REPUBLIC OF IRAQ

MINISTRY OF HIGHER EDUCATION AND SCIENTIFIC RESEARCH

AL-FURAT AL-AWSAT TECHNICAL UNIVERSITY

ENGINEERING TECHNICAL COLLEGE – NAJAF

Production of Fresh Water Using Effective Solar Still Using Different Absorbing Materials

By

Mays Alaa Noori

(B.Sc. Mechanical Power Technology. Eng. 2021)

M.TECH.

IN MECHANICAL ENGINEERING TECHNIQUES OF POWER

2024 A.D **1446 A.H**

Production of Fresh Water Using Effective Solar Still Using Different Absorbing Materials

A THESIS

SUBMITTED TO THE DEPARTMENT OF MECHANICAL ENGINEERING TECHNIQUES OF POWER

IN PARTIAL FULFILLMENT OF THE REQUIREMENTS FOR

MASTER OF THERMAL TECHNOLOGIES DEGREE IN MECHANICAL ENGINEERING TECHNIQUES OF POWER (M.TECH.)

BY

Mays Alaa Noori

(B.Sc. Mechanical Power Technology. Eng. 2021)

Supervised by

Lec. Dr. Basil Noori Merzah

Prof. Dr. Montadhar Al-Moussawi

2024 A.D **1446 A.H**

بسم الله الرحمن الرحيم

﴿ وَأَنْ لَيْسَ لِلْإِنْسَانِ إِلَّا مَا سَعَى (٣٩) وَأَنَّ سَعْيَهُ
سَوْفَ يُرَى (٤٠) ثُمَّ يُجْزَاهُ الْجَزَاءَ الْأَوْفَى (٤١)﴾

صدق الله العلي العظيم

سورة النجم

Acknowledgements

First and foremost, I am profoundly grateful to Allah, whose guidance and grace have been my strength and light throughout this journey.

I extend my most profound appreciation to my supervisors, (**Lec. Dr. Basil Noori Merzah and Prof. Dr. Montadhar Al-Moussawi**) Whose invaluable expertise, patience, and encouragement have been instrumental in shaping this work. Their insights and mentorship have been an enduring source of inspiration and growth.

I also wish to thank the head of my department (**Prof. Dr. Adel A. Eidan**) and the esteemed faculty members for their unwavering support, guidance, and belief in my potential. Their dedication to academic excellence and encouragement have enriched my experience and driven me to achieve my best.

To my beloved family, whose love, sacrifices, and encouragement have been my steadfast foundation, your belief in me has been a constant source of motivation. For that, I am eternally grateful.

Finally, I thank my colleagues and friends, whose support, companionship, and kindness have been invaluable. Their presence and understanding made the challenges of this journey far more bearable.

Thank you all for helping me reach this important milestone.

DEDICATION

I dedicate this humble work to all I hold dear, especially my family, the light guiding my path to success.

To my beloved father, whose existence grounds me and to whom I owe boundless respect and admiration

To my dear mother, whose unwavering strength and endless care taught me resilience in all circumstances

I extend my heartfelt gratitude to my cherished brothers, my sisters-in-law, and my precious nieces.

To the miraculous woman whose patience and steadfast support make all things possible, my beloved sister (Amna), my guardian angel and steadfast supporter from the beginning of this journey to its end

I also honour all who, with their knowledge, have illuminated the minds of others or dispelled confusion with wisdom, embodying the humility of scholars and the grace of the truly wise.

Finally, to the martyrs of Iraq, martyrs of pride and dignity, martyrs of honour and nobility, you who led the battles to protect the land, honour, and defended the religion of God, Iraq, and the sacred places, peace be upon your pure souls, the day you were born, the day you were martyred, and the day you are resurrected alive.

Mays Alaa Noori

Declaration

I hereby affirm that the work contained in this thesis is solely my own and has not been submitted to any other organization or for the purpose of obtaining any other degree.

Signature:

Name: **Mays Alaa Noori**

Date: / / 2024

Supervisor Certification

We certify that this thesis entitled "**Production of Fresh Water Using Effective Solar Still Using Different Absorbing Materials**" which is being submitted by Mays Alaa Noori was prepared under our supervision at the Department of Mechanical Engineering Techniques of Power, College of Technical Engineering-Najaf, AL-Furat Al-Awsat Technical University, as partial fulfillment of the requirements for the degree of Master of Techniques in Thermal Engineering.

Signature:
Name: Lec. Dr. Basil Noori Merzah
(Supervisor)
Date: / / 2024

Signature:
Name: Prof. Dr. Montadhar Al Moussawi
(Co-Supervisor)
Date: / / 2024

In view of the available recommendation, we forward this thesis for debate by the examining committee.

Signature:
Name: Prof. Dr. Adel A. Eidan
Head of Mechanical Eng.Tech. of Power Dept.
Date: / / 2024

Committee Report

We certify that we have read this thesis titled "**Production of Fresh Water Using Effective Solar Still Using Different Absorbing Materials",** which is being submitted by **Mays Alaa Noori** and as Examining Committee, examined the student in its contents. In our opinion, the thesis is adequate for the award of the degree of Master of Techniques in Thermal Engineering

Signature:
Prof. Dr. Hafidh Hasan Mohammed
(Chairman)
Date: / / 2024

Signature:
Asst.Prof. Dr. Ahmed Razzaq
(Member)
Date: / / 2024

Signature:
Asst.Prof. Dr. Ahmed Salim Naser Almurshedi
(Member)
Date: / / 2024

Signature:
Lec. Dr. Basil Noori Merzah
(Supervisor)
Date: / / 2024

Signature:
Prof. Dr. Montadhar Al Moussawi
(Co-Supervisor)
Date: / / 2024

Approval of the Engineering Technical College- Najaf

Signature:
Name: Prof. Dr. Hassanain Ghani Hameed
Dean of Engineering Technical College- Najaf

List of Figures

List of Table

Table of Contents

Abbreviations

Symbol	Description
N / E	North / East
CFD	Computational Fluid Dynamics
SSSS	Single Slope Solar Still
SS	Solar Still
PCM	Phase Change Material
PV	Photovoltaic
TDS	Total Dissolved Solids
SSSS	Conventional single-slope solar Still
3-D	Three dimensional
NPs	Nanoparticles
NFs	Nano-fluids
MSSSS	Modified Single Slope Solar Still

Nomenclature

Symbol	Definition	Unit
A	Collector area	m^2
$\bar{\mathbf{F}}$	External force per unit volume.	N/m^3 or $kg/(m \cdot s^2)$
$\bar{\mathbf{g}}$	Gravitational acceleration vector	m/s^2
$\mathbf{H_{vap}}$	The heat of vaporisation of water	J/Kg
$\mathbf{I_{sun}}$	Solar intensity	W/m^2
$\boldsymbol{\mu_m}$	Dynamic viscosity of the mixture	$Pa \cdot s$ or $kg/(m \cdot s)$
P	The productivity	Kg or L
p	Pressure	N/m^2 or Pa (Pascals)
$\boldsymbol{\rho_m}$	The mass density of the mixture	kg/m^3
$\mathbf{T_{amb}}$	Temperatures of ambient	°C
$\mathbf{T_{gi}}$	Temperatures of glass cover bottom	°C
$\mathbf{T_w}$	Temperatures of water	°C

t	Time	sec
$\bar{v}_m$	The mass-averaged velocity	m/s
η	Efficiency per hour during the day	
M	Mass	Kg
U	Velocity field	m/s
K	Thermal conductivity	W/m.K
t	Thickness	Cm or mm
Q_{ev}	Evaporation heat	J/s
M_{ev}	The mass flow rate of water	Kg/s
L_{ev}	Latent heat for evaporation water	KJ/kg
Q_r	Radiation heat transfer	J/s
Q_c	Convection heat transfer	J/s
Q_{ev}	Evaporation heat	J/s
Q_{cond}	Condensation heat	J/s
H	Convection heat transfer coefficient between glass cover and Ambient	$W/m^2.K$

Subscripts

Symbol	**Definition**
Amb	Ambient
B	Basin
G	Glass
W	water

Abstract

The numerical investigation was conducted numerically with ANSYS Fluent software version 18.2. A CFD numerical model was used in order to select the best absorbing materials. The absorbing materials used in the current work were crushed black marble with different average sizes (0.5–4 cm) and natural black leather, which are easily available and cost-effective materials.

It was found that crushed black marble with a size of 4 cm and 2 cm yielded the highest productivity of 6035 mL/day and 5760 mL/day, respectively, while natural black leather produced 5600 mL/day. A strong agreement was found between the experimental findings of the current investigation and the numerical data. The CFD results were validated by comparing with previous published work and with the experimental results too, which indicate a percentage error of less than 5%.

Experimental tests were done on specific days of March, April, and May at particular times, starting from (7 am) in the morning until (5 pm) in the afternoon. The findings from experimental and numerical investigations suggested that the techniques used in this work can potentially enhance the performance of the solar distiller. This may be accomplished by improving the distiller's production by increasing the water temperature and facilitating rapid vaporisation. Using a stepped solar still with absorbing materials and a preheating unit was the most effective method to accomplish this objective. The function of the absorbing materials is relatively little relative to that of the stepped solar still and preheating unit. Consequently, the combined use of these strategies (stepped solar still incorporated with a preheated water unit and 4 cm of crushed marble) has enhanced the freshwater efficiency and productivity of the solar still by 44.02% and 75.57%, respectively, in comparison with conventional solar stills.

Chapter One

Introduction

1.1. General Introduction

Water is a vital component for sustaining life. Despite water accounting for 71% of the Earth's surface area, 98% is saline and unsuitable for human consumption. The issue of water scarcity is a significant challenge confronting contemporary society. Most countries globally utilise desalination systems that rely on electric or thermal energy, resulting in substantial energy consumption. These systems incur production costs approximately 50% higher than systems powered by renewable energy sources. Additionally, they contribute to environmental damage. Humanity turned to alternate energy sources to solve the water shortage, seeking long-lasting and environmentally beneficial options. A significant obstacle faced is the decreasing need for fossil fuels. Renewable energy is the most optimal choice and has been extensively studied globally. Recently, substantial efforts have been made to identify alternative energy sources and improve their efficiency to address problems associated with fossil fuel use and promote the use of green energy [1].

1.2. Solar energy

Solar energy is a promising alternative solution with significant potential in various regions across the globe. In contrast to other energy sources, the primary advantage of solar energy is its inherent purity and ability to be generated without any atmospheric pollution [2]. Solar energy is a clean, sustainable, potent, and renewable source. It is generated by the sun and emitted as electromagnetic waves throughout the cosmos. When these waves reach a body and are absorbed, they cause an increase in its internal energy and temperature [3]. The sun is a crucial and inexhaustible source of energy on Earth. Solar energy is using solar radiation or thermal energy derived from solar radiation. The spatial distribution of solar energy on Earth's surface exhibits variations based on latitude and longitude. Certain countries, such as Iraq, at 32.1° N/44.19° E, receive ample sun radiation. Iraq gets a yearly average of 1968-2244 kWh/m^2 of direct radiation, as shown in Figure (1.1) [4], [5].

1.3. Solar Energy Application

The sun, the nearest celestial body to our planet, supplies it with vital energy and sustains life. The sun radiates a vast quantity of energy, with around 1367 W/m^2 of our ionosphere. Approximately 80% of the energy can reach the Earth's surface and be utilised for many purposes, including power generation, water heating, solar cooking, air heating, greenhouse operations, and water distillation [6].

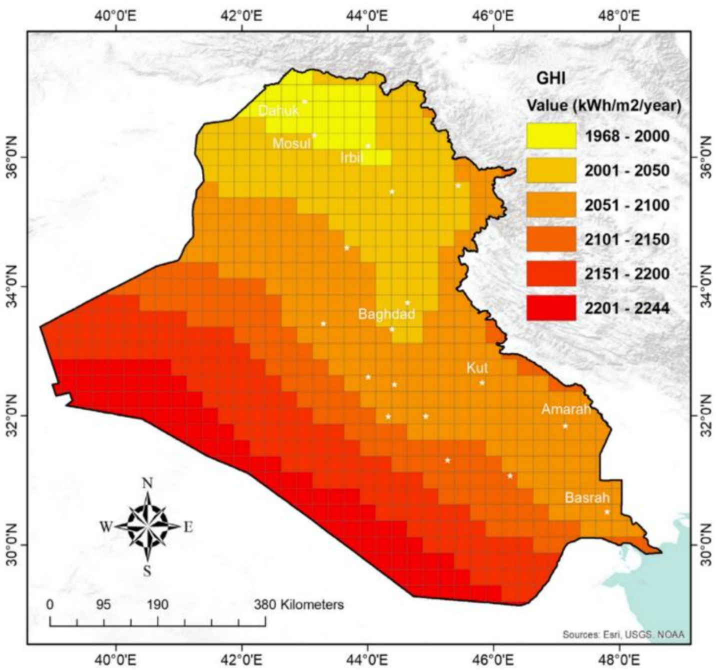

Figure 1.1: Map of horizontal solar radiation in Iraq [5]

1.4. Solar Desalination

Solar distillation is an established technique. In 1551, the Arab chemist was the initial individual to utilise it. Della Porta employed the approach in question in 1589, Lavoisier in 1862, and Mauchot in 1869. "Solar Still" commonly refers to a solar water distillation apparatus. The Solar Still can be utilised to purify seawater and eliminate salt and mineral constituents such as sodium (Na), calcium (Ca), arsenic (As), iron (Fe), and manganese (Mn). Bacteria such as E.coli, Cholera, and Botulinus can also be eliminated. Solar energy still functions based on a principle identical to the natural water cycle. Every water treatment process in Table 1-1 needs considerable energy to extract clean water from a saline source. The procedure involves introducing salt (feed) water and producing two separate streams: clean water and high-salt effluent [7].

According to calculations, producing 1000 m^3 of fresh water daily would necessitate 10,000 tons of oil annually. This is crucial because it involves a repetitive consumption of electricity that can only be afforded by a limited number of water-scarce locations worldwide. Several oil-rich countries utilise large-scale commercial desalination plants powered by fossil fuels to supplement their traditional water sources. Solar energy is being selected for the desalination process due to the demand for energy and the expensive nature of conventional power facilities. Other countries worldwide lack the financial means or oil reserves necessary to facilitate such growth [8].

Table 1.1: Different Types of Water Treatment Methods [7]

	Designation of the Category	**Explanation**
1	Reverse osmosis	saline solution is forced through selective membranes under elevated pressure, enabling the passage of water molecules while preventing the passage of dissolved salts.
2	Vapour Compression	In this process, the water vapour is compressed adiabatically, increasing temperature beyond its boiling point. When the vapour temperature attains saturation, it condenses at a steady pressure. This procedure employs mechanical energy.
3	Distillation	Several processes, such as distillation, can purify water. This process requires an energy input, which can be supplied by solar radiation. In this process, water undergoes evaporation, causing the separation of water vapour from dissolved particles. The water vapour is then condensed to get clean water.
4	Multistage flash distillation	The MSF approach comprises a sequence of specific steps known as phases. Steam condensation is used to preheat the seawater at each stage. The method aims to achieve maximum efficiency in recovering latent heat by dividing the temperature difference between the

		warm source and saltwater into numerous phases. This system's functionality necessitates the presence of pressure gradients inside the facility.
5	Multiple-effect distillation	Multiple-effect basin stills are distillation apparatuses with two or more chambers. The lower chamber's condensing surface is the higher chamber's floor. The condensing vapour generates enough heat to cause the feed water above it to evaporate. Because multiple-effect solar desalination systems use the latent heat of condensation, they exhibit more productivity than single-effect systems.
6	Freezing	The concept is intriguing since freezing necessitates a lower amount of thermodynamic energy compared to evaporation. This is attributable to the fusion latent heat of water, which is 6.01 kJ/mole, in contrast to the latent heat of vaporisation at 100°C, which is 40.66 kJ/mole. The water stream is chilled by a conventional refrigeration cycle until it attains the freezing point, resulting in ice formation. The ice is eliminated via scraping, subsequently melting.

1.5. Solar desalination types

Solar desalination systems are categorised into two main types: direct systems, which utilise solar energy to directly generate distillate, and indirect systems, which consist of two sub-systems: one for collecting solar energy and another for desalinating water [9]. Solar energy is divided into two distinct types: passive solar energy and active solar energy. Passive solar energy encompasses the collection and retention of solar heat, while active solar systems capture solar radiation and convert it into thermal or electrical energy using electrical or mechanical equipment like fans and pumps. Active solar energy is classified into two categories: active solar thermal energy technology and photovoltaic technology. Solar thermal energy is used for several purposes in homes and businesses, including drying, heating, cooling, and cooking [10].

Multiple factors affect the efficiency of a solar distillation system, including the strength of radiation from the sun, wind velocity, ambient temperature, thermal disparity between water and glass, surface area of the absorption plate, inlet water temperature, angle of glass inclination, and depth of salt water in the basin. The solar desalination technologies are classified according to the evaporation and condensation mechanisms employed, as shown in Figure (1.2) [11], [12]

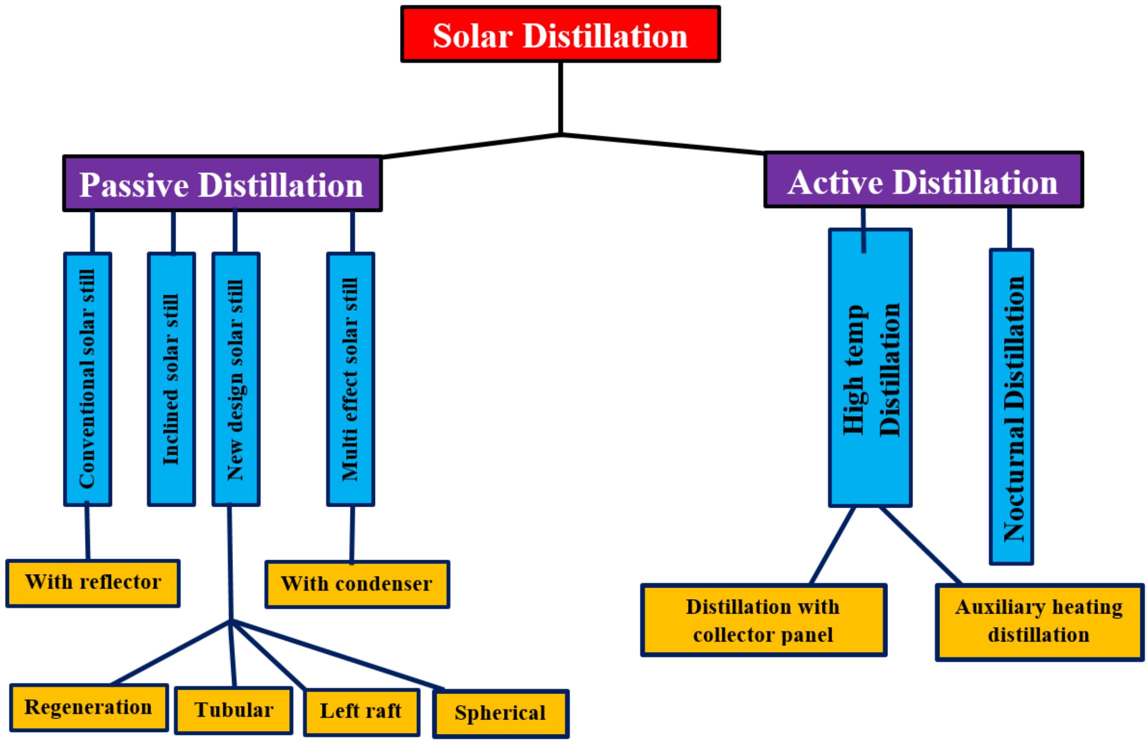

Figure 1.2: Solar Distillation Classifications [12]

1.6. Passive solar distillation

There are many types of passive solar distillers. The primary common type is Single Slope Solar Still (SSSS) which are straightforward solar distillation systems that are user-friendly and quick to construct. Due to their restricted production capacity, they are primarily used for small and modest household purposes. The operational mechanism of the solar still is uncomplicated and can be delineated into five distinct stages [6].

The solar radiation infiltrates the top glass cover and enters the sealed and insulated container. When the radiation reaches the water in the basin, only a small portion is absorbed, while the majority passes through and is absorbed by the black-painted basin. As a result, the basin heats up and increases the temperature of the water. Due to the system's isolation, thermal equilibrium occurs between the base plate and the layers of water. A saturated vapour is emitted from the water as its temperature rises. As the water vapour ascends, it encounters the glass cover with a lower surface temperature. The water vapour then condenses upon contact with the glass, generating pure water droplets on the inner side. The water drops naturally descend and are gathered by a specialised collector to utilise them as pure water [6].

Single-slope solar stills generally feature a right-angled cross-section and semi-triangular shape. The bottom is typically made of a galvanised rectangular plane sheet. The top side is covered by a transparent material with a tilt angle determined by the global position of the still. To minimise thermal dissipation, the bottom and sides of the still are coated with insulation material. Figure (1.3) shows a single slope solar still general configuration [13]

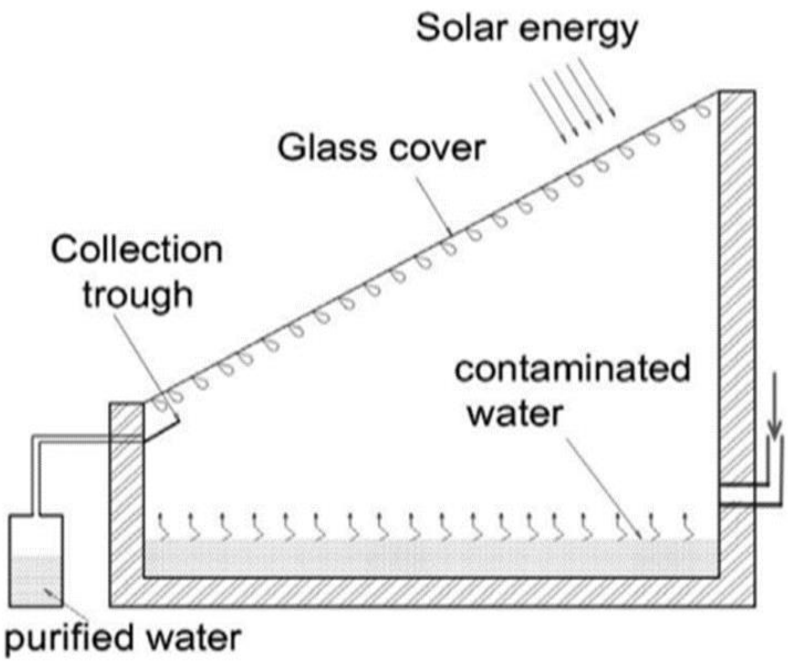

Figure 1.3: Conventional Single Slope Solar Still's general design [13]

1.7. Active solar distillation

Diverse methods enhance freshwater productivity due to decreased passive distillate production [14]. The temperature of salty water is elevated during active distillation using many external sources, including reflecting mirrors, Fresnel lenses, solar energy concentrators, evacuated tubes, etc [12]. as seen in Figure (1.4)

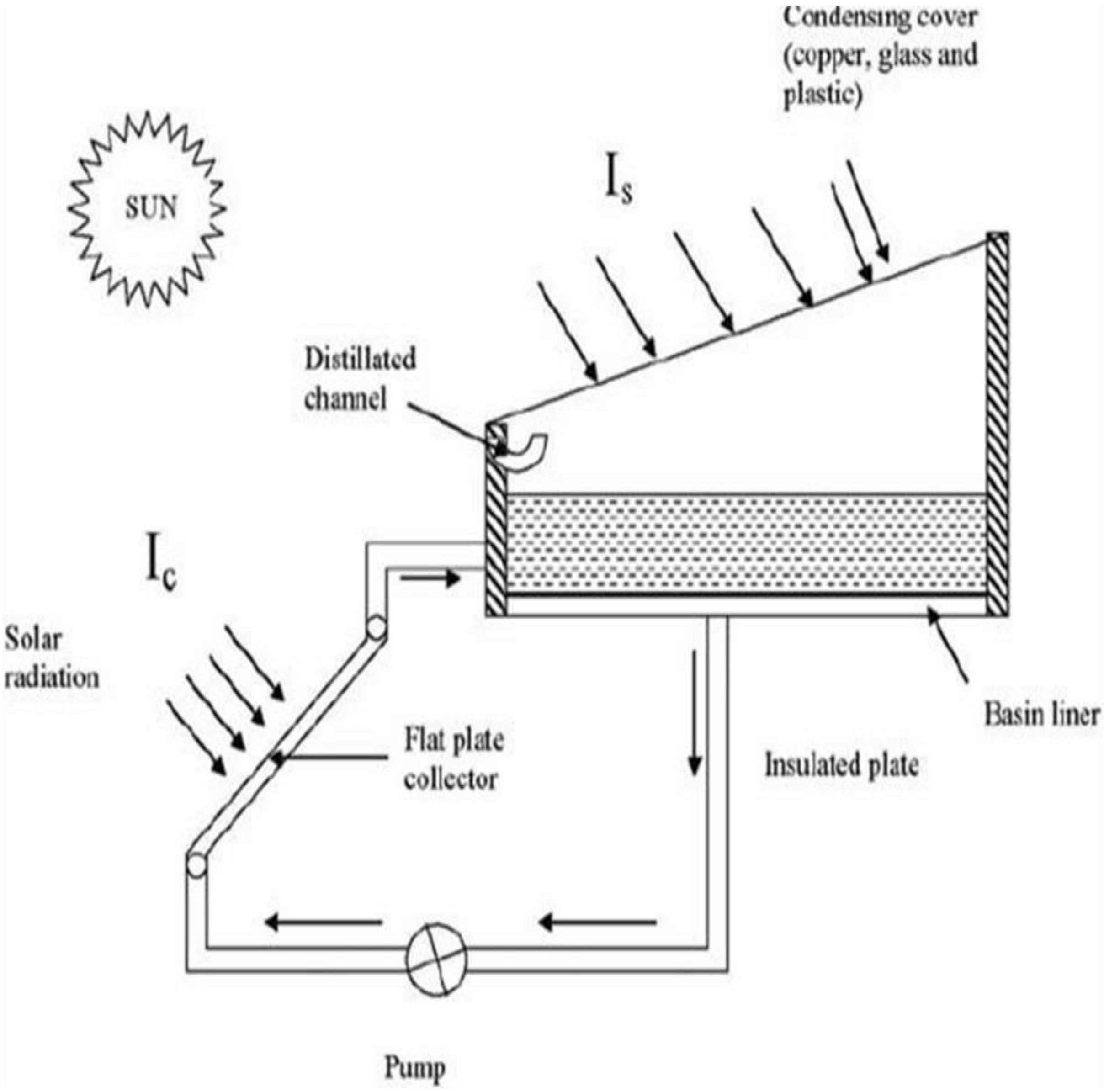

Figure 1 4: View of active solar still with flat collector [14]

1.8. Advantage of Solar Distillation

1) The cost-effective and efficient installation method is suitable for supplying clean water to households and small communities. It features a compact design and does not rely on stationary accessories such as vanes or motors [7].
2) Moreover, it is environmentally friendly as it solely depends on renewable energy and does not cause pollution [7].
3) The operator does not need to possess a substantial comprehension of the tasks, upkeep, or possible malfunctions. Iraq experiences abundant sunshine throughout the year, distinguishing it as one of the select nations globally [7].

1.9. Disadvantages of Solar Distillation

1) This strategy requires vast expanses of land with ample solar radiation. It is vulnerable to weather conditions. The level of productivity and efficiency is now suboptimal[7].
2) Typically, the water temperature in the solar system still fails to reach the boiling point, hence the failure to effectively eliminate germs and bacteria. Moreover, the productivity of conventional solar stills in generating freshwater is often low due to the decreased efficiency caused by the improperly inclined glass cover[1].

1.10. Problem statement

The issue of water pollution is a pressing concern that necessitates the implementation of effective strategies to enhance the efficiency of freshwater resources. Contaminated water harms health and presents a substantial risk to individual well-being. The main purpose of this research is to examine the efficiency of SSSS using an effective CFD model, as well as carrying out experiments which include a stepped solar still system design connected to a solar heater that consists of a reflector, which can significantly improve freshwater productivity compared to prior attempts. In addition, several absorbent materials were employed to enhance output even further. A comparison was conducted between the outcomes of utilising water alone and those with absorbent materials, revealing an improved capacity for thermal enhancement within the solar still.

1.11. Scope and Objectives

The primary objective of this project is to create an effective small-scale solar desalination system in Najaf city. This will be achieved by using local resources to improve the production of distilled water. The main aim is to address the challenges of electricity availability and the scarcity of purified water. Hence, the subsequent goals are considered to examine the efficiency of a SSSS.

The aims can be listed as following:

1- To study the performance of a single slope solar still under the environmental conditions of Al-Najaf city.

2- Preheat the water using the solar heater to enhance evaporation.

3- To enhance the condensation process by using an external reflector.

4- To develop a 3-D mathematical model with the aid of ANSYS-FLUENT software, as well as, to validate the developed model for reliability purposes and to develop the numerical simulation for the best solar still design.

5- To evaluate the performance of the solar still systems with absorbing materials.

6- To Promote technological innovation that may inspire future innovations in sustainable water treatment and purification.

1.12. Thesis Outline

This thesis is divided into six chapters, each one dealing with a different part of the work's scope:

Chapter One: This chapter presents background information about solar desalination.

Chapter Two: This chapter presents some previous studies of experimental and numerical effects of different solar still types on freshwater productivity.

Chapter Three: This chapter discusses the development of the 3-D model and the validation process.

Chapter Four will present the experimental work, including manufacturing solar stills and devices used for experimental tests.

Chapter Five: The numerical and experimental investigation findings are presented and discussed in this chapter.

Chapter Six: Conclusion and future recommendations.

Finally, the references used in this study are listed.

Chapter Two

Literature Review

2.1. Introduction

Numerous techniques exist for desalinating seawater and brackish water. This category encompasses several processes, including flash distillation, multi-effect distillation, membrane distillation, reverse osmosis, forward osmosis, ion exchange, capacitive deionisation, electro dialysis, and seawater greenhouse technology [15], [16]. The energy required for desalination may be sourced from conventional fossil fuels or alternative energy sources, including biomass, wind, solar, geothermal energy, or industrial waste heat.

Solar stills possess several advantages in solar desalination: simplicity, affordability, ease of maintenance, and minimal ecological footprint. Nevertheless, it is essential to acknowledge that these technologies also possess certain drawbacks, notably their subpar performance, which deter their widespread adoption in commercial settings.

Solar still's function based on the principles of evaporation and condensation. Solar energy is utilised to evaporate the brine contained within the SS, resulting in the collection of condensed water as the output of purified water. Within a dual-or multi-effect SS, the procedure above is iterated in a manner that utilises the heat generated during condensation to facilitate a subsequent evaporation phase. The utilisation of multiple effects has been observed to enhance performance; however, it is accompanied by a concomitant cost penalty. Utilising dynamic elements, such as pumps and fans, presents an alternative approach to improve performance; however, it also entails certain drawbacks regarding increased expenses and heightened intricacy.

Numerous scholarly articles have been published on the topic of solar stills, mainly focusing on aspects such as creation and advancement [17]-[20] efficiency optimisation [21]-[25], type of wick [26], and simulation [27]. However, the latest advancements, which utilise novel materials like PCMs and Nano-composites, hold the potential for substantial enhancements in efficiency. Consequently, this necessitates a comprehensive reassessment. In this chapter, A current and thorough examination of the latest advancements in solar stills technology is provided.

2.2. Key factors influencing the performance of Solar Stills

2.2.1. Weather conditions

The primary climatic characteristic that impacts production is solar radiation intensity. Under the assumption of constant efficiency, daily productivity will exhibit a direct proportionality to sun irradiation, and the unit of measurement is ($kJ/m^2.day$). Nevertheless, the performance is also influenced by wind speed and ambient temperature. Tiwari et al. (2014) evaluated the impacts of different meteorological circumstances on distillation systems, active and passive. They showed that wind enhanced the execution to an identical threshold velocity of 4.5 m/s, and the output stayed consistent [28]. The reason for this phenomenon is that wind facilitates the process of heat transfer from the cover, leading to an increase in condensing up to a certain threshold velocity. Beyond this critical speed, the augmentation of condensation becomes minimal [29], [30].

2.2.2. Depth of water

In their study, Sourabh K. N. et al. (2021) employed various methodologies to enhance the performance of SS by optimising water depth. They reported that the system exhibits high efficiency and produces significant distillate when operating at a shallow basin water depth of 1-2 cm. The productivity levels during workdays and non-workdays vary based on the basin water depth. The design, operation, and climatic parameters substantially influence the performance of a still. The relationship between salt concentrations in basin input water and productivity indicates that lower salt concentrations are associated with higher productivity levels. The thermal performance of a stagnant liquid can be enhanced by incorporating NPs with different water depths. The utilisation of paraffin as a PCM in SS has demonstrated its significance over alternative materials owing to its advantageous physical, chemical, and economic characteristics, which contribute to enhanced safety and reliability [31].

2.3. Passive Solar Stills

A passive SS refers to a system whereby evaporating and condensing occurs spontaneously. Passive SSs may be classified based on several factors, such as the structure and components of the evaporator (including wicks), alternative methods of storing heat, the forms, and the number of basins. Utilising numerous basins or wicks may facilitate the implementation of multiple-effect distillation, resulting in significantly increased production [32]

2.3.1. Basic single-effect solar still

The fundamental form of passive still, the single-slope, single-basin SS, is a benchmark for comparing more sophisticated designs. Numerous research has been conducted on the subject, exploring different factors such as the material type, the inclination of the glass lid, the cooling mechanism, the material employed within the SS for absorption purposes, the chemical makeup of the water used for feeding, and the kind of basin lining [33].

The impact on performance is influenced by the selection of materials, as shown by Panchal's (2011) study, which included trials with several kinds of SS, such as those made of aluminium and galvanised iron. The study revealed that the aluminium SS exhibited a higher distillate production of around 3.8 L/m^2.day.

In comparison, galvanised iron only produced 2.6 L/m^2.day. This disparity in performance was attributable to the enhanced heat conductivity of the aluminium material [34].

The angular tilt of the glass surface exerts a substantial influence on several measures, including the output and the efficiency at any given moment. Nevertheless, various researchers arrived at disparate results regarding the most favourable disposition. While it may be proposed that the angle of inclination must be equivalent to the angle of latitude, this alignment needs to be regularly seen in the conceptual and empirical research that has been documented.

According to reference [35], the system's effectiveness improves as the temperature of the incoming water supply rises. Zurigat (2010) examined the efficiency of an SS equipped with a double glass covering, including brine preheating and cover cooling. The study unveiled a significant improvement in efficiency as a result of an escalation in the rate of evaporation, leading to an increase in efficiency of up to 25% [36]

The overall productivity of the still is influenced by the makeup of the feed water used. The output of single-basin stills is subject to variation based on the type of basin liner employed.

Several scholars have conducted studies to analyse and define heat coefficients' thermal capacity and transference in SS. Rabbar (2013) observed the relationship between the rate of heat transfer through evaporation and convection is contingent upon the temperatures of the glass and water [37]. In their study, Narjes et al. (2011) modelled the solar desalination still's heat transfer coefficient using computational fluid dynamics. Their findings indicated that the rate of potable water generation remains relatively stable across varying radiation heat transfer coefficients. However, they observed that the water's temperature and the glass lid's presence influenced this rate [38].

Sivakumar et al. (2015) conceptualised a singular slope solar still, concentrating on the effects of the glass lid's and basin's heat capacity. According to the study, a decrease in the heat capacity of the glass cover and basin led to a 10.38% overall increase in yield. Additionally, the destruction of exergy for the glass and basin dropped, with reductions of 7.53% and 15.84%, correspondingly the study concluded an inverse relationship exists between heat capacity and production [39].

In conclusion, the output of an SS with a single-effect design varies between 2-4 L/m^2.day for a basic iteration but can reach 3-5 L/m^2.day for enhanced editions featuring upgraded basin liners or optimised geometries. The relatively modest numbers have compelled researchers to propose additional design alterations, which will be elaborated upon in the following discussion.

2.3.2. Solar Reflectors

One potential strategy for enhancing production involves augmenting the incident solar radiation captured by the SS. This task can be accomplished by employing a reflector. In their study, Hiroshi (2011) conducted trials utilising an SS with a single basin equipped with both reflectors inside and outside. Research has indicated that distillate production can be enhanced by adjusting the angle of the outer reflector, namely by tilting it rearward in the summer and onward in the other periods [40], [41]. In a study by Boubekri (2011), the author used numerical modelling techniques to investigate the effect of incorporating reflectors inside and outside SS. The objective was to assess the resulting increase in productivity, which was found to be 72.8% [42]. The overall conclusions indicate that maximum allowable tilt angles for exterior and interior reflectors should not surpass 25°. Additionally, the optimal angle of inclination for the glass lid varies between 10° and 50° depending on the time of year.

2.3.3. Thermal energy storage

An alternative method for enhancing execution is the utilisation of thermal energy storage. Storage of thermal energy media can assimilate thermal energy during periods of intense solar radiation and discharge the stored thermal energy when the radiation level diminishes. The SS has the potential to operate beyond sunset. Diverse substances have been used to retain both latent and sensible heat. Several studies have explored placement strategies for heat storage materials, including those below the water surface, immersed within and underneath the basin [32].

2.3.3.1. Effective heat storage

Dudul Das et al. (2020) defined various methodologies to improve the efficiency of SS and increase distilled water production. Key aspects include modifying absorber plates, integrating condensers, using reflectors, incorporating dehumidification units, incorporating thermal energy storage materials, and implementing thermoelectric coolers. Some significant findings include incorporating baffles to enhance water residence time within basins, allowing for increased water temperature and accelerated evaporation. Sponges are suitable materials for solid-state applications due to their high absorptivity and permeability. Cuprous oxide NPs have shown enhanced efficiency in distillate output, and combining them with active systems like hoovers can significantly improve productivity. PCM infused with NPs can also enhance SS efficiency, producing distilled water at a cost comparable to bottled water. Paraffin wax and sand can be highly efficient heat storage mediums in solar systems, mitigating overall costs [33].

Certain substances can simultaneously store heat and absorb optical radiation. Pankaj (2013) conducted a study on the impact of a buoyant permeable absorber. The basin of a singular slope SS was examined both experimentally and theoretically. The outcomes demonstrated that a modified still setup yielded approximately 68% of the distillate yield [43]. These findings align closely with the outcomes reported by Velmurugan [43], who investigated an SS consisting of only one basin and one slope, featuring a stepped design incorporating thermally efficient material for storing heat.

Other studies focused on integrating solar still with thermal energy storage on the roof, recording a daily productivity of around 3.5 L/m^2.day [44], [45].

An SS with a single basin and a double slope was built using feasible materials for storing heat energy, including quartzite pebbles, fragments of red brick, shards of cement concrete, washed stones, and iron debris, according to research done by Kalidasa et al. (in 2010). The researchers concluded that using quartzite rock resulted in the maximum production, as indicated by their findings [46]. In their study, Kalidasa et al. (2011) researched utilising different wick materials and determining the minimal water mass required in the SS [47].

2.3.3.2. Latent heat storage

The utilisation of PCM enabled the attainment of latent heat storage. The effects of earlier upgrades on Egypt's energy efficiency, production costs, and pure water productivity were studied by Mohamed Abdelgaied et al. (2022). Saving money on water production while improving sustainability, economic feasibility, and competitiveness can be achieved by utilising solar heat and waste heat in desalination systems. The cost of producing pure water drops from 6.80 \$/m^3 to 1.6 \$/m^3 when compared to grid electricity-based systems, and the permeation rate of pure water increases as the input water temperature increases. From 46.6% to 61.8%, system efficiency is enhanced with a pre-cooling unit on the permeate flow loop. PCM improves pure water productivity with an estimated improvement rate ranging from 33.11% to 43.18%. By raising the cumulative yield by 43.2% and the output ratio by 34.4%, thermal storage materials improve membrane distillation units' overall efficiency and productivity. Multi-walled carbon nanotubes (MWNTs) are added to enhance water flux, but salt rejection efficiency is decreased. With rates of 40.98% and 57.4%, respectively, the solar collector for preheating input water significantly improves pure water productivity. Pure water production costs only 0.0102 $/L with this method, and the productivity of SSs can be increased by up to 116% with NFs and 105.5% with thermal storage materials, particularly PCM [48].

Shahin Shoeibi et al. (2021) conducted an empirical study on several configurations of SSs throughout a four-day experimental period, focussing on the use of porous absorber surfaces, Nano-enhanced phase transition materials, and Nano-coatings. The porous media absorber used in this investigation consisted of a bed of anthracite with a homogeneity coefficient of 0.0013 m. To improve the thermal conductivity of PCM, paraffin wax was supplemented with aluminium oxide and copper oxide nanoparticles at concentrations of 0.1% and 0.3%, respectively. The CuO nanoparticles were added to the black dye solution at a concentration of 10%. The mixture was then applied to the twelve copper pipes to improve thermal conductivity and solar energy absorption. In every instance of SSs, the benefit-cost ratio surpassed one. Compared to conventional SSs, the daily energy efficiency of the SS using CuO (0.3 wt%) Nano-enhanced PCM shown a 55.86% improvement. The melting temperatures of CuO and Al2O3 nano-enhanced phase transition materials decreased by 2.1 and 1.8 °C, respectively, at 0.1% concentrations, and by 2.7 and 2.3 °C at 0.3% concentrations.

Compared to saline water, the use of nano-coating on copper pipes enhanced the quality parameters of distilled water, such as TDS, EC, TSS, turbidity, pH, thermal conductivity, and solar intensity absorption [49].

T. Arunkumar et al. (2019) investigated the use of solar-absorbing materials, including metallic, semiconductor, and carbon-based substances, in the photo-thermal conversion process in China. These materials effectively promote the evaporation of many aqueous solutions, including seawater, synthetic seawater, river water, acidic water, and alkaline wastewater. The exceptional efficiency of plasmonic metals is attributed to the local surface plasmon resonance phenomena (LSPR). Concurrently, carbon-based materials demonstrate enhanced thermal retention, an essential consideration. Cu_2O, Al_2O_3, SiO_2, ZnO, TiO_2, and carbon nanotubes (CNTs) were examined in solid-state systems (SSs) to enhance thermal conductivity with bulk water. Phase Change Materials (PCMs) boost energy storage capacity in solar systems; nevertheless, they are limited by low thermal conductivity and the need for appropriate encapsulation. Nanoparticles were integrated into paraffin wax to improve thermal conductivity, hence lowering the melting and solidification temperatures of phase transition materials. Supplementary materials, including as fins, pebbles, cotton fabric, and jute wick, were included into SS to augment the evaporation surface area. Energy-efficient materials revealed an exceptional sun absorption capacity exceeding 96% and indicated higher effectiveness in minimising heat loss compared to energy exchange and storage materials. However, incorporating nanoparticles into liquids or black paint resulted in a little increase in the evaporation rate [50].

In their study, Omar et al. (2013) carried out trials using an SS equipped with PCM below the basin. The researchers observed that the inclusion of PCM resulted in improved productivity and efficiency of the SS. However, the study needed precise performance data to allow for meaningful comparisons. The efficiency observed in this study was comparatively higher than the reported efficiencies of Rahim (47.2%) and Zurigat (25%) [51], [52].

In their study, Mohammad et al. (2011) conducted a thermal evaluation on an SS with a stepped design that incorporated a PCM consisting of paraffin wax positioned below the absorption plate. This integration of PCM resulted in enhanced SS output. Additionally, it was noticed that the time of residence increased as a result of the water distribution on the evaporation surface [53].

In their study, Swetha et al. (2011) accomplished scientific investigations involving a SSSS that utilised PCM consisting of the acid Lauric positioned underneath the basin. Their findings revealed a notable increase of up to 36% in distillate production [54]. This contrasts with the results reported by Silakhori (2011), who suggested that paraffin wax and acetamide exhibit more excellent stability in this context. In summary, latent heat storage has demonstrated superior performance [55], and it is advisable to choose PCM with a relatively low melting point, approximately 30-45 °C [56], to align with the lower temperature range for operation often associated with passive stills. The optimal placement for the medium for thermal preservation is situated below the basin, while the most suitable components for this purpose are acetamide and paraffin.

2.3.4. Non-traditional forms

The standard SS exhibits a rectangular shape from above and a trapezoidal shape from the side. Nevertheless, several other geometries have been documented for their application in passive SSs, as elaborated in subsequent segments [57]-[73]

2.3.4.1. Triangular stills

Multiple scholars have undertaken a range of assessments of triangular SSs, including thermal analysis, exergy analysis, and parametric analysis. The optimal production of the pyramid glass cover is achieved at an angle of 50°. In their study, Kianifar et al. (2012) performed an exergy assessment on a photovoltaic desalination system with a pyramid design, comparing its performance with and without using a fan positioned alongside the glass. The research indicated that the evaporation rate augmented in the system fitted with a fan. Additionally, the daily production experienced a notable enhancement of approximately 15-20%, while the exergy efficiency had a positive correlation with lower water depths [58].

A parametric analysis was undertaken by Ahsan (2014) on a passive triangular SS. The study involved the manipulation of water depth and several environmental conditions. The study suggested a negative relationship between water depth and daily production [59], [60]. Ravishankar et al. (2014) completed experimental investigations within a triangular pyramid and subsequently analysed the various aspects that influence its performance. The study suggests that the highest level of productivity was observed at the lowest water depth, and it is implied that a wind velocity of approximately 4.5 m/s is necessary to generate a 15% improvement in output (refer to segment 2) [28].

Triangular SS has also been implemented in conjunction with reflectors. In their study, Arunkumar et al. (2010) researched the thermophysical parameters of a pyramid-shaped SS equipped with mirror boosters. The investigation involved measuring the thermal conductivity and dynamic viscosity; the values obtained were 29.64×10^{-2} W m^{-2} C^{-1} and 20.2×10^{-6} N s m^{-2}, correspondingly [61]. One notable discovery derived from the research is that the distillate output significantly increases from 1.52 to 2.9 L/m^2.day when using the mirror booster.

The overarching finding suggests that while triangular SSs may enhance productivity on some days, their year-round performance is not advantageous due to radiation losses.

2.3.4.2. Tubular stills

Tubular SSs are created to optimise the building process. In their study, Amimul et al. (2010) created a computational representation for a tubular SS. The model incorporated thermal and fluid dynamics phenomena and introduced new equations to account for the presence of humid air in addition to the usual equations. In a study by Zhili (2013), an experimental investigation was conducted using three tubular SS. The results indicated a direct relationship between the temperature and the output; as the temperature rises, the yield also increases [62]. Rahbar et al. (2015) completed an investigation analysing the convection heat transfer coefficient and water production using CFD. The results indicate an adverse correlation between the temperatures of the glass and water, affecting the system's overall effectiveness [63]

Regarding the material used for the cover, Amimul et al. (2012) performed trials on a cylindrical solar distillation apparatus outfitted with polyethene film. The researchers modified the trough arrangement and investigated the creation of a direct correlation between coefficients of heat transfer and mass transfer coefficients [64] Implementing a thin polythene sheet resulted in a notable enhancement of the mean cumulative coefficient of mass transfer due to condensation, reaching a value of 305 W/m^2K. Consequently, this improvement positively impacted production levels.

2.3.4.3. Hemispherical stills

Hemispherical covers have been employed to enhance the solar energy absorption of the SS. Arunkumar et al. (2012) empirically investigated a hemispherical solar still by comparing its performance with and without water flow over the cover. The study revealed a significant improvement in efficiency when water flow was present in a still, with a 42% increase compared to a still without water flow, which only achieved 34% efficiency [65]. The efficiency achieved by Aboul [74] in SSs with two or three basins with a pyramid lid is similar to the result obtained. When comparing the effectiveness of a hemispherical SS to Panchal's standard slope single-basin SS [34], The efficiency of the hemispherical SS is superior. The main conclusion about hemispherical sun stills is that increasing the water depth decreases output and effectiveness. Additionally, the rejuvenating impact enhances the amount of distilled water produced. Enhanced performance could be achieved by incorporating a reflector into the still, warranting more investigation.

2.3.4.4. Multiple slopes

Like hemispherical SSs, SSs with multiple slopes can harness sunlight from different angles. Several experiments were conducted on SS with dual inclinations to examine heat storage, explore different parameters, analyse the coefficient of heat loss, and consider the impact of orientation.

Parametric variation is crucial for optimising system efficiency. Researchers have examined several characteristics: architecture, functional, weather-related, and non-dimensional.

Rahul et al. (2011) formulated the equation of characteristic for a dual slope passive SS using non-dimensional variables, including immediate effectiveness. Subsequently, they performed experiments on the distillation apparatus under the environmental circumstances prevailing in Delhi. The results indicate that non-linear characteristic curves exhibit greater precision than linear characteristic curves [66]. Hanane et al. (2012) performed studies utilising an SS with a dual incline to desalinate saltwater. They investigated different operational parameters, including the temperature of water and glass. It was deduced that a more significant thermal gradient between water and glass resulted in increased output, producing an output rate of 4 L/m^2.day [67]

Rajamanickam et al. (2012) performed an experimental investigation using a dual slope SS to examine the influence of water level on the coefficients of internal thermal and fluid dynamics. The output of 3.07 L/m^2.day was higher at a depth of 0.1 m. However, this result contradicts the findings of Hanane (2012), who claimed that the double-slope SS produced 4 L/m^2.day [68]. Trad et al. (2013) performed an analysis of comparison of a symmetrical SS with a double slope and an asymmetrical SS. The study demonstrated that an SS positioned asymmetrically in a north-south alignment is more effective than a symmetrical one with a double-slope design [69]

The primary conclusions regarding the basic dual-incline solar distillation apparatus are that to maximise efficiency; it is crucial to maintain an optimal water depth and ensure that the still is asymmetrical with a north-south alignment.

2.3.4.5. Vertical stills

Most solar stills are horizontal, distinguished by width and breadth proportions that far surpass height dimensions. Vertical solar stills, distinguished by their elevation, have also been assessed. The examination of variables such as saline water input, output temperature of the still, ambient temperature, glass cover temperature, and still productivity revealed that performance depended on solar radiation, ambient temperature, and solar orientation [70]. Additionally, it was noted that the utilisation of a flat plate reflector resulted in an enhancement of productivity [71] figure 2.1 Nevertheless, implementing many divisions in a vertical SS has resulted in productivity of about 3.45 L/m^2.day [72], [73]. The SSs listed are, nevertheless, far more limited in scope than other varieties. Single-basin regenerative stills with Jute fabric; single-basin stepped stills; singular-basin triangular stills; dual-slope stills; triple- and dual-basin stills; and dual-slope stills with revolving cylinders and condensers are a few examples of SS designs. However, compared to the single-basin triangle SS with fan and mirror booster, the productivity of the single-basin greenhouse-type double-slope SS is higher. Vertical SSs usually have low outputs and are best suited for particular uses requiring a compact footprint.

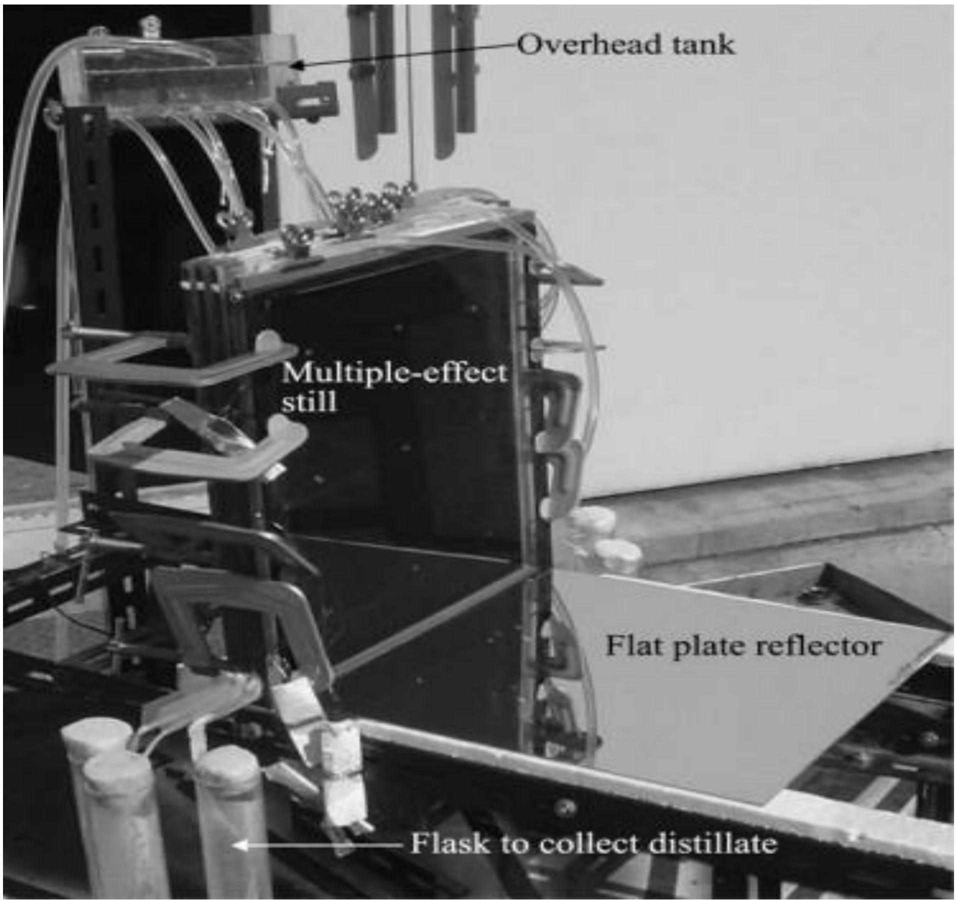

Figure 2.1: Snapshot of an experimental apparatus [71].

2.3.5. Multiple-effect passive solar stills

Using condensation heat, multiple-effect SSs can significantly improve efficiency by repeatedly evaporating water. Multi-effect SS can be categorised as either multi-wick or multi-basin.

2.3.5.1. Multi-wick solar stills

Sodha et al. (1981) examined an SS equipped with many wicks and covered with blackened, damp jute fabric to capture the maximum radiation from the sun. The evaluation relies on Dunkle's relationship and demonstrates a maximum efficiency of 34% for SSs with multiple wicks. This represents a 4% rise in efficiency compared to the type of basin still [75]

2.3.5.2. Multi-basin solar stills

Additional studies examine the efficiency and output of multi-effect SSs employing numerous basins. Sangeeta et al. (1998) used an abstract framework that relied on ordinary differential equations to ascertain that the optimal quantity of basins in a reversed absorber still is 7 [76].

Tanaka (2002) experimented with an SS that utilises multiple-effect diffusion coupling and is equipped with a reflector near the base to determine the impact of the inclination angle. The findings indicated that the distillate yield was 13% higher than a traditional SS [77], [78].

Hilal et al. (2004) compared one-basin and multiple-basin stills to assess their productivity. They found that the multi-basin still had higher productivity, which they attributed to the reduction of thermal dissipation in the bottom basin due to the presence of the top basin [79].

In Sebaii's (2005) study, the output of a three-basin SS was evaluated. It was determined that the daily productivity of the still exhibited an inverse relationship with the amount of water in each basin. The productivity reached a value of 12.6 L/m^2.day, surpassing that of any still, single or double [80]. The yield and efficiency of an SS with two plastic basins were meagre [81], [82].

Madhlopa et al. (2009) performed research to assess the influence of a condenser in a multi-effect steam system. They concluded that the final product of the altered still was 62% greater compared to that of the conventional still [83]

Utilising multi-effect SSs is advised to optimise profits. The drawback lies in the amplified maintenance endeavour and expenses commonly linked to the supplementary basins.

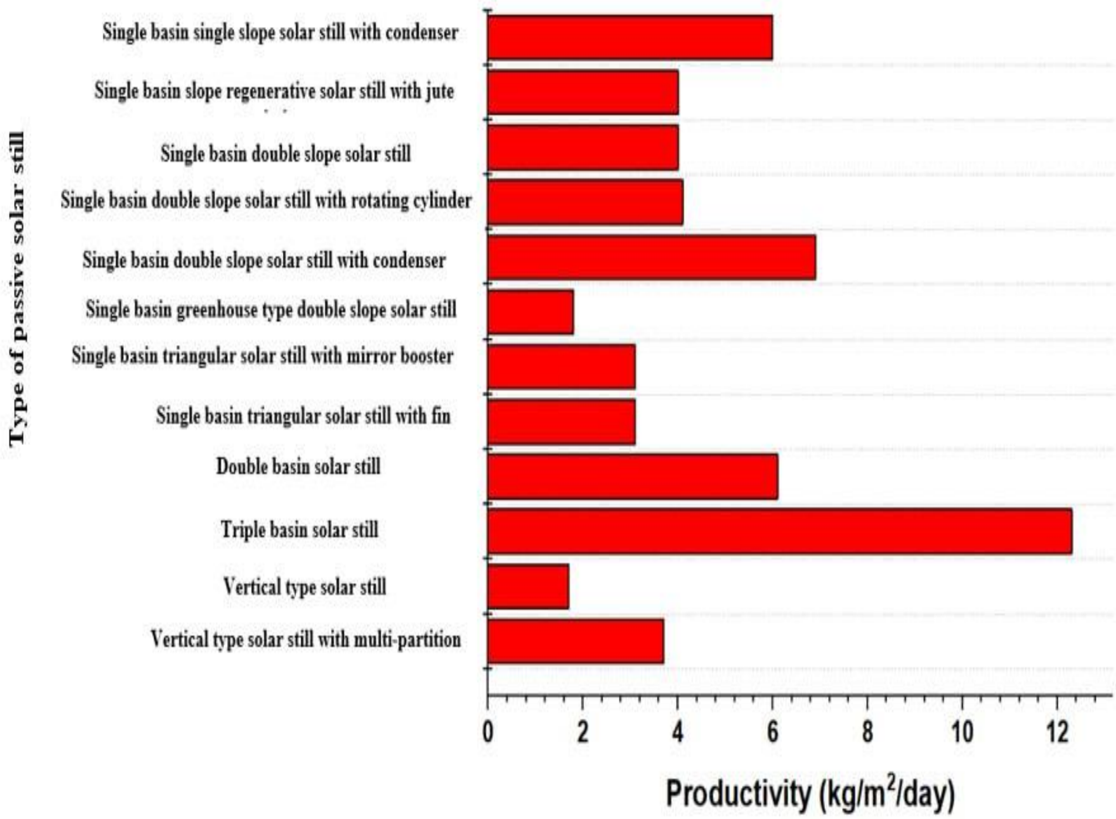

Figure 2.2: Productivity of different passive types SS [32].

2.4. Active Solar Stills

Active SSs include additional components, like solar collectors, condensers, coolers, or other devices to enhance efficiency. Generally, this equipment's operation necessitates using pumps, fans, or other energy-driven devices. In contrast to passive SS, active SS usually requires the utilisation of energy [32].

2.4.1. Solar collectors

External solar collectors may enhance or replace the outer layer of the still's collector. The primary material delineates the eventual use of several types of collectors [32].

2.4.1.1. Flat plate collectors

Using a collector increases the heat provided to the still, hence requiring an enhancement of the thermal energy generated to enable condensation. This process has been accomplished using a humidification tower and a condensation lid. Farhad et al. (2015) investigated the exergy and energy of a photovoltaic desalination system with a flat-plate solar collector. They conducted an experimental and theoretical analysis. Their findings revealed that extending the height of the humidification tower resulted in a decrease in exergy efficiency. Additionally, they observed that exergy efficiency increased when the ambient air temperature decreased, and the diameter of the tower decreased [84].

The performance of the SS may be influenced by its shape, similar to passive SSs, albeit in a distinct manner. Arslan et al. (2012) performed trials utilising different types of SSs, including circular box SS, rectangular box SS, and single tube SS combined with a solar collector. According to the evidence, the circular box SS demonstrates higher efficiency than a cylindrical tube or rectangular box [85].

Rajaseenivasan (2014) combined a flat plate collector with an altered SS that included Jute fabric and obsidian gravel. This modification aimed to improve the rate at which the still evaporates and its capacity to store heat, resulting in a 60% increase in distillate production compared to the conventional version [86].

Kabeel et al. (2012) performed an experimental and theoretical investigation of a stepped evaporator flat-plate collector for desalination applications. The study indicated that preheating the feed water slightly improves productivity but significantly decreases system efficiency [87].

Badran et al. (2007) devised an experimental configuration in a SSSS, including a mirror affixed to its interior and combined with a flat plate collector, resulting in a 36% increase in production [88]. However, Badran's SS with mirror [88]had lower productivity in contrast to an SS that has only one basin and one slope and utilises a flat plate collector [89], [90].

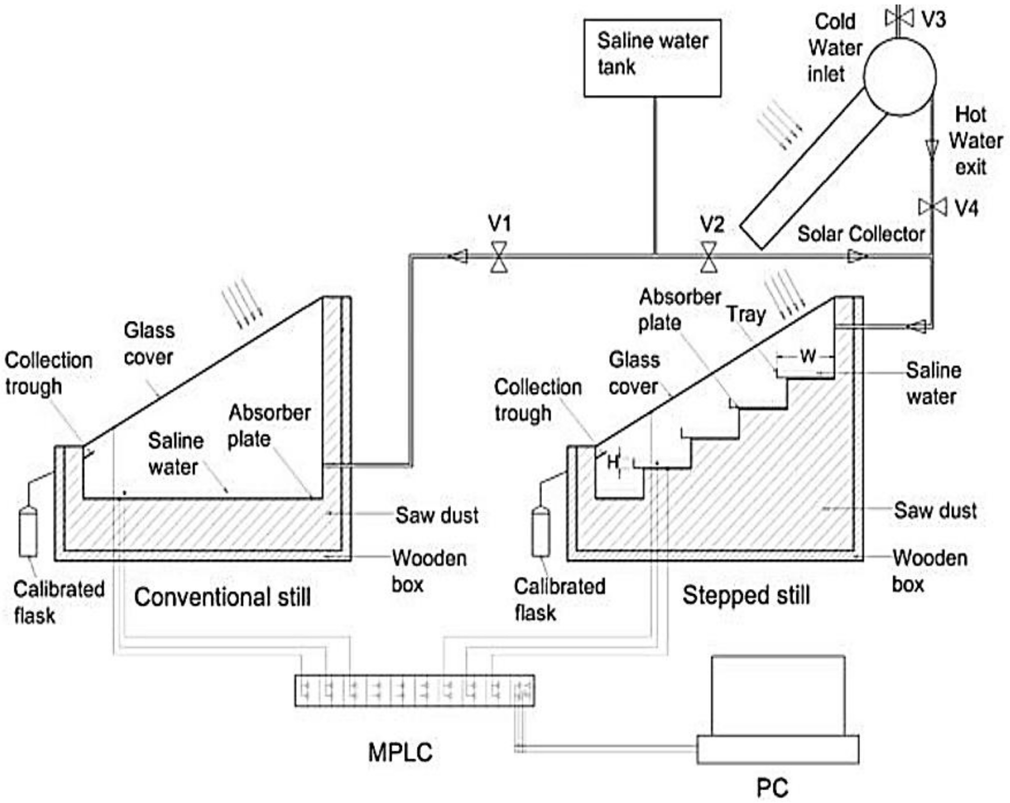

Figure 2.3: Visual representation of a stepped SS system with a single basin and a collector [87].

2.4.1.2. Evacuated tube collectors

The evacuated tube collector consists of several glass tubes including internal absorber surfaces. Shiv et al. (2014) constructed a single slope design SS with a forced-mode evacuated tube collector. The use of the combination model enhanced both temperature and yield. The attained energy efficiency was around 33.8% [91].

Eugenio et al. (2007) investigated the efficiency of a combined solar-still evacuated tube collector. The freshwater production for the integrated model was found to be lower compared to the conventional model [92].

2.4.1.3. Solar ponds

The solar pond has three separate strata: an upper convective layer, a non-convective layer, and a lower convective layer. The solar pond functions as a thermal energy reservoir. The integration of a solar pond with the still enhances the preheating of the supply water, hence augmenting profitability. Multiple studies aimed to assess the efficiency of solar ponds combined with distillation systems with various changes. Sebaii et al. (2011) investigated the thermal performance of an operational solitary basin solar still linked to a small solar pond. This approach shown improved productivity and efficiency compared to a conventional still. Furthermore, they determined that this gadget might serve as a source of boiling water for several purposes [93]

2.4.1.4. Concentrating collectors

A solar concentrator captures solar radiation over a wide surface and concentrates it into a smaller receiver area. This solar concentration will enhance the desalination process within the still. A study has examined the correlation between the velocity of the air, surrounding temperature, intensity of sunlight, and performance and production. In their research, Javad et al. (2011) experimented using concentrators linked to active SS. They discovered that the output of freshwater decreased as wind speed rose but rose with higher environmental temperature and radiation of the sun [94]

Zeinab (2007) conducted examinations on solar desalination. Utilising an altered configuration that involved a parabolic trough concentrator for solar energy. The results showed an improvement in productivity yield of approximately 18% [95]

Scientists furthermore experimented with concentrators equipped with thermal storage of energy. Arunkumar et al. (2013) constructed an SS connected to a concentrator, both with and without PCM. The productivity output experienced a 26% boost when using the PCM [96].

Farshad et al. (2010) examined an SS connected to a concentrator and a heat reservoir. The purpose of this system was to provide fresh water even during periods of low sunlight, such as at night or on cloudy days, during the overnight period, a water production of 12% was noted [97].

2.4.1.5. Air heating

Incorporating an air heater into the solar distillation system elevates the water temperature in the basin, hence accelerating the evaporation rate. Sampathkumar et al. (2012) examined several active solar systems and discovered that the incorporation of an air heater resulted in an output enhancement of up to 70% [98].

Abdullah (2013) carried out a test using an SS with a stepped design equipped with solar thermal energy storage and solar air heating to examine the impact of thermal preservation, the study revealed that the combination yielded a 53% increase in earnings compared to a traditional setup [99].

Zahaby et al. (2011) conducted an experimental study to enhance the efficiency of SSs equipped with air heaters. They achieved an efficiency of 77.4%, utilising a reciprocating water supply system [100]

Younes et al. (2022) provided an extensive review of the techniques for reducing the losses of the back walls in solar stills. In their thorough review, they discussed, clarified, and evaluated the state of the art about the many methods, such as spinning wicks, vertical wicks, drums, trays, discs, and so on, employed to lower losses in the rear wall of solar distillers. The relevance of rotating parts was illustrated by a variety of outputs, comprising the following: drum distiller (9.22 L/m²/d & 350%), moving wick solar still (9.17 L/m²/d & 315%), vertical disc distiller (16.5 L/m²/d & 617.4%), and vertical wick distiller (7.2 L/m²/d & 154%) [101].

2.4.1.6. Water heating

In their study, A.S. Zedan et al. (2015) examined techniques to enhance the efficiency of solar stills, which are vital in regions with few clean water supplies. Their research included comparing a traditional solar still and an altered version with a flat plate collector for preheating and a vacuum pump for reducing pressure. The results indicated that preheating led to a productivity gain ranging from 27.7% to 29.3% while decreasing pressure using the vacuum pump resulted in a productivity enhancement ranging from 21.8% to 23.9%. These enhancements are incredibly efficient at high elevations, where reduced boiling points enhance effectiveness [102].

V.S. Winstor Jebakumar et al. (2021) assessed the efficiency of passive and active solar stills in Coimbatore, Tamil Nadu. The study revealed that active solar stills, equipped with a spiral collector for preheating, significantly outperformed passive stills. The active still yielded 3.2 kg/d compared to 1.5 kg/d from the passive still, demonstrating higher efficiency. The optimal water depth in passive stills was found to be 1 cm. Factors like basin temperature, solar intensity, and wind velocity influenced productivity, with the active still showing a 42.7% efficiency versus 32.57% for the passive model. Despite its higher cost, the active solar still's increased productivity makes it a more practical option for water desalination [103]

A.S. Abdullah et al. (2023) evaluated the performance of modified sun stills (MSS) compared to standard solar stills (SSSS) for water distillation. Their investigation demonstrated that MSS fitted with internal reflectors (MSS-IR) and phase change materials (PCM) significantly boost productivity. MSS-IR-PCM achieved 115% better productivity than SSSS, with PCM enhancing production by 34%. The addition of silver nanoparticles to PCM further enhanced productivity by 8%. Economically, MSS-IR-PCM generated distilled water for \$0.0235/L, making it more cost-effective than SSSS at \$0.03/L[104].

Many previous works have attempted to simulate the solar distillation process to investigate the ability to increase the efficiency of solar stills; this may include changing the geometry design or the material type of the solar still basin. Vaibhav Rai Khare et al. (2016) constructed a computational fluid dynamics (CFD) model of a single inclined solar still using ANSYS FLUENT software. They performed transient state simulations verified by experimental data collected from Jaipur's climate conditions. Parametric assessments, which examined various basin materials and water depths, optimised solar productivity. The study confirms the CFD model's precision, showing increased thermal efficiency in solar stills between 16:00 and 17:00 hours and greater efficiency when reducing water depth [105]

Mahmoud S. El-Sebaey et al. (2020) made a computational fluid dynamics (CFD) simulation for a solar still with a basin design in Egypt. They showed that it could accurately predict performance in several locations and environmental conditions. The model showed slightly higher simulated productivities at 1.982 L/m^2 compared to 1.785 L/m^2 experimentally, with a 2 cm water depth. The daily simulated efficiency was marginally higher at 16.79%, compared to 15.5% under specific weather and solar conditions. The model demonstrated potential in analysing the performance of intricate solar still designs, indicating its applicability to other cases beyond the one under investigation [106].

In areas with water scarcity, Hameed et al. (2022) aimed to improve the efficiency of solar stills in single-slope, single-basin systems for clean drinking water. Hameed *et al*. (2022) used the CFD technique to investigate an innovative methodology that involved reconfiguring absorbent bases with stainless steel geometries to increase surface area for evaporation. Results show that changing size has significantly improved evaporation rates and overall productivity. The cones were identified as the geometry with the highest productivity, resulting in a total freshwater production of 4.13 kg/m^2 with an enhancement ratio of 38.2%. The study underscores the importance of CFD in enhancing solar still designs and provides valuable insights for progress in freshwater generation using solar energy [107]

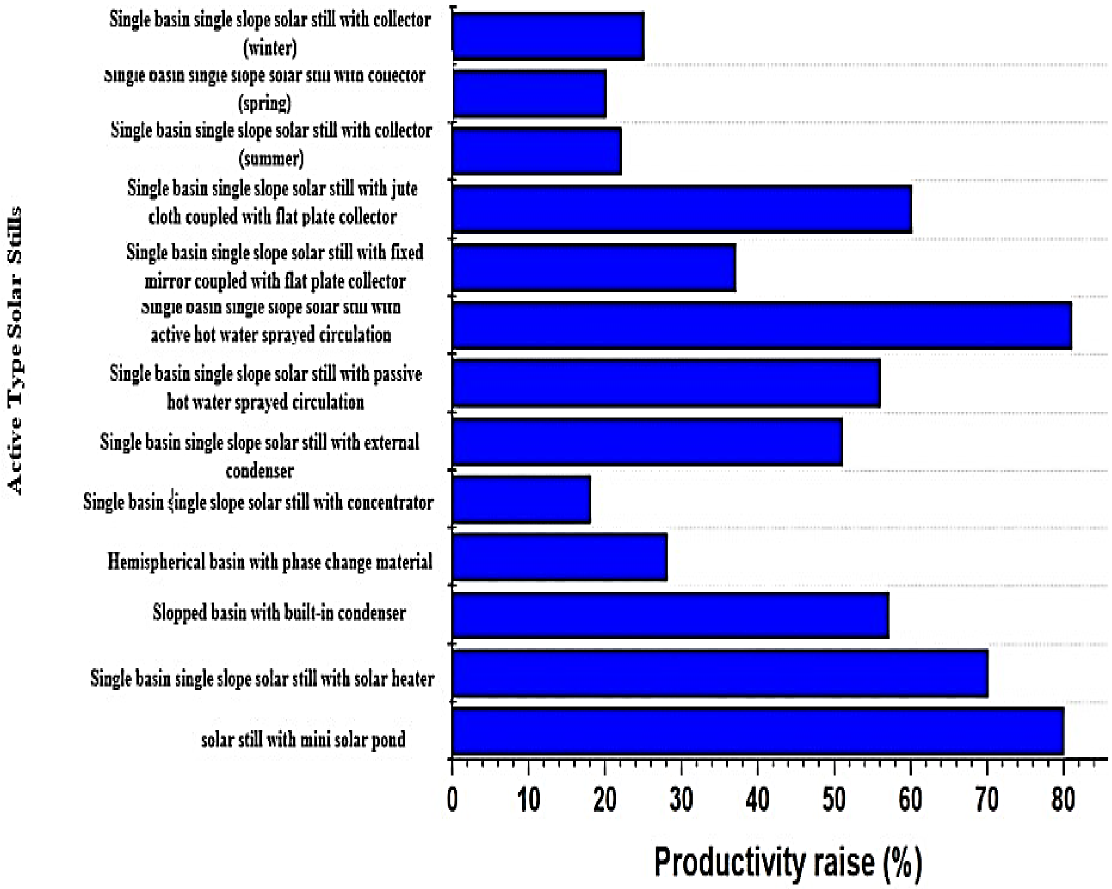

Figure 2.4: Enhancement of Productivity through Different Active SS Types [32].

Table 2.1: Presents an overview of the solar stills examined in this work, including their primary categorisation, changes, the percentage increase in production resulting from the adjustments, and the ultimate daily productivity attained (where data is available).

	Researchers	Categories	Geographical Position	Percentage rise in production (%)	Cumulative Productivity (L/m^2/day)	Modifications, Observation
1	Sodha et al. (1981) [75]	Passive with multiple effects	New Delhi, India	34	2.5	Various wick types , All surfaces exposed to sunlight will remain continuously damp in this arrangement.
2	Sebaii et al. (1998) [73]	Unconventional	Tanta, Egypt		4.2	Vertical SS , A minimum of 3.5 m^2 is optimal for vertical SS.
3	Tanaka et al. (2002) [77]	Passive with multiple effects	Fukuoka, Japan	13		Utilising a reflector to achieve various effects , The ideal inclination angle for a multi-effect solar still is 23°.
4	Hilal et al. (2002) [79]	Passive with multiple effects	Muscat, Oman		6	Dual and single-effect , Double-effect SSs provide a superior output level in comparison to single-effect SSs.

5	Cappelletti (2002) [81]	Passive with multiple effects	Foggia, Italy		1.8	Plastic, **The** yield rate and productivity might significantly increase, rendering it superfluous.
6	Hiroshi et al. (2005) [72]	Passive with multiple effects	Fukuoka, Japan		34.5	Various effects of using mirror , **Productivity** based on forecasts is 50% more than productivity based on tests.
7	Badran et al. (2007) [88]	Active	Amman, Jordan	36		A flat plate collector with a mirror, **The** productivity was markedly worse in comparison to the solar system use a flat plate collector.
8	Zeinab et al. (2007) [95]	Active	Cairo, Egypt	18		A parabolic trough with only one inclination, **the** system's productivity surpasses that of conventional stills.
9	Madhlopa (2009) [83]	Multi-effect passive solar stills	Blantyre, Malawi	62		Utilizing a condenser achieves multiple effects, **These** sorts of SS provide enhanced production at the penalty of elevated maintenance expenses.

10	Hiroshi Tanaka (2010) [40]	Passive	Fukuoka, Japan	48		Interior and exterior reflectors , **The** incorporation of both interior and exterior reflectors demonstrated more efficiency than the exclusive use of an interior reflector.
11	Kalidasa et al. (2010) [46]	Singular effect passive	Tamil Nadu, India			Diverse wicks , **A** more effective thermal storage medium than red brick fragments, cement concrete fragments, washed stones, and iron debris.
12	Arunkumar et al. (2010) [61]	nontraditional	Tamil Nadu, India		2.9	Triangular configuration with reflective amplifier , **The** decreased yearly production is attributable to radiation losses.
13	Tabrizi et al. (2010) [97]	Active	Zahedan, Iran	75		Using a sandy thermal storage , **Distillate** yield was attainable even at night by the use of a heat reservoir.
14	Panchal et al. (2011) [34]	Singular effect passive	Ahmedabad India		3.8	The basin liner is made of aluminium SS and galvanized iron, **The** employment of

						galvanised iron type SS led to enhanced output owing to improved heat conductivity.
15	Boubekri et al. (2011) [42]	Singular effect passive	Constantine Algeria	72.8		Solar reflectors, **The** ideal output requires an inclination angle of under 25°.
16	Mohammad Dashtban et al. (2011) [53]	Passive	Zahedan, Iran		6.7	Using PCM in a cascade solar system , **The** still's efficiency was improved with the integration of PCM.
17	Rajamanickam et al. (2012) [68]	Passive with a singular effect	Muscat, Oman	20		A cooling system consisting of an individual basin with a dual glass cover, **The** efficiency was improved by preheating the water and then chilling the glass cover.
18	Amimul et al. (2012) [64]	Unconventional	Selangor, Malaysia		5	Tubular SS, **The** temperature difference between the water and the glass cover dictates the pace of water production. The heat transmission coefficient for evaporation exceeds that of convection.

19	Sampathkumar et al. (2012) [98]	Active	Tamil Nadu, India	70		Air heater , **The** elevation of water temperature in the basin immediately connects with an augmented rate of evaporation.
20	Arslan (2012) [85]	Active	Yozgat, Turkey		12.37	Open cycle mode with multiple active stills , **In** comparison to rectangular boxes and individual tubes, the circular box SS generates a higher yield.
21	Kianifar et al. (2012) [58]	nontraditional	Mashhad, Iran	20	3.14	Triangular , **Enhanced** exergy efficiency is attained at reduced water depths.
22	Hanane et al. (2012) [67]	Unconventional	Tipaza, Algeria		4	Multiple inclines , **The** SS must possess an asymmetrical configuration aligned from south to north.
23	Pankaj et al. (2013) [43]	Passive	Allahabad, India	68	2.0	Singular slope with permeable absorbers , **The** porous absorber's little thermal inertia facilitates a greater working temperature.
24	Arunkumar et al.(2013) [96]	Active	Tamil Nadu, India	26	4.4	A concentrator that is connected to copper balls filled with PCM,

						This study uses paraffin as a PCM.
25	Abdullah et al.(2013) [99]	Active	Tanta, Egypt	48		Stepped solar **, The** use of a cooling cover enhances the efficiency of SS.
26	Shiv et al. (2014) [91]	Active	Delhi, India		3.9	Forced mode operation of an evacuated tube collector **, To** get optimal results, sustain a water depth of 0.03 m and a mass flow rate of 0.06 kg/s.
27	Rajaseenivasan et al. (2014) [86]	Active	Tamil Nadu, India	60	5.68	A flat plate collector integrating jute fabric and black pebbles**, The** evaporation rate and the heat capacity of the still both augmented.
28	Shiva et al. (2014) [108]	Active	Tehran, Iran		5.12	Stand-alone point focus **, Productivity** is uninfluenced by air temperature or water salinity.
29	Manivel et al. (2014) [44]	Passive	Tamil Nadu, India		4.5	Heating system for roofs **, The** elevation in feed water temperature due to roof heating prolongs the evaporation and condensation process for many extra hours into the night.

30	A. S. Zedan et al. (2015) [102]	Active	Abha, Saudi Arabia	28.5 22.85		Preheating Water and Vacuum Pump , **The** combination of preheating the inlet water and reducing pressure inside the still significantly enhances productivity.
31	Vaibhav R. K. et al. (2017) [105]	Passive	Jaipur, India	32 for 5 L 29 for 10 L 27 for 15 L		Use of CFD to model and optimize the performance of a single slope solar still, **The** study focuses on numerical simulations for performance improvement, such as optimized basin design, better heat retention, and increased productivity. Increased distillation rate due to modifications can be highlighted.
32	Mahmoud S. El-Sebaey et al. (2020) [106]	Passive	Sheben El-Kom, Egypt	11.04	1.982 Simulated 1.785 Experiment	Experimental analysis combined with CFD modelling for a conventional basin-type solar still, **The** study compares experimental results with CFD predictions, highlighting

						improvements in thermal performance and distillation efficiency. Optimization may lead to better heat management and water evaporation rates.
33	V.S. Winstor J. et al. (2021) [103]	Passive and Active	Tamil Nadu, India	113	1.5 for passive 3.2 for active	Passive: Basin is painted black for better heat absorption. Depths of saline water (1, 2, and 3 cm) are tested, with 1 cm yielding the best results. Active: Includes a spiral copper collector for preheating inlet water, **Optimal** water depth of 1 cm results in higher productivity for both systems. Preheating in the active still enhances the evaporation and condensation processes. Wind velocity and solar intensity positively influence the productivity of both stills. The active solar

						still achieves higher efficiency due to better heat transfer and evaporation rates.
34	Shahin Shoeibi et al. (2021) [49]	Passive SS	Tehran, Iran	55.8 and 49.5	1.3833	Utilizing anthracite media in saline water, **The use** of porous media and Nano-coated copper pipes in solar desalination markedly enhanced water productivity, energy efficiency, environmental advantages and financial gain.
35	A.S. Abdullah et al. (2023) [104]	passive	Kharj, Saudia Arabia	115	6.665	Use of two spiral copper water heating coils, an internal reflector (MSS-IR), and a Nano-Phase Change Material bed enhanced with silver nanoparticles (MSS-IR-PCM-Ag), **These** modifications increased evaporation rates and distillate production, with the enhanced PCM further boosting efficiency. Overall, the modified solar still

						outperformed the conventional design, offering a more effective solution for water distillation.
36	Hassanain G. H. et al. (2023) [107]	passive	Najaf, Iraq	38.24	4.13	Use of different shapes and sizes of geometries were tested to enhance the evaporation process in a conventional single-slope single-basin solar still, **Modifying** a conventional solar still with stainless steel basin plate geometries, particularly using cone-shaped enhancers, is a practical, low-cost, and effective way to improve water productivity.
37	Current Study (2024)	passive and active	Najaf, Iraq	75.57	9.99	Utilising absorbing materials and a preheating water unit with stepped solar still**, The** use of a combination (4-cm-thickness crushed marble and solar heater with stepped solar still) has significantly

						enhanced the productivity and efficiency of the solar still.

2.5. Research gap: In this study, different absorbing materials were utilized in the solar still basin to enhance water productivity. Readily available and cost-effective materials such as marble (solid and crushed with average sizes ranging from 0.5 to 4 cm) and leather were employed. Both materials demonstrated improvements in water productivity compared to the solar still without absorbing materials. Notably, crushed marble of 4 cm size achieved the highest enhancement in productivity, showcasing its effectiveness as an absorbing material.

Chapter Three

Mathematical Model and Numerical Simulation

3.1. Introduction

This chapter is structured into two primary sections: the initial section comprises the mathematical equations that dictate the heat transmission within the solar water distillation system, and the second section provides a comprehensive explanation of the ANSYS constitutive numerical model. This research aims to quantitatively analyse the temperatures of water and vapour inside the distiller, together with the temperatures of the base and glass cover of the solar distiller.

3.2. Mathematical Model

This section presents the governing partial differential equations that describe the thermal properties of phase transition materials within the solar distillation system.

3.3. Governing Equations

The governing equations pertinent to the current case study are as follows [109]

The Equation of Continuity (The Equation of mass conservation):

$$\frac{\partial \rho}{\partial t} + \nabla . (\rho u) = 0 \qquad (3-1)$$

The Equation of Navier-Stokes (The Equation of Momentum Conservation):

$$\rho \left(\frac{\partial u}{\partial t} + u . \nabla u\right) = -\nabla P + \nabla . (\mu(\nabla u + (\nabla u)^{T})) + F + \rho g \qquad (3-2)$$

Equation of Energy Conservation:

$$\rho C_P \frac{\partial T}{\partial t} + \rho C_P u.\nabla T = \nabla.(k \nabla T) + Q \qquad (3-3)$$

Equation of Concentration:

$$\frac{\partial c}{\partial t} + \nabla cu = D_{ab} (\nabla^2 c) \qquad (3-4)$$

D_{ab}: Mass diffusivity of water vapour

C: Concentration of water vapour

The governing equations for several regional models may be described as following [110] [111]

3.4. Glass Cover

The energy equation governs the state of the transparent material, which is subjected to solar radiation, inducing heat convection. Thus, the numerical simulation utilizes the following thermal and energy parameters:

$$m_g\ c_p \left(\frac{dT_g}{dt}\right) = Q^{\circ} - Q_{r,\,g\_a} - Q_{c,\,g\_a} + Q_{ev} + Q_{c,\,w\_g} + Q_{r,\,w\_g} \qquad (3-5)$$

Primary thermal source (Solar radiation):

$$Q^{\circ} = A_G \grave{\alpha}_g\ I \qquad (3-6)$$

Where

$$\acute{\alpha}_g = (1 - R_G)\,\alpha_G \qquad (3-7)$$

The thermal radiation emitted by transparent material to the surrounding environment:

$$Q_{r,g_a} = \varepsilon_G \sigma\,(T^4{}_{amb} - T^4{}_G) \qquad (3-8)$$

Heat convection from glass to the surrounding environment:

$$Q_{c,g\_a} = h\,(T_{amb} - T_G) \qquad (3-9)$$

$$h = 2.8+3v \qquad if\, v \leq 5\ (m/s) \tag{3-10}$$

$$h = 2.8+3.8v \qquad if\ v > 5\ (m/s) \tag{3-11}$$

Condensation of water vapour (on the inside surface of glass):

$$\mathrm{Q_{cond}} = \mathrm{L_{ev}}.\mathrm{M_{ev}} \tag{3-12}$$

M_{ev}: mass flow rate of water (kg/s)

3.5. Basin Water

The governing equation of energy for water from a basin is predicated by the upcoming expression:

$$\mathrm{m_w}\, C_{pw}\, \left(\frac{\mathrm{dT_w}}{\mathrm{dt}}\right) = Q^{\circ} - Q_{r,\,w\_g} - Q_{ev} + Q_{c,\mathrm{b}\_w} - Q_{c,\,w\_g} \tag{3-13}$$

Source of heat

$$Q^{\circ} = A_w\, \acute{\alpha}_w\, \mathrm{I} \tag{3-14}$$

$$\acute{\alpha}_w = (1 - \mathrm{R_G})(1 - \alpha_\mathrm{G})(1 - \mathrm{R_w})\, \alpha_\mathrm{w} \tag{3-15}$$

Radiation of heat from water to transparent material:

$$Q_{r,w\_g} = \varepsilon\sigma(\mathrm{T_{G,i}}^4 - \mathrm{T_w}^4) \tag{3-16}$$

$$\varepsilon = \frac{1}{\frac{1}{\varepsilon_\mathrm{w}} + \frac{1}{\varepsilon_\mathrm{G}} - 1} \tag{3-17}$$

Evaporation of heat from the water to the glass:

$$\mathrm{Q_{ev}} = -\,\mathrm{L_{ev}}\ .\ \mathrm{M_{ev}} \tag{3-18}$$

3.6. Absorber Plate

$$m_b\, c_{pb}\, \left(\frac{dT_b}{dt}\right) = Q^{\circ} - Q_{c,\, b\_w} - Q_{sides} \qquad (3-19)$$

Source of heat

$$Q^{\circ} = A_b\, \acute{\alpha}_b\, I \qquad (3-20)$$

$$\acute{\alpha}_b = (1 - R_G)(1 - \alpha_G)(1 - R_w)(1 - \alpha_w)(1 - R_b)\, \alpha_b \qquad (3-21)$$

Heat transmission from the base and sidewalls of the container to the environment:

$$Q_{sides} = U\, (T_{amb} - T_b\,) \qquad (3-22)$$

$$U = \frac{k_{ins}}{t_{ins}} \qquad (3-23)$$

Where k_{ins}: Thermal conductivity of insulation material, t_{ins}: the thickness of insulation material

Yield is calculated from condensation rate as follows [112]

Instantaneous productivity of distillate (kg/m² - hr) = $\dot{m}_c \times 3600$/Basin area (3−24)

3.7. Solar Still Efficiency

The efficiency of solar still can be calculated as follows [113]

$$\eta = \frac{\boldsymbol{P} \times H_{vap}}{I_{sun} \times A \times t} \qquad (3-25)$$

Where η: *is the efficiency, P: Productivity in Kg,* H_{vap}: *The heat of vaporisation of water J/Kg*

I_{sun}: *Solar intensity W/m², A: Collector area = 1.179 m², t: Time sec,* H_{vap}: *can be expressed as* [113]

$$H_{vap} = 10^3 * [2501.9 - 2.40706T_w + 1.192217 * 10^{-3}T_W^2 - 1.5863 * 10^{-5}\, T_W^3] \tag{3–26}$$

3.8. Numerical Simulation

This section overviews the ANSYS software that simulates heat transfer in solar water distillation systems. It includes details on the software's construction phases, such as the geometry and mesh creation. The solver utilised in the present study is Fluent, a component of ANSYS (Version 18.2). The reason for selecting (Fluent) is its ability to provide more accurate results that closely match the experimental data. Furthermore, it can solve the equations of conservation for (energy, mass and momentum) in various scenarios, including two or three-dimensional flow, steady or unstable state, and other situations. Moreover, it has been employed in different research domains, including the science of heat transfer (the current area of study). The process of producing the ANSYS programme involves several steps: first, creating the geometry of the test model; then, generating the mesh; next, forming the setup; and finally, displaying the results.

3.9. Problem Statement

This study will use a practical numerical CFD to simulate the evaporation-condensation process and productivity of SSSS. The model will try to approach the experiments, and the results will be compared with previous published work. The first comparison pertains to the study conducted in the climatic circumstances of Jaipur, India [105] and the other relates to the survey conducted in Sheben El-Kom, Egypt [106]. Various new absorbent materials will be used in the solar still basin, including black marble, crushed black marble of varying sizes (0.5 cm to 4 cm), and natural black leather. The optimal material for achieving the highest productivity from the SSSS will be determined. Additionally, experiments will be conducted to validate the CFD model.

3.10. Geometry and Meshing

The ANSYS Workbench generated a 3D model of the traditional basin-style solar still. Since there are no curved surfaces in the geometry of the basin-type solar PV, the cut-cell meshing technique proved the most suitable for the scenario. The mesh quality was checked regarding skewness, orthogonal, and aspect ratio and found the final mesh quality to be 0.97; it's important to note that the maximum mesh quality is 1, Figure (**3. 1**)

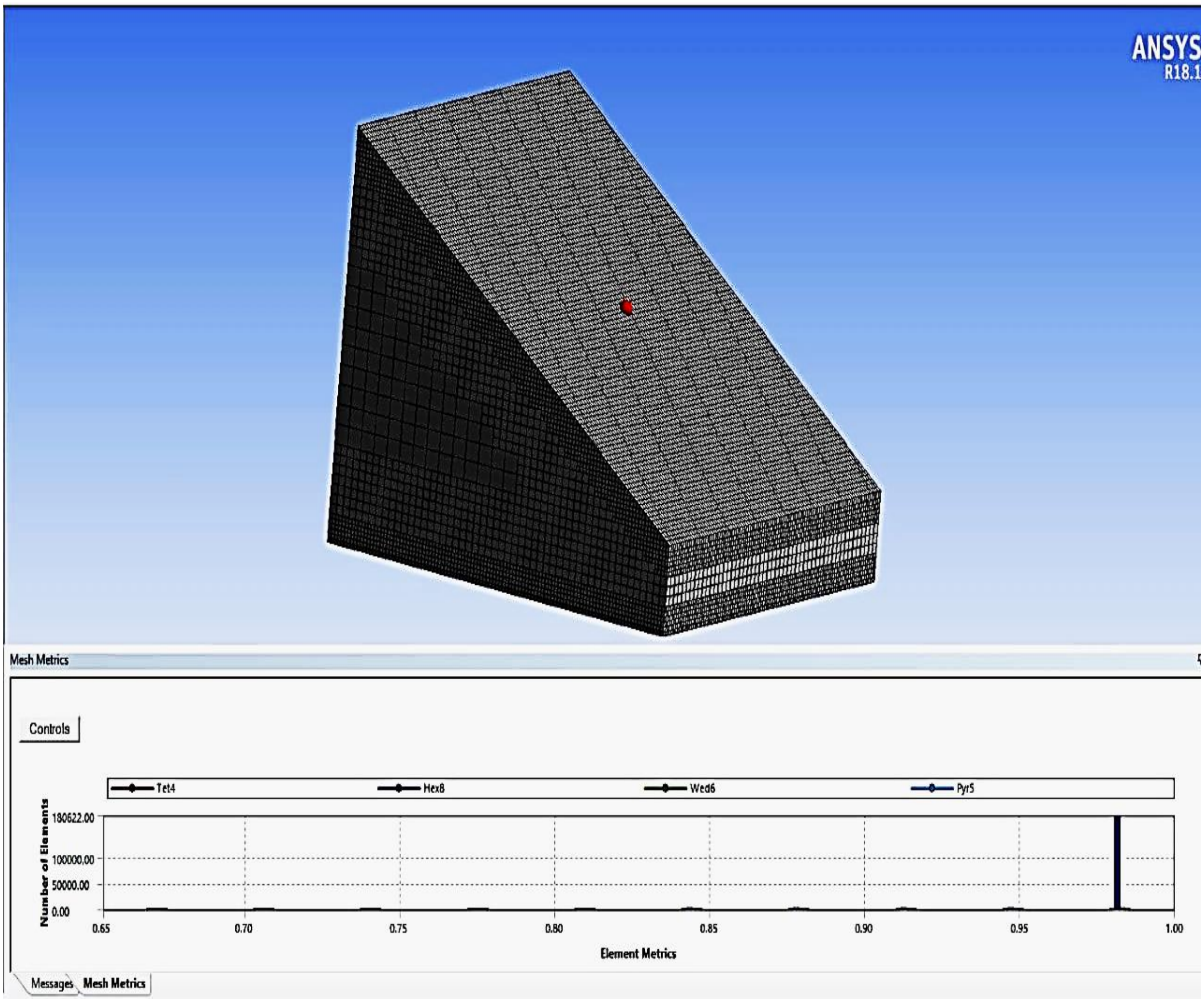

Figure 3- 1 Mesh quality for the CFD model of SSSS

The mesh on the basin and glass cover Was refined using the face sizing technique, with a mesh size of 1 cm and a growth rate of 1.1, to align with the physics of evaporation-condensation and meet the convergence criteria for the energy equation, velocity, and continuity.

This method could produce correct results with minimal computation time using ANSYS. A mesh study was conducted to assess the mesh independence and identify the optimal meshing refinement (Figure **3. 2)**

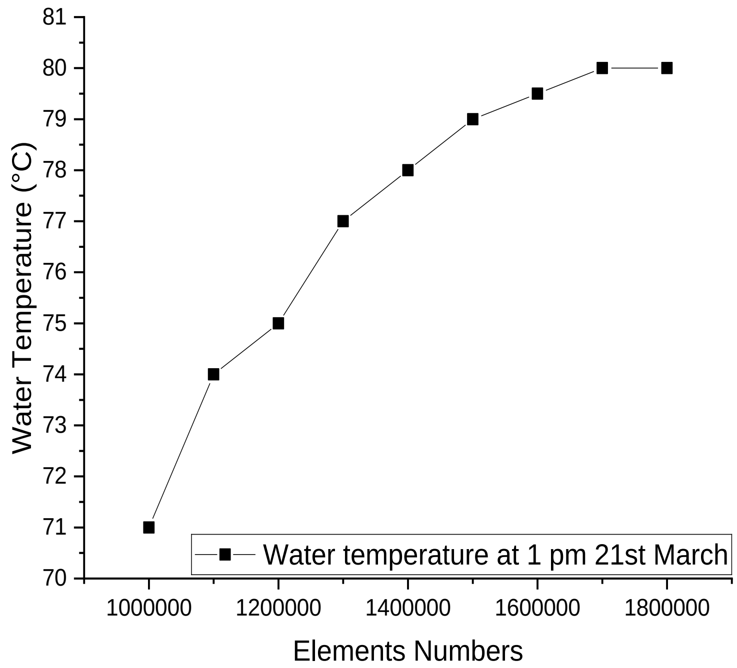

Figure 3- 2 Mesh independency study for the CFD model of SSSS

The absorber plate (basin) was selected for comparison with the mesh refinement and determined the mesh refinement's stopping point based on the stability of this temperature. Given the complexity of the problem, there were 1,735,234 total nodes and 1,678,459 total elements within the mesh domain. The still basin, front and back walls, side walls, and transparent cover was designed using the designated selection function. Figure **3. 3** shows the geometry and mesh generated for the CFD modelling. The mesh is finer at the glass cover and basin to catch the physics of evaporation-condensation phenomena.

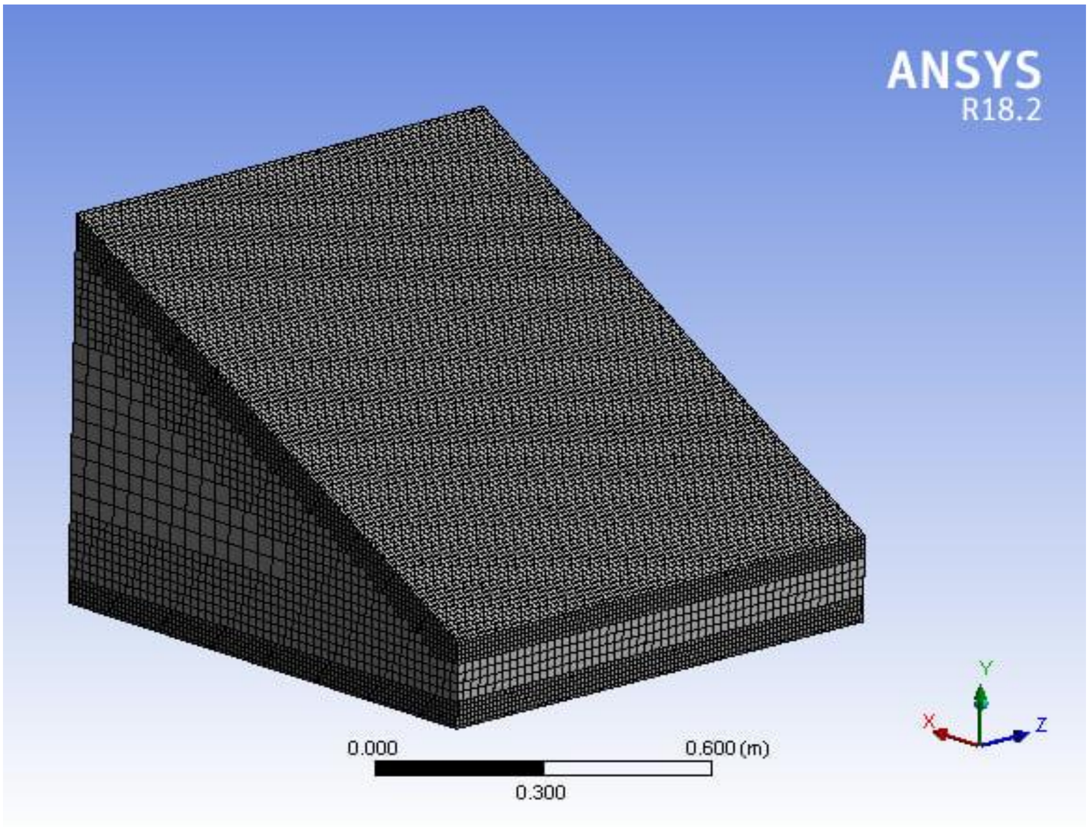

Figure 3- 3 Geometry and meshing for the CFD model of SSSS

3.11. CFD model assumption

Some presumptions have to be taken into account when building the CFD simulation modelling, and they are as follows:

1. Only free convection was considered, and the effect of wind velocity was disregarded due to the low ambient wind velocity.
2. Only film condensation type was occurring.
3. The still contained no source of thermal energy generating.
4. The system did not experience any leaks. Furthermore, the still's side and bottom walls were insulated, which made them adiabatic.

5. The inflow and outlet saltwater masses barely conveyed any heat, and the water level within the basin was maintained constantly.
6. Despite the low-temperature variation, the walls' physical characteristics were considered constant.
7. The water in the solar still's basin and glass cover did not have different temperatures. The density, specific heat, and viscosity of water liquids were considered functions of temperature, as shown in appendix (A). Glass thermal properties are shown in Table 3.

Table 3. 1 Thermal properties of marble, natural leather and glass

Material	Density (kg/m^3)	Thermal Conductivity (W/m.K)	Specific heat (J/kg.K)
Black Marble	2500-2700	3-4	880
Natural leather	1400-1500	0.4-0.6	1500-1700
Ordinary glass	2500	1	800

3.12. Boundary Conditions

1) Absorptivity and Transmissivity of the Glass Cover

Solar radiation is absorbed by the absorber plate, raising the water's temperature.

2) Initial Water Level for Modelling

The solar still's starting water level was taken to be 1 cm.

3) Volume Fractions of Water and Air

The volume fractions were 0.1 and 0.9, respectively.

4) **Experimental Data Collection**

Hourly data was used to determine the radiation dose and the initial water temperature.

5) **Boundary Conditions for Equations**

Proper boundary conditions were applied at each boundary to solve the continuity and momentum equations.

6) **CFD Simulation Duration**

The simulation ran for ten hours due to computer time constraints and many time steps.

7) **Assumptions for One-Hour Intervals**

It was assumed that water and glass temperatures, as well as solar radiation received by the basin, were determined using a solar calculator under ideal weather conditions.

8) **Boundary Conditions for Surfaces**

Constant temperature boundary conditions were applied to the collecting surface, bottom, and glass.

9) **Simplifying Assumptions**

a) Glass, water, and air all have consistent Thermophysical properties during the process.
b) The glass, the solar still basin's walls, and its surroundings all have perfect thermal contact.
c) The solar still wall's temperature is considered equal and unaltered.

10) **Simulation Time Period**

The trial ran from 8:00 a.m. to 5:00 p.m.

11) Hourly Boundary Conditions

The average temperature served as the boundary condition for each 1-hour time interval.

12) Solar Intensity Calculations

The absorption factor and the emissivity of the bottom, glass, and water were used for these calculations.

13) Heat Transmission Coefficient for Sidewalls

It was determined and maintained throughout the procedure.

14) Boundary Conditions for Phases

a) A free-slip boundary condition was applied for the gas phase.
b) A no-slip wall boundary condition was used for the liquid phase

3.13. CFD Model set-up

The following steps were taken to simulate evaporation-condensation in the solar still using the FLUENT solver: The General Solver type was configured as Pressure-Based with Velocity Formulation set to Absolute and Time specified as Transient in the ANSYS setup tree. The Gravity option was activated and set at (0, -9.81 ,0) m/s^2 for (X, Y, Z), respectively. Subsequently, the multiphase model was established as a Volume of Fluid with three Eulerian phases, and the Volume Fraction parameters were formulated Implicitly with a Volume Fraction Cutoff at 1e-06. The Interface Modelling type was set to Sharp. The three phases are arranged: (air-water-vapour) and (Primary-Secondary-Secondary). Additionally, the Phase Material is assigned as (air-water-liquid-water-vapour) respectively, with their properties detailed in Table 2.

Table 3. 2 Three phases properties

	Air	**Water-liquid**	**Water-Vapor**
Density (Kg/m^3)	Constant 1.225	Piecewise-liner	Incompressible-ideal-gas
Cp Specific Heat (j/kg.k)	Constant 1006.43	Constant 4082	Piecewise-polynomial
Thermal Conductivity (W/m.k)	Constant 0.0242	Constant 0.6	Constant 0.0261
Viscosity (kg/m.s)	Constant 1.7894e-05	Constant 0.001003	Constant 1.34e-05

The specific properties mentioned for the Secondary phases are Molecular Weight (kg/km), Standard State Enthalpy (j/kg.mol), Reference Temperature (°C), Absorption coefficient (1/m), Scattering coefficient (1/m), Scattering Phase Function, and Refractive Index.

Regarding phase interactions, there are two mass transfer mechanisms to consider: one from water to vapour and the other from vapour to water, which can be referred to as the evaporation-condensation mechanism. The Surface Tension Force was configured to Continuum Surface Force, and the wall Adhesion option was activated.

The coefficients for surface tension (dyne/cm) for water to air, vapour to air, and vapour to water are all consistently set at 73. The energy option has been activated to enable the energy equation. The K-epsilon (2 eqn) viscous model and Standard Wall Functions for Near-Wall Treatment were utilised. Additionally, other model constants, including Cmu, C1-Epsilon, C2-Epsilon, TKE Prandtl

Number, TDR Prandtl Number, Energy Prandtl Number, and Wall Prandtl Number, have been established.

The Radiation Model has been configured as Rosseland, while the Solar Load Model has been set to Solar Ray Tracing. The option to use the direction computed from the Solar Calculator has also been activated for the Sun Direction Vector (X.Y.Z).

The global position coordinates are 32.00°N 44.33°E, located explicitly in Najaf city, Iraq. The designated Time zone is set at 3, with the Starting Date and Time established as March 21st at 1 PM. The Solar Irradiation Method is defined as Fair Weather Conditions with a corresponding Sunshine Factor of 1.

The remaining options, including Heat Exchanger, Species, Discrete Phase, Solidification and Melting, Acoustics, and Eulerian Wall Film, have all been deactivated.

In the setup tree, the third option pertains to Materials categorised as Fluids (water vapour, water liquid, air) and Solids (granite, glass, wood, aluminium). These materials are defined by their respective chemical formulas and properties.

The region adaptation from the "Setting Up Domain" was executed in a hexagonal shape, which was selected from the "Region Adaptation" box along with other options, including the input coordinates (X, Y, Z) set to (0.1, 1, -1) respectively. Upon activating the option, a specific number of cells will be designated for refinement. Subsequently, upon selecting "manage" and "display", the hexagonal shape will be visually distinguished in a different colour.

Upon inputting the parameters, the solution was initialised, and the patch with water as the designated phase and volume fraction as the variable was activated. The ease of convergence and the efficient simulation duration influenced the decision to set the time step for over 1000 iterations at 30-second intervals.

3.14. Solution Method

Four numerical solution methods are available for a fluent solver: SIMPLE, SIMPLEC, COUPLED, and PISO. The appropriate solution approach can also be chosen based on prior researches in the same domain or by four tests (one test for each solution method). This is the result of selecting the turbulence model. To ascertain the most suitable approach, the outcomes of the approaches above are individually compared with the experimental findings of the identical study or other studies conducted under identical test settings.

In this study, the solution approach was chosen based on earlier researches on the same subject, where the COUPLED method was adopted to solve the partial differential equations.

3.15. Flow Chart of Computational Model

Figure (5) is a flow chart illustrating the sequential process of constructing a computational model using the 18.2 version of ANSYS software for simulating the solar distillation system.

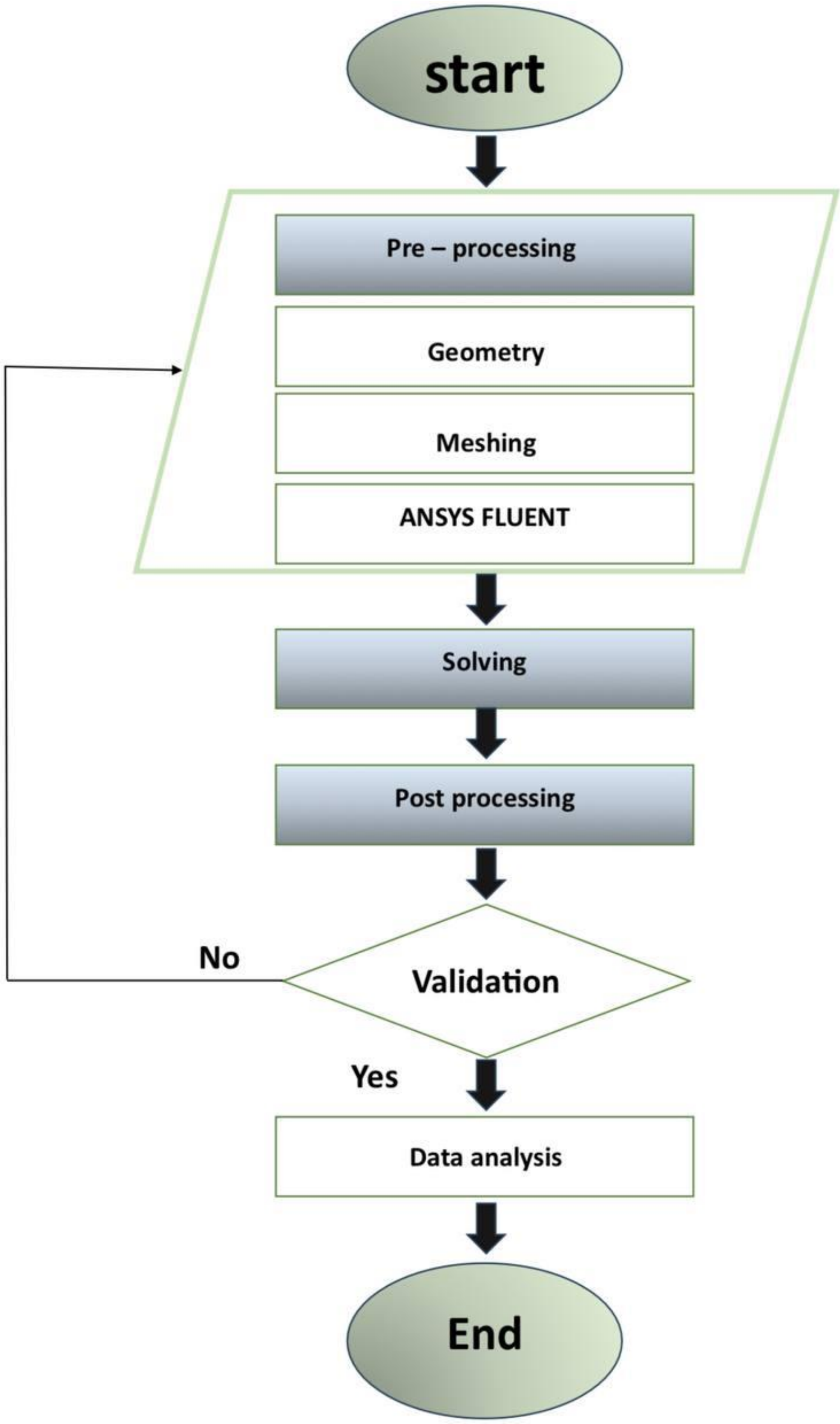

Figure 3- 4 The schematic diagram illustrating the flow chart of steps involved in constructing a computational model using ANSYS-Fluent software

Chapter Four

Experimental Work

4.1. Introduction

The main goal of the experimental tests is to evaluate the impact of particular operational variables and improvement factors on SSSS's performance. Furthermore, their objective is to validate the quantitative and CFD findings. This section summarises the experimental setup, measurement systems, timeline, and technique.

4.2. Experimental Set-up

The fabricated systems were positioned in Najaf, Iraq, at coordinates 31.9955° N and 44.3168° E. The experimental setup consisted of building a conventional single-slope solar still (SSSS) and a modified single-slope solar still (MSSSS). Multiple materials were utilised during the construction process. The selection of these materials was based on their cost-effectiveness and operational characteristics. Figure 4-1 A & B illustrates the process of manufacturing single-slope solar stills.

A

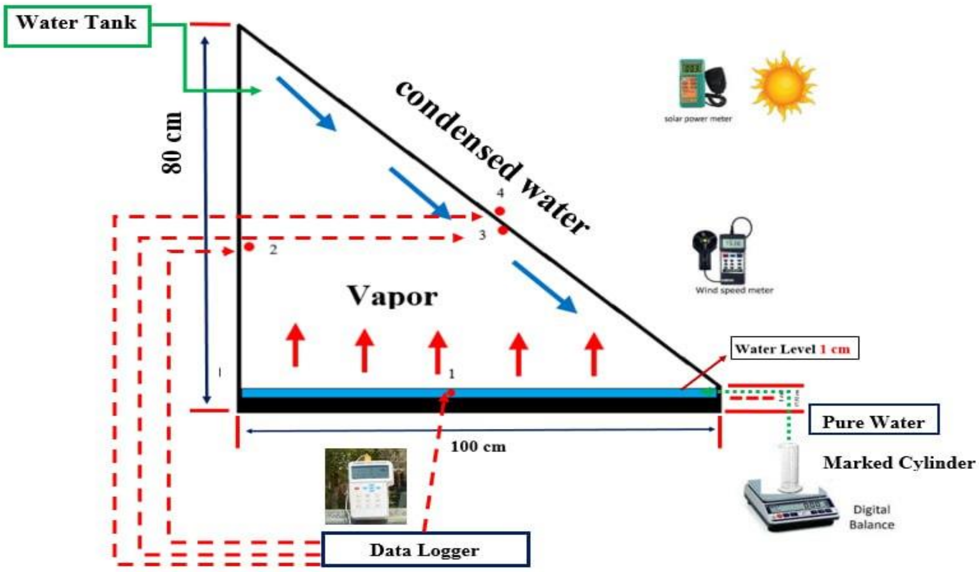

B

Figure 4. 1 A , B: Experimental Setup Photograph

4.2.1.Single Slope Solar Still Enclosure

The solar still basin was constructed from a rectangular box composed of a galvanised steel plate with a thickness of 2 mm. The box was cut at a 32° angle using a CNC machine to achieve a neat appearance, as shown in Figure 4.2. Due to this box's effective sealing and insulation, the likelihood of any leakage is minimal. The sides and bottom of the steel box were insulated using Polystyrene, an insulating material with a thermal conductivity of 0.030 W/m.k [109] The box has a surface area of 1 m^2, a height of 80 cm at the rear, 17.52 cm at the front, and an insulation thickness of 5 cm for the side and bottom walls. As depicted in Figure 4.2

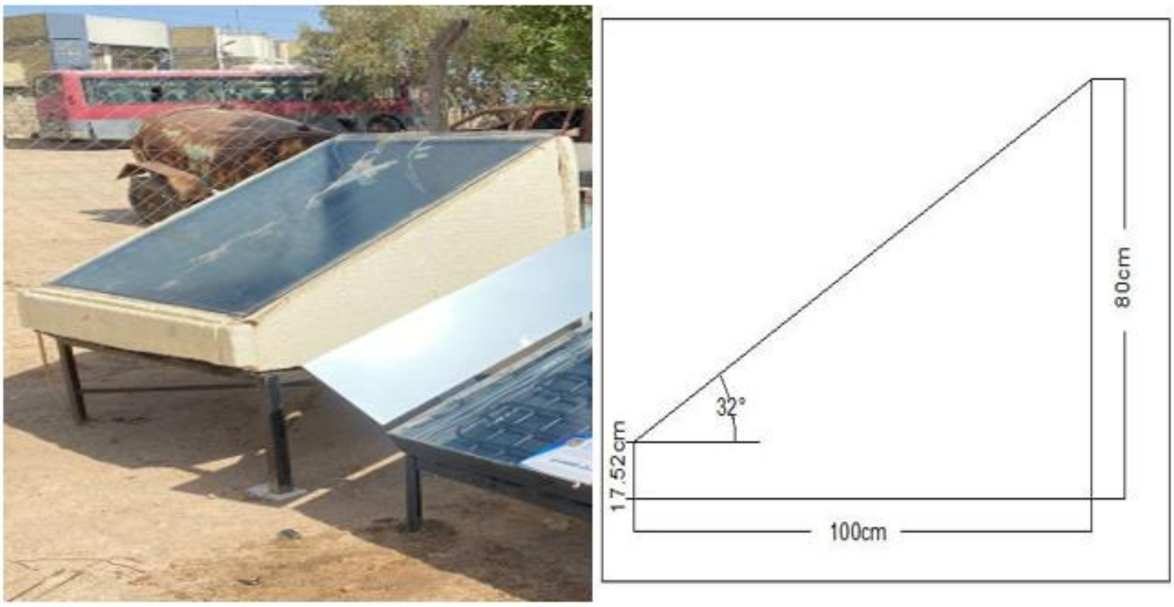

Figure 4.2: The Single Slope Solar Still Enclosure

4.2.2. Basin Absorber Plate

The bottom of the basin was covered with a 2 mm thick galvanized iron sheet painted black to maximize heat absorption from the sun. This sheet functions as an absorber plate, with the matte black thermal paint minimizing reflection of incoming radiation and enhancing both corrosion resistance and sunlight absorption.

4.2.3. Solar Still Cover

According to the literature reviews, several materials may be used as cover materials. Glass is particularly advantageous owing to its superior ability to transmit solar radiation, healthfulness, and relatively low cost. The glass cover used had a thickness of 4 mm, for optimal condensation, the effective glass cover thickness should be between 3 and 5 mm [114] and an average transmission rate of 0.88 [7]. An elastic rubber band with adhesive characteristics was placed between the transparent cover and the inclined surfaces of the solar still.

4.2.4. Water Collecting Channel

A collecting channel, 2 cm in width and inclined at a 5° angle from the horizontal axis, is placed on the upper border of the bottom part of the Polystyrene enclosure. Water droplets will fall into this channel as they reach the bottom end of the glass cover's surface. As a result, the liquid collected will flow into a flask positioned underneath the solar still.

Table 4. 1 Solar still dimensions

Parameters	Values	Units
Length	100	Cm
Width	100	Cm
Right side height	80	Cm
Left side height	17.52	Cm
Basin and sides thickness	2	Mm
Glass cover thickness	4	Mm
Water depth	1	Cm
Insulation thickness	5	Cm
Inclined angle	32	Degree

4.3. Measurement Instruments

The experiments have been carried out for solar still involved the use of various measurement apparatuses, as outlined below:

4.3.1. Temperature sensing measurement

Four calibrated K-type thermocouples were utilised to get measurements, with an error margin 0.2% ± 1°C. These thermocouples were placed at various positions along both the SSSS and MSSSS. One thermocouple was employed to measure the temperature of the moist air inside the still, with one dedicated to measuring the temperature of the water basin. A thermocouple was installed on the absorber plate of the basin, while two additional thermocouples were used to monitor both the interior and exterior surfaces of the glass cover. The four thermocouples were connected to a 4-channel digital omega data logger thermometer (type HH1384), with a measurement range of -150 to 2000°C. The accuracy of the device is within ± 0.5°C. Figure 4-4 displays a K-Type thermocouple and the accompanying data logger. The positioning of thermocouples was depicted as seen in Figure 4-5.

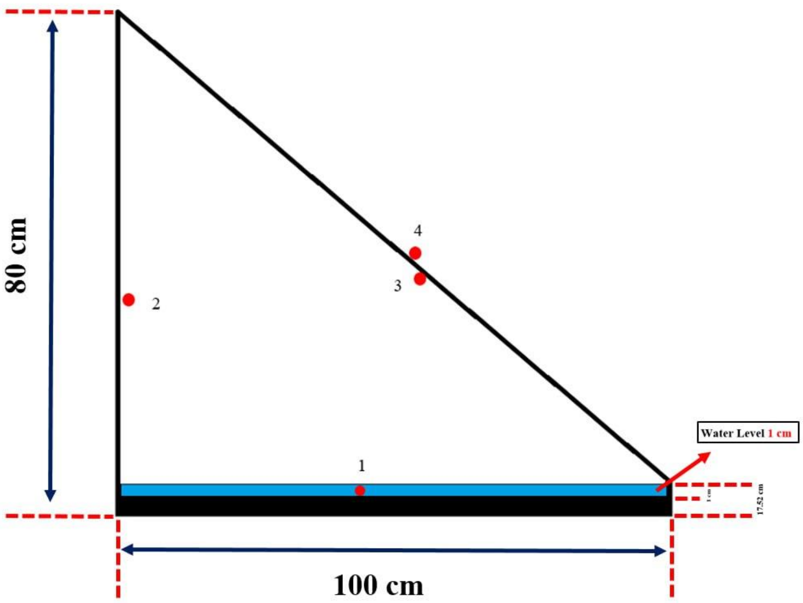

Figure 4.3: Thermocouple probe distribution in SSSS

Table 4.2: Thermocouple Location

Thermocouple No.	1	2	3	4
Location	Basin's water	Mostly air (vapour region)	Internal glass surfaces	External glass surfaces

4.3.2. Solar radiation measurement

The intensity of the incident solar radiation was measured hourly. Figures 4-6 depict the use of the TENMARS (TM-207) solar power meter for measuring solar radiation intensities. The solar power meter has an error margin of ±5% to ±10 W/m² and a measurement range of 0–2000 W/m². Appendix (B) provides a comprehensive explanation of the procedure for calibrating the solar power meter that has been previously utilised.

Figure 4.4: TENMARS (TM-207) solar power meter

4.3.3. Wind Speed Measurement

Airflow, particularly as it moves across the glass surface of the solar still, significantly enhances the condensation process. Hence, the Anemometer (AM-4206M), as seen in Figure 4-7, has a velocity range from 0 to 35 m/s and is used to measure the wind's velocity. The device's accuracy is within ±0.2 m/s. The anemometer calibration is provided in Appendix C.

Figure 4.5: Anemometer device (AM-4206M)

4.3.4. TDS-3 hold meter

A salinity assessment of the water was conducted before and after the enhancement process using the (TDS-3 hold meter), as seen in Figure 4-8, which measures the total concentration of dissolved salts in water. This device includes stirring the meter to remove any air bubbles to prevent interference between electrodes; afterwards, there should be a waiting time of 10-20 seconds to stabilise the reading. Before the enhancement, the salinity level was recorded as range of 580 ppm (mg/L), whereas it was measured as range of 50 ppm (mg/L) following the enhancement.

Figure 4.6: The TDS-3 hold meter

4.3.5. Distilled Water Collector

A marked flask was used to collect the distilled water, which was used to compare the hourly production of the traditional and enhanced solar stills. The graded flask had a capacity of 2.5 L and an accuracy of ±5 mL

Table 2 illustrates the accuracy and range of all the measuring apparatuses used in this investigation.

Table 4.3: The accuracy and range of all the measuring apparatuses

Apparatuses	Accuracy	Measurement Range	Measurement Units
Thermocouples	±1°C	0 –50°C	°C
Solar power meter	±5 W/m^2	0 –2000 w/m^2	W/m^2
Anemometer	±0.2 m/s	0 –35 m/s	m/s
TDS-3 hold meter	±10 ppm	0 –2000 ppm	ppm or mg/L
Scaled flask	±5 mL	0 – 1000 mL	mL
Data logger	±0.5°C	-150- 2000°C	°C

4.4. Single Slope Solar Still Improvements

Three main enhancement methods were used in the tests conducted in this study to achieve performance improvement of solar stills.

4.4.1. Absorbing materials

To enhance the efficiency and productivity of the SSSS, the first improvement approach included integrating new absorbent materials, such as marble and black leather. Further details on this technique will be provided in section 4.5, denoted by Figure 4-12, table 4.3. The choice of these materials has been achieved with the aid of the numerical CFD study conducted in this research.

4.4.2. Stepped single slope solar still with reflector

A stepped solar still is constructed to achieve the second improvement, as seen in Figure 4-9. A stepped solar still, which has a step-shaped design, is similar to a conventional one.

The glass roof and insulated box are similar to those of a standard fixed model. Conversely, the stepped-type basin supplants the singular basin; the glass cover had identical proportions to those in the SSSS. Water is kept stagnant and exposed to incoming radiation at each phase to ensure adequate depth. This design is adopted to enhance the production and efficiency of the solar still for two reasons: firstly, the reduced air volume, and secondly, the increased surface area for heat and mass transmission [115]. The stepped solar still has a surface area of 1.6 m^2, representing a 60% increase compared to the SSSS under study.

A

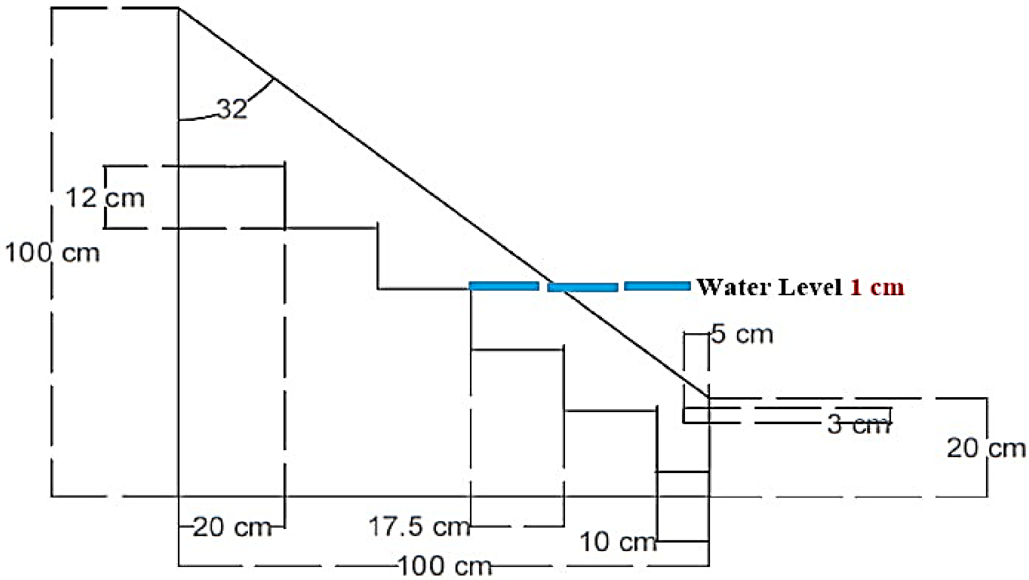

B

Figure 4.7: A & B stepped solar still.

4.4.3. Preheated water unit with reflector

Figure 4-10 A & B shows that the third enhancement involves linking the solar still system with solar heater to employ solar energy in pre-heating the water before entering the solar still to promote evaporation. The solar heater surface is positioned at a 30° angle and comprises a series of components to measure water temperature within a system. The arrangement begins with a tank, which serves as the water reservoir. Attached to the tank is a pump that drives water through the system. The water is then directed through a flowmeter, positioned directly after the pump, to measure the flow rate. Following the flowmeter, the water travels through a pipe and into a black U-shaped copper tube with a 10 mm diameter and a length of 20 m. A temperature sensor is mounted on the U-shaped copper tube to measure the water temperature as it flows through accurately. This configuration ensures precise monitoring and measurement of the water temperature within the system.

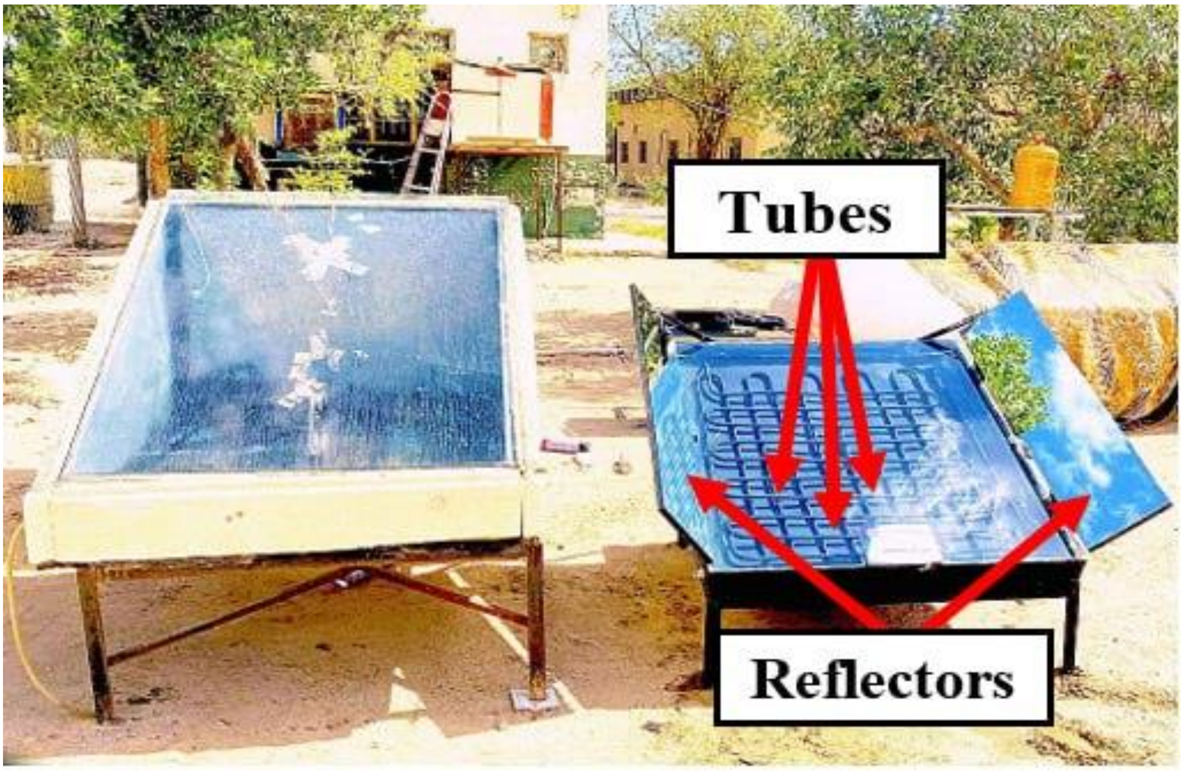

A

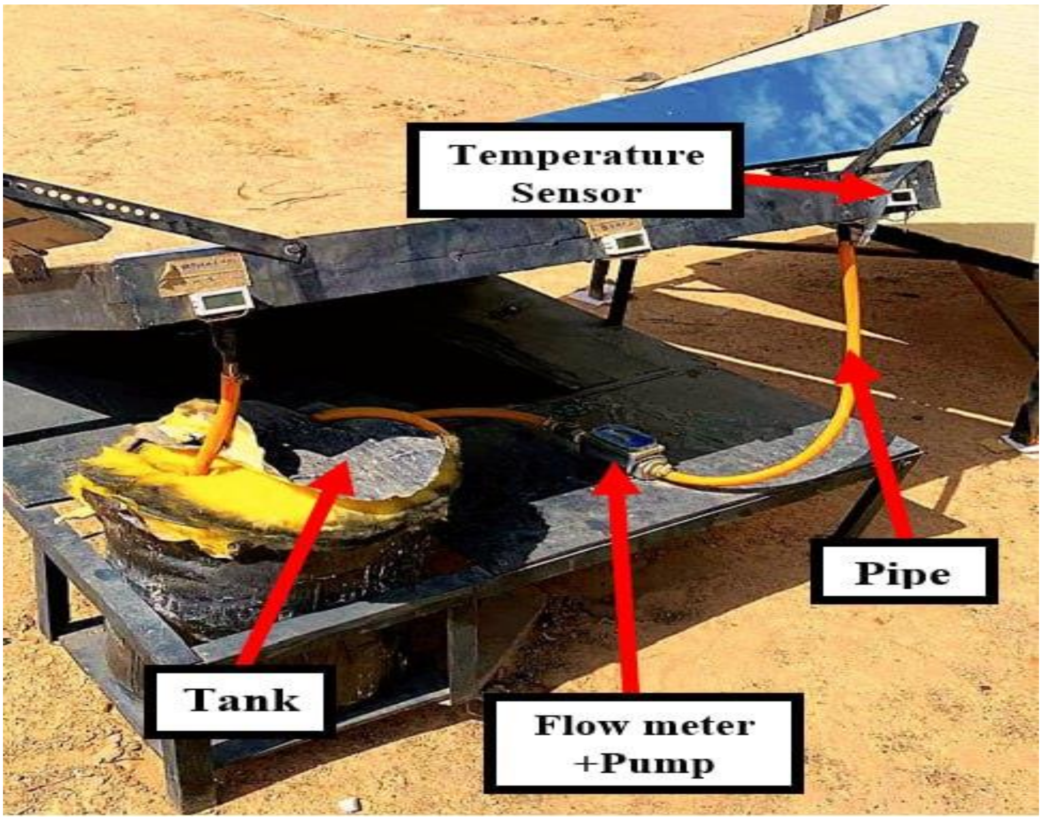

B

Figure 4. 8 A & B Front view of Solar heater

4.5. Summary of Experimental Procedure

Figure 4-11 shows that a 1 m^2 base solar still with an inclined angle of 32° using galvanised steel plates with a wall thickness of 2 mm is constructed. The outer sides are perfectly insulated with 5 cm thick white cork boards, while the base wall is painted black. A transparent, 4-mm-thick glass covering and sealing the top surface was placed with an inclined angle of 32°, allowing the solar rays to heat the inner walls. Thermocouples K-types with a 4-channel Omega data logger were used to measure the temperature of the basin's water and vapour region and the glass cover of the solar still. Wind speed was measured using an anemometer device (AM-4206M). Solar intensity was measured using a solar power meter (Tenmars 207). The average relative humidity information was taken from the weather station for Najaf/Iraq, which was 29% on March 21 and 23%

on April 21 [116]. The productivity of fresh water was measured using a scaled jar. The experimental work has been compared to numerical results to validate the CFD model. Black marble, 40 kg each, solid at 1.5 cm thickness and crushed at 0.5–4 cm sizes, were used as absorbent materials. 2 mm thick natural black leather was also tested in the SSSS basin to investigate the increase in SSSS productivity, as shown in Figure 4. Table 1 shows the thermal properties of these materials. The number of elements in water, including salts, ions, metals, and minerals known as total dissolved solids (TDS), were measured using a TDS-3 hold meter. The TDS value of the water under investigation (tap water) was at range of 580 mg/l or ppm. A small floating arm was also used to ensure and maintain the water level at 1 cm in the solar still basin.

A

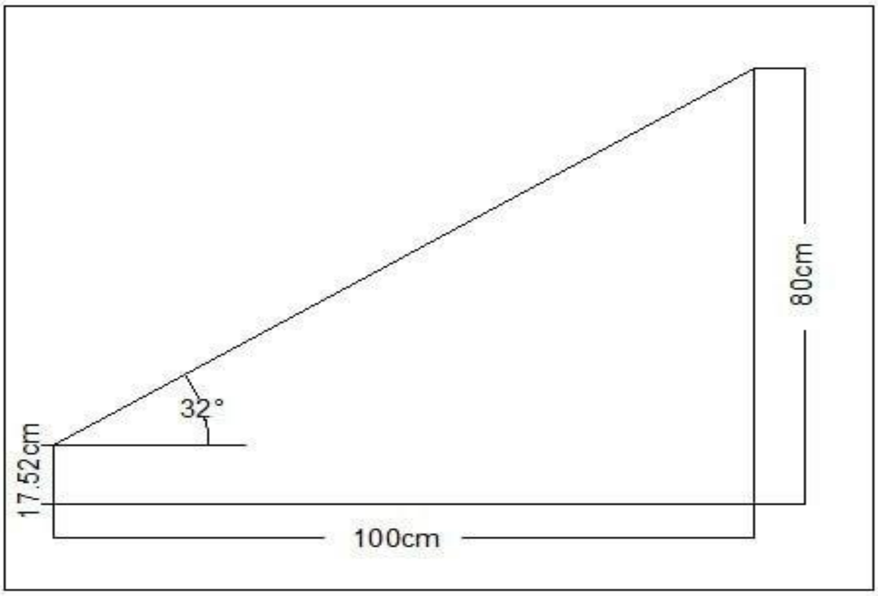

B

Figure 4. 9: A & B 1 m^2 base SSSS, with inclined angle of 32^o using galvanised steel plates with a wall thickness of 2 mm.

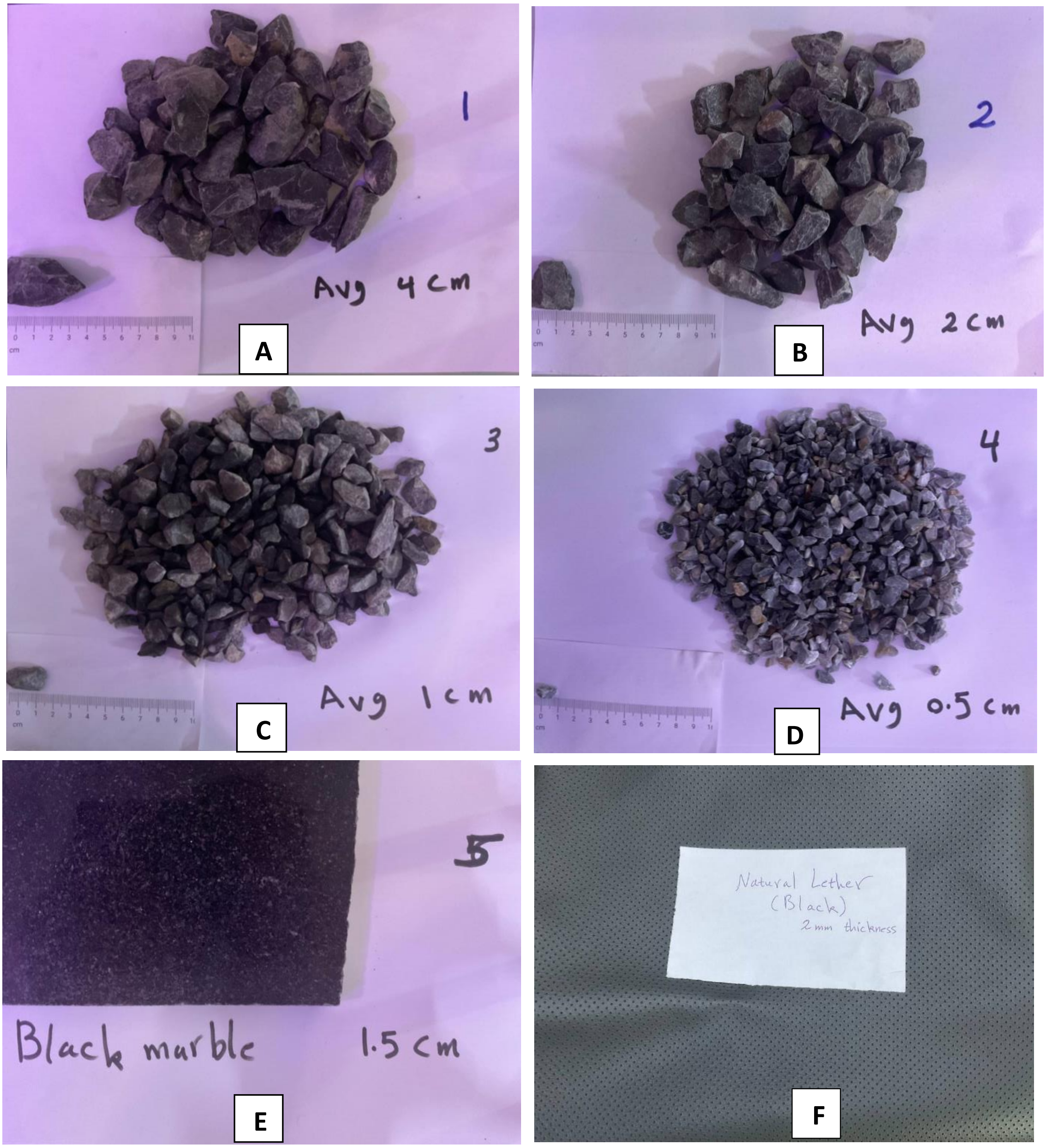

Figure 4. 10 Black marble (crushed and solid) and natural black leather were used to investigate increased SSSS productivity

Chapter Five
Results and Discussion

5.1. Introduction

This chapter discusses the results of the numerical and experimental works that were conducted at the Technical Engineering College of Najaf, Iraq (32.1 N 44.19 E). The experiment period was from 7:00 a.m. to 5:00 p.m. and lasted for several months. The numerical work included an improvement process by using different absorbing materials. The proposed materials are black marble and natural leather to investigate the effect of using different absorbing materials in the basin on the solar still productivity. The study comprised cases for SSSS with and without preheated water units and absorbing materials. Also, experimental cases relied on the use of stepped solar stills with and without preheated water units and absorbing materials. The experimental work for each case was repeated more than once to obtain the best and most accurate results. The results of the experimental work are compared with those of the numerical work, and good agreements are obtained. The following sections illustrate the results obtained from the studies that were conducted.

5.2. Numerical model validation

Numerical and experimental work has been compared with previous work to validate the CFD model. Figure 5.1 (A and B) compares the glass cover and basin-water temperatures of the tested solar still, while Figure 5.1 (C and D) compares the productivity and cumulative productivity of the tested solar still at a water depth of 2 cm with the work of [106], which was conducted on June 14, Egypt weather conditions, at an SS inclined angle of 30.5^{o}.

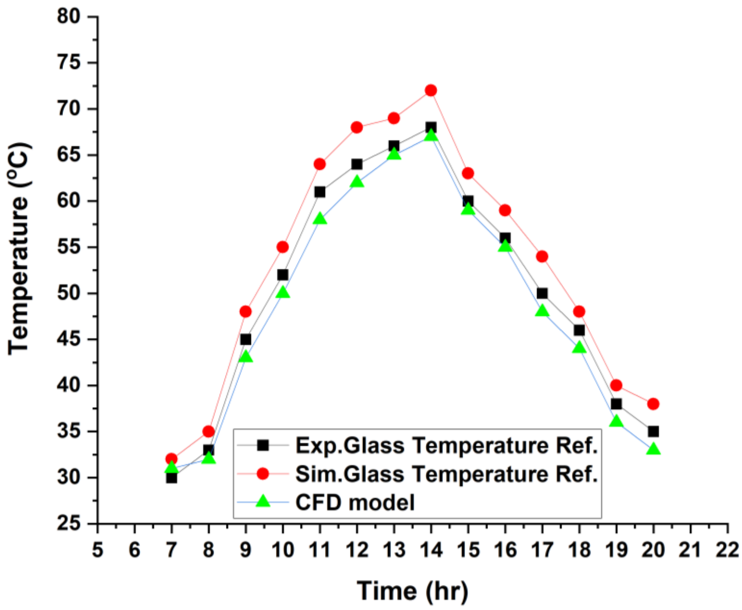
Temperature (°C)
Time (hr)
Exp.Glass Temperature Ref.
Sim.Glass Temperature Ref.
CFD model

A

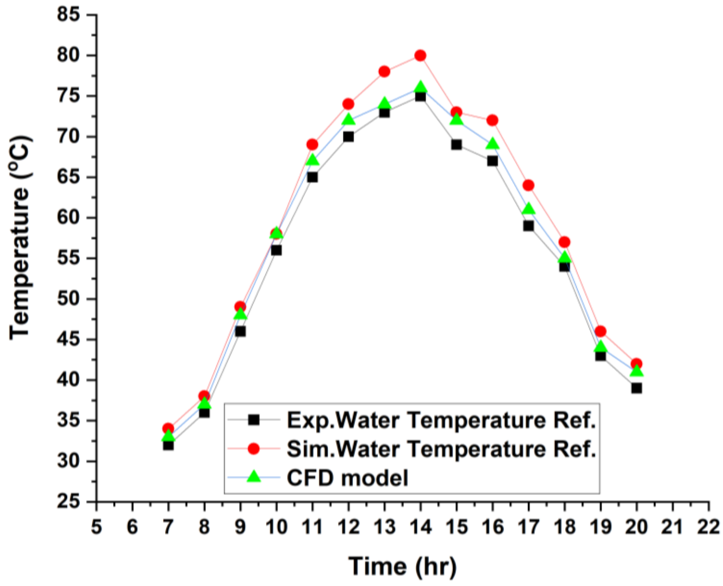
Temperature (°C)
Time (hr)
Exp.Water Temperature Ref.
Sim.Water Temperature Ref.
CFD model

B

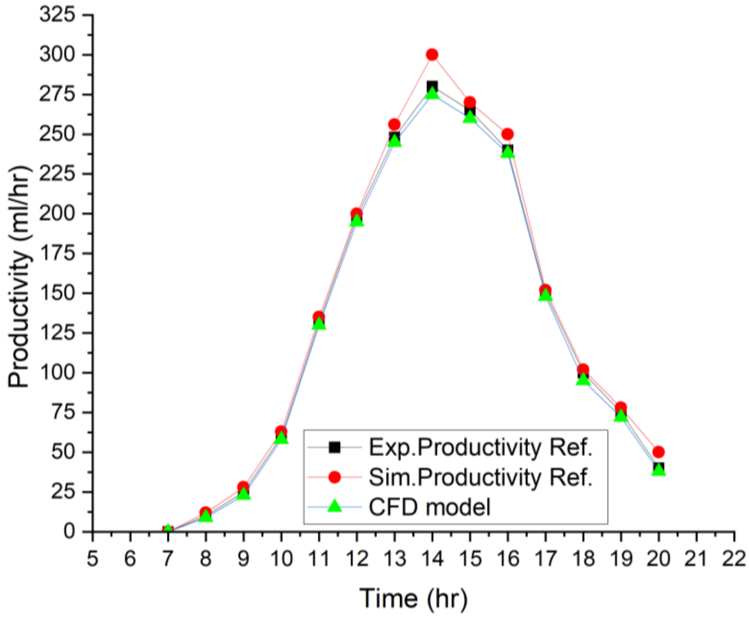

C

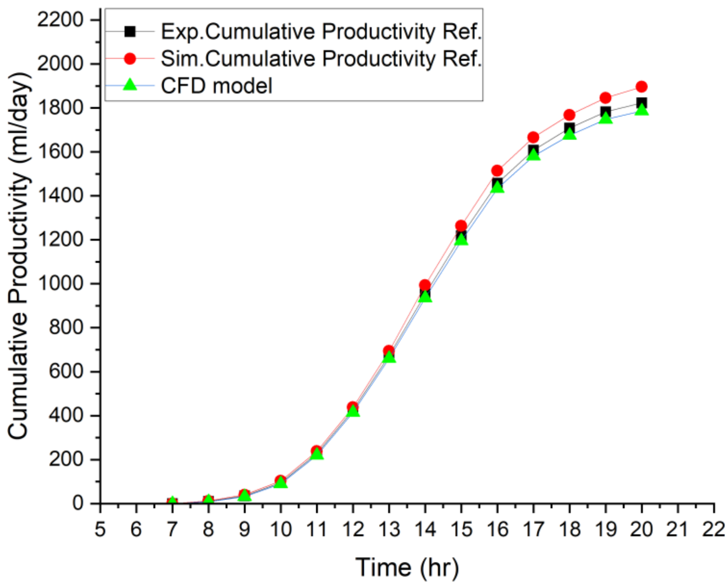

D

Figure 5. 1: Comparison of the water and glass cover temperatures, productivity and cumulative productivity of the tested solar still for ref. [106]**. (A) glass cover (B) Basin-water (c) productivity (D) cumulative productivity.**

Figure 5.2 (A and B) compare the tested solar still's basin-water and water-vapour temperatures for numerical and experimental results [105], whereas Figure 5.2 (C) compares the solar still efficiency. The work conditions used were an inclined angle of 26° a water depth of 3 cm on June 21st, 8 a.m. to 6 p.m., India weather conditions. The results from the current CFD model were found to match closely the experimental findings of previous works. There is a small percentage of difference, which is lower than 5%, between measured and simulated temperatures, productivity, and cumulative production. This indicates that the CFD model is accurate and suitable for enhancing the SSSS's efficiency.

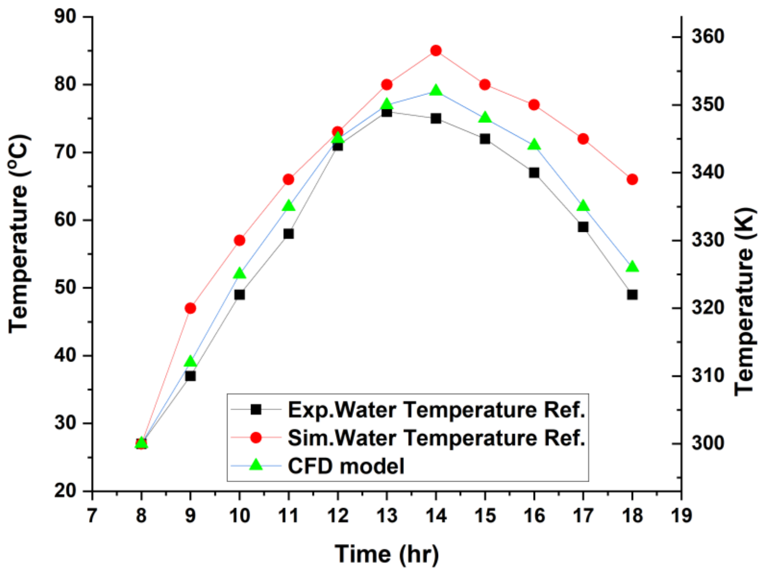

A

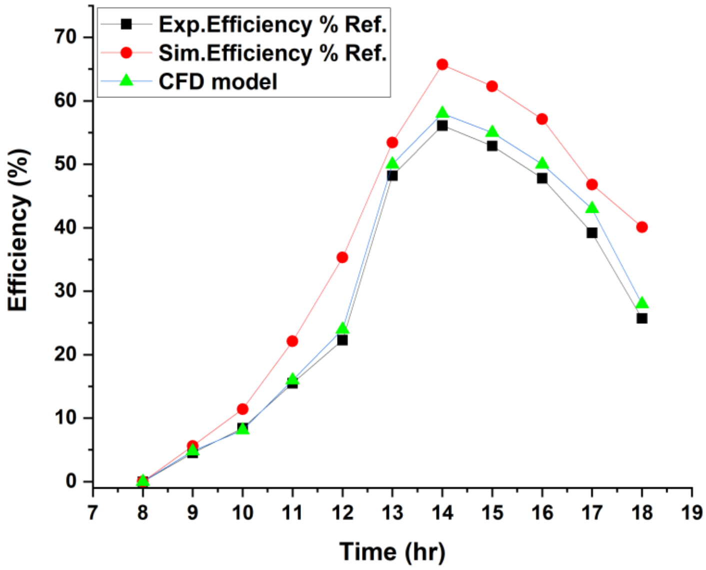

B

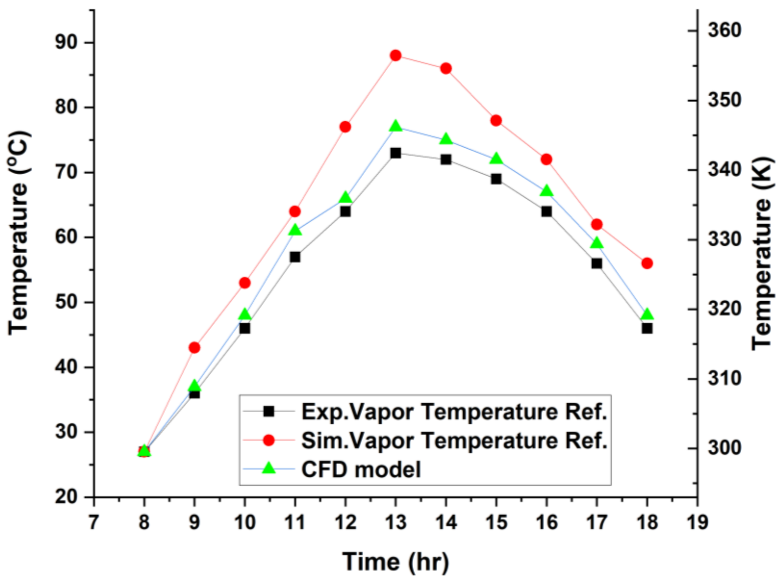

C

Figure 5. 2 Comparison of the basin-water, water- vapour temperatures and efficiency of the tested solar still for ref. [105] **(A) Basin-water (B) Water-vapour (C) Efficiency**

In addition, validation was conducted between the numerical and experimental results for SSSS using black solid marble on the 21st of March from 7:00 a.m. to 5:00 p.m. The results demonstrated a percentage error of less than 5% for productivity, cumulative productivity, and efficiency, indicating strong agreement between the CFD simulations and the experimental results, as illustrated in Fig. 5.3 (A, B, and C)

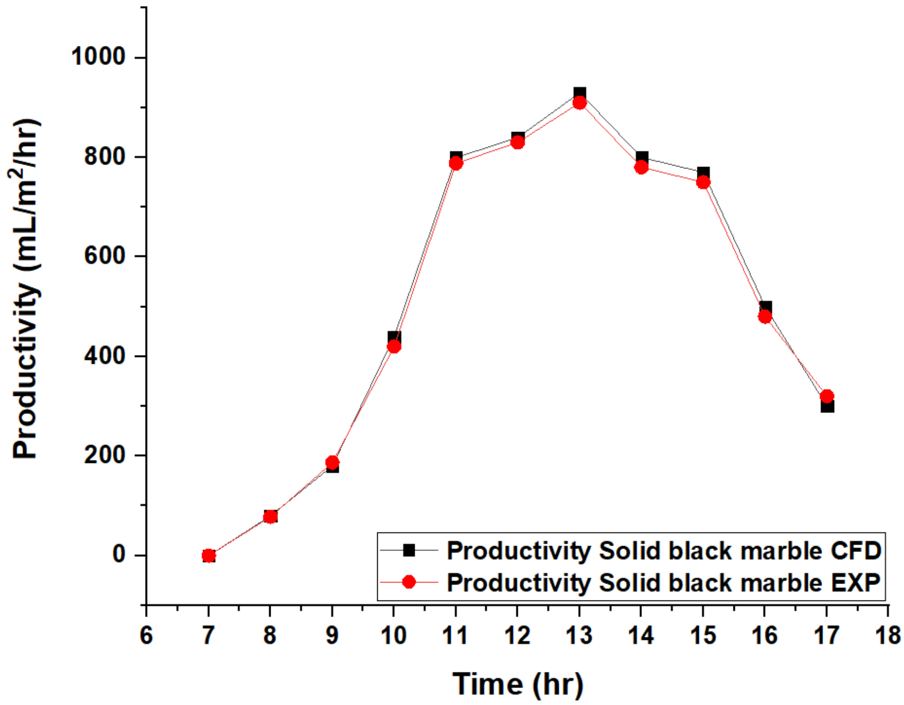

A

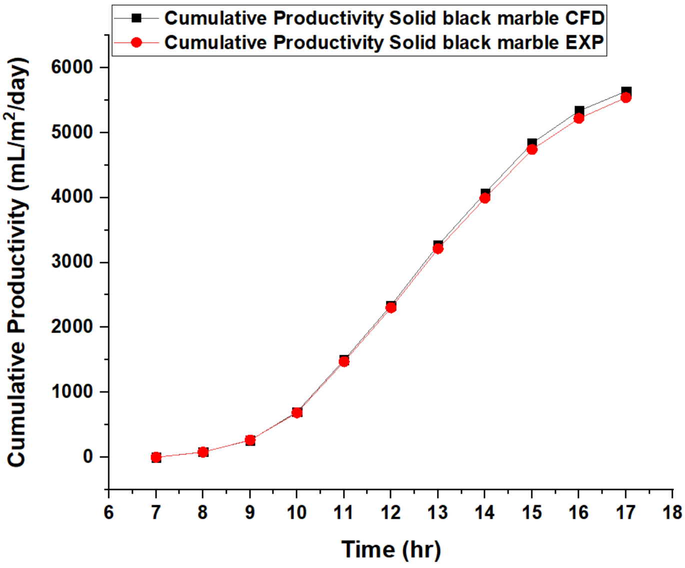

B

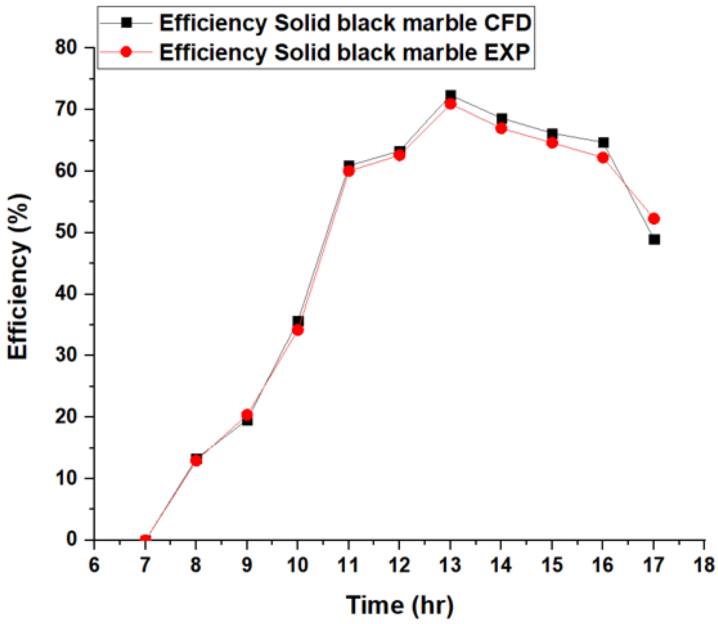

C

Figure 5. 3 Comparison of the CFD simulation and experimental results for SSSS with solid black marble (A) Productivity (B) Cumulative productivity and (C) Efficiency.

5.3. Numerical CFD Result

Figure 5.4 displays the CFD results from the work conducted in Najaf, Iraq, which included an inclined angle of 32°, a water depth of 1 cm, and a solid black marble basin with a thickness of 1.5 cm. The solar intensity was applied on the 21st of March at 1 pm. The vapour density inside the SSSS is depicted in Fig 5.4 (A), which reaches its maximum value near the bottom of the glass cover due to the combined effects of the inclined angle and gravity.

The same behaviour for the vapour volume fraction Fig 5.4 (B) is observed, reaching its maximum value at the glass cover's inner side and increasing towards the bottom. This result coincides with the previous work of [105], [106] & [107] Which simulates the evaporation-condensation process for SS. The volume fraction also increases near the SSSS basin as the temperature rises and the water transforms into vapour.

Fig 5.4 (C) illustrates the velocity of the vapour, which appears to behave laminarly from the SSSS basin towards the top before becoming turbulent until it reaches the inner surface of the glass cover. When the vapour reaches the glass cover's bottom, turbulence movement increases.

Fig 5.4 (D) shows the temperature distribution inside the solar still; basin water has a maximum temperature of 354 K (81°C). The only source of radiation passes through the glass cover, causing a temperature rise inside the solar still; the plate painted black will absorb the most heat, causing an increase in the water temperature, which is in direct contact with the base surface.

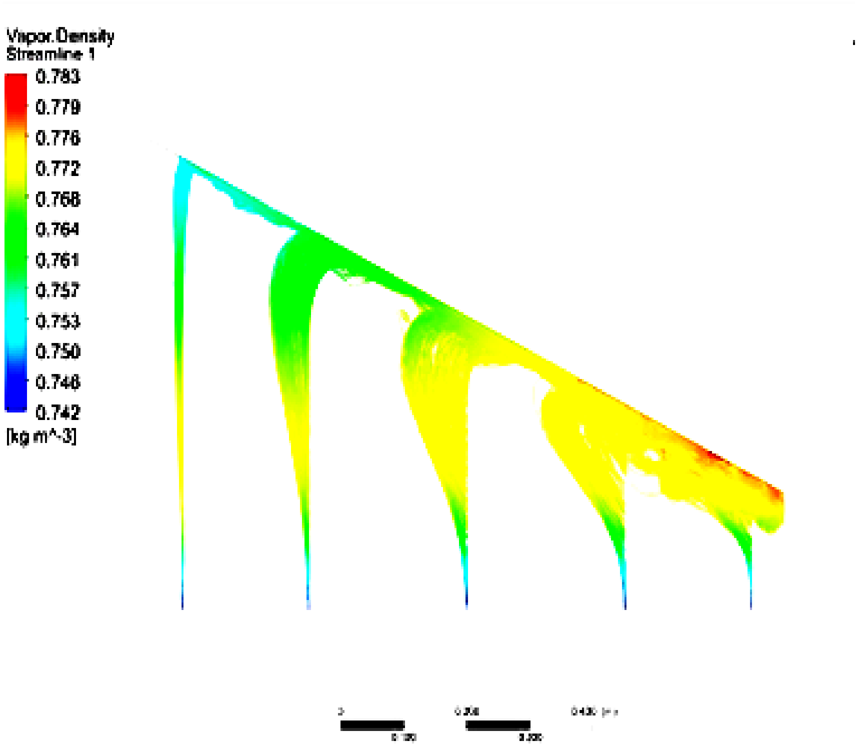

-A- Vapor density

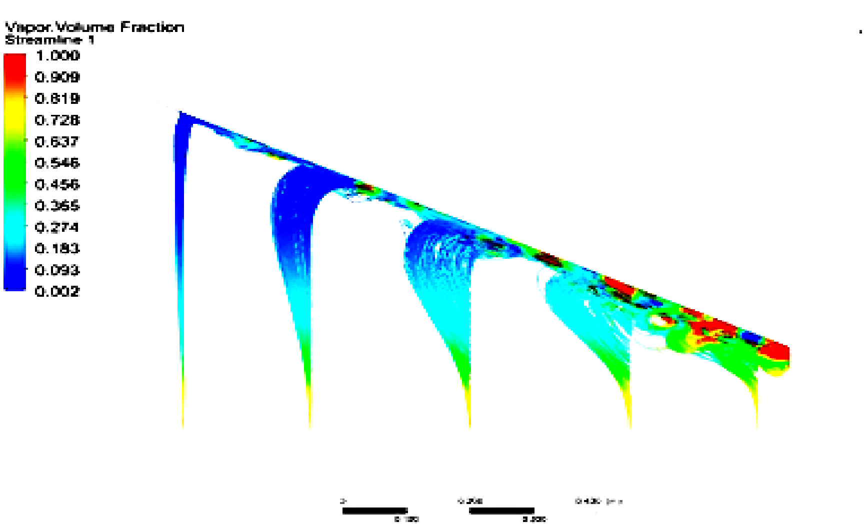

-B- Vapor volume fraction

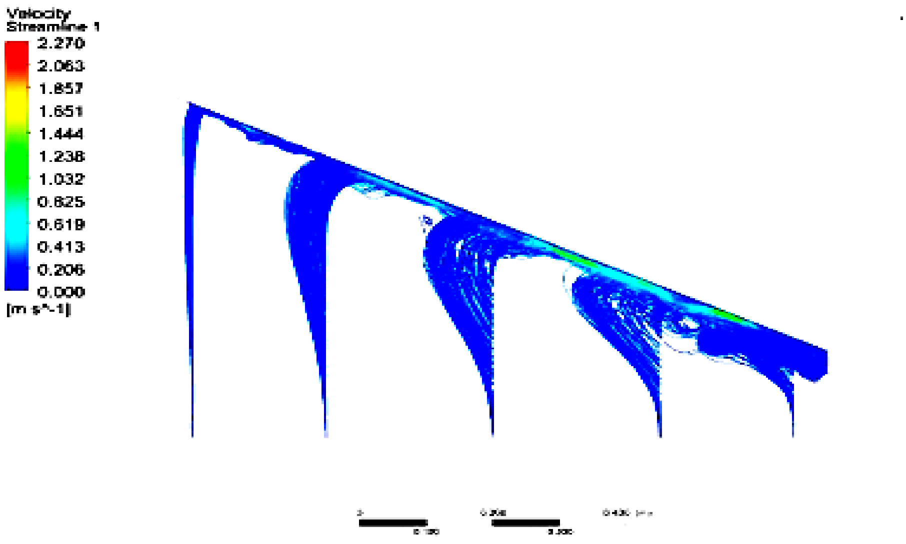

-C- Vapor Velocity

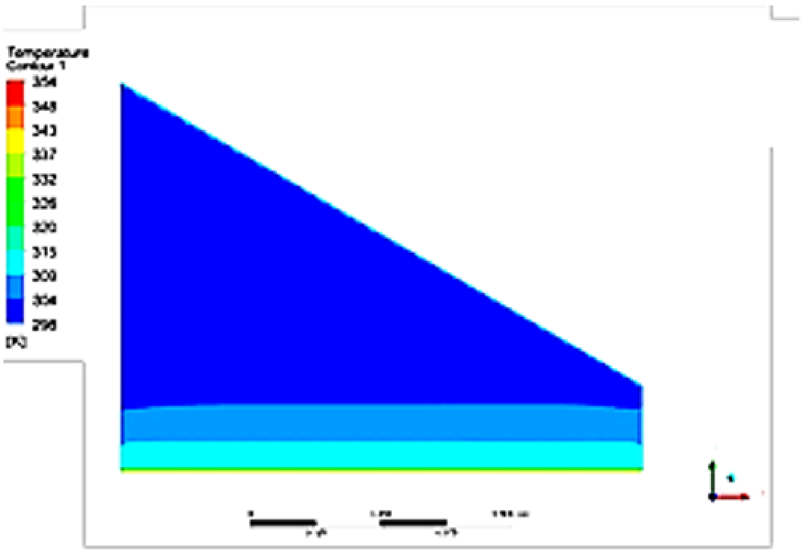

D – Temperature

Figure 5. 4 CFD results of the work carried out in Najaf/Iraq, inclined angle 32°, water depth 1 cm, on 21st of March at 1 pm (A) Vapor density (B) Volume fraction of vapour, (C) Vapor velocity and (D) Temperature contours.

Figure 5.5 shows the CFD results of 21st March from 7 am to 5 pm for three cases SSSS, SSSS with 1 m^2 black marble basin and 1 m^2 black leather. Fig 5.5 (A) displays the water's temperature from 7 a.m. to 5 p.m. Fig 5.5 (B) shows the solar still's productivity calculation using eq. (3-24), while Fig 5.5 (C) displays the cumulative productivity. In all these figures, solar intensity plays an important role in rising temperatures as more solar rays reach the S base, causing an increase in productivity. Low solar intensity in the early morning leads to low temperatures and thus low productivity, while high solar intensity between 12 and 2 p.m. yields maximum productivity. Despite the high decrease in solar intensity, the water temperature, as shown in Fig 5.5 (A) gradually drops after 2 p.m. because the SSSS is closed and insulated from its surroundings. Fig 5.5 (A, B and C) demonstrates that absorbing materials such as black marble and natural leather have increased water temperature and productivity compared to the SSSS. The absorbed materials worked as a heat absorber, keeping the SSSS hot enough to produce more fresh water despite the decrease in solar intensity after 4 p.m. The suggested absorbing materials from the CFD simulation will be tested in experiments to determine their potential to increase SSSS productivity. Fig 5.5 (D) compares the efficiency of the SSSS, as calculated from eq. (3-25), and the one including absorbing materials. Using the absorbing materials has increased the efficiency by 4 to 7% when using natural black leather and black marble, respectively, which promises to improve the yield of solar stills.

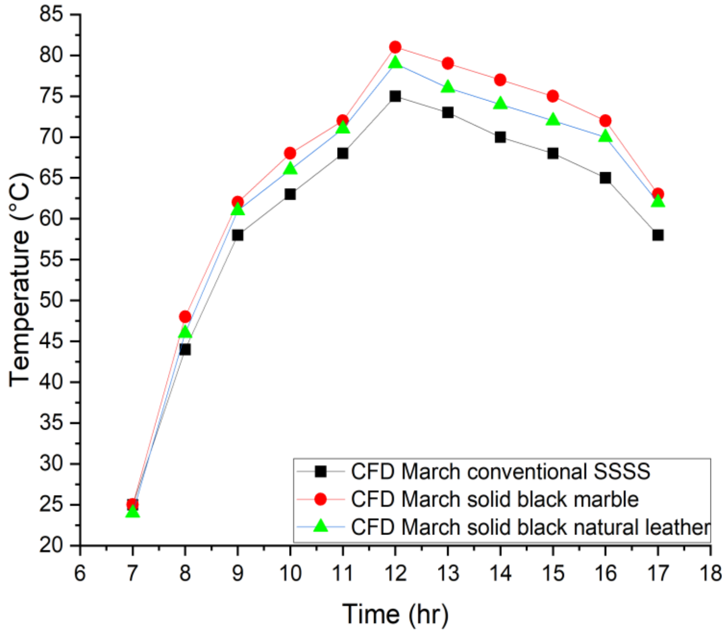

85
80
75
70
65
60
55
50
45
40
35
30
25
20
Temperature (°C)
6
7
8
9
10
11
12
13
14
15
16
17
18
Time (hr)
CFD March conventional SSSS
CFD March solid black marble
CFD March solid black natural leather

A

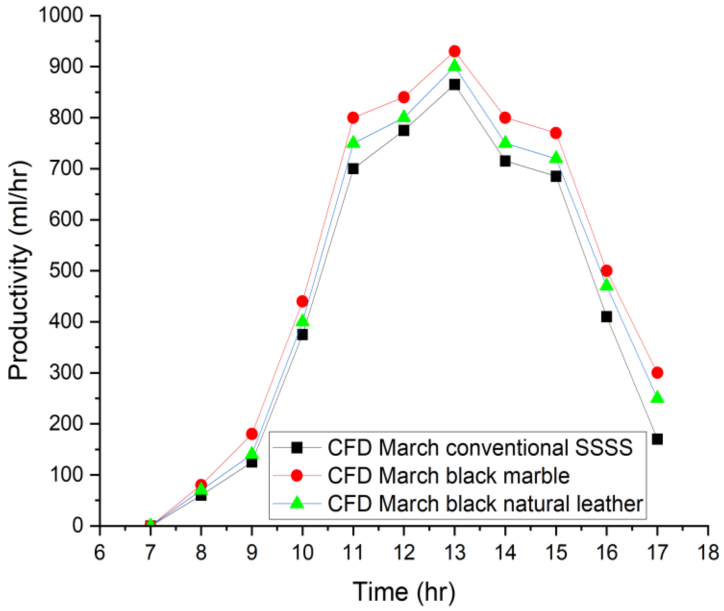

1000
900
800
700
600
500
400
300
200
100
0
Productivity (ml/hr)
6
7
8
9
10
11
12
13
14
15
16
17
18
Time (hr)
CFD March conventional SSSS
CFD March black marble
CFD March black natural leather

B

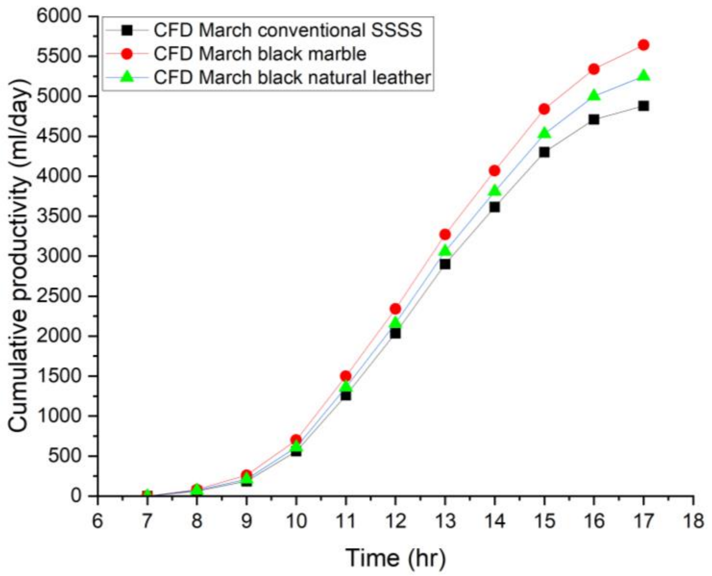

C

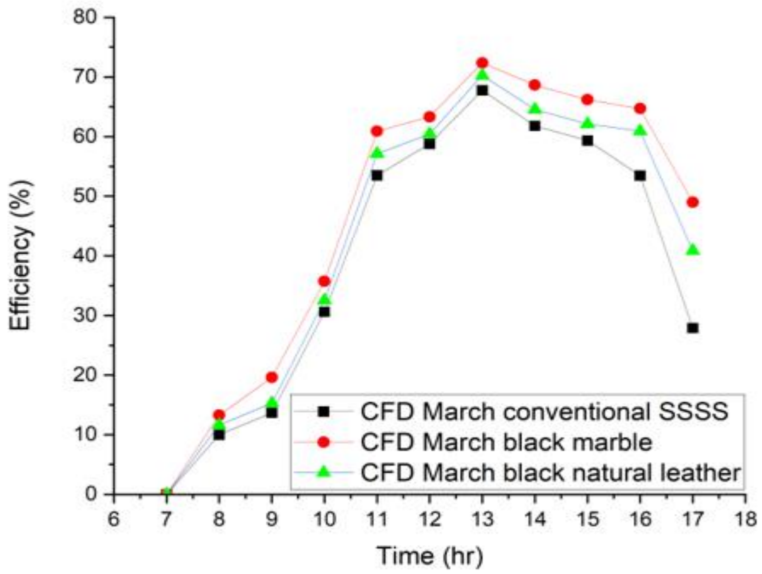

Figure 5. 5 (A) Water temperature of S, (B) Productivity and (C) Cumulative productivity (D) Efficiency of solar still, CFD result on 21st March for three cases SSSS, S with 1 m2 black marble basin and 1 m2 black leather

Figure 5.6 demonstrates the vapour movement steps; it can be seen that the water starts to evaporate due to the temperature increase inside the solar still. Due to its low density compared to air, the water vapour rises towards the glass cover. The lower temperature of the glass cover and the high surface tension cause the vapour to condense into the water, which then slides down due to the glass's inclined angle and the gravity effect. This coincides with the results published in[117], as the gravity and glass tension force are the main factors for the vapour stick/slide mechanism.

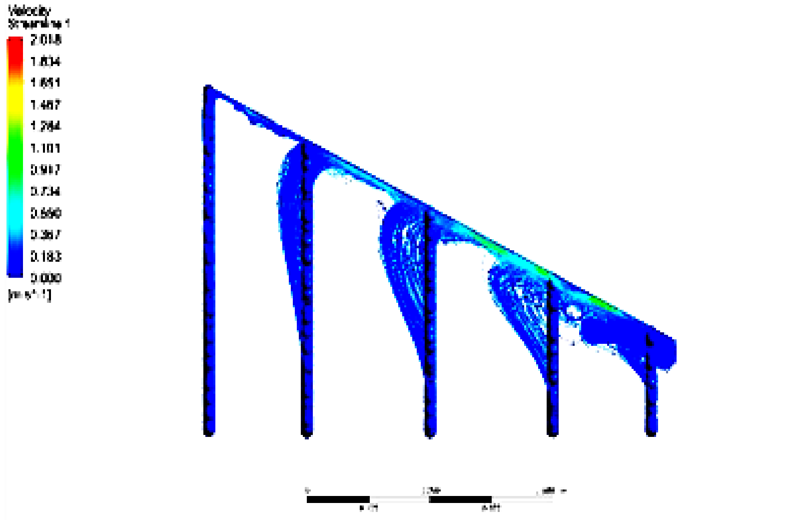

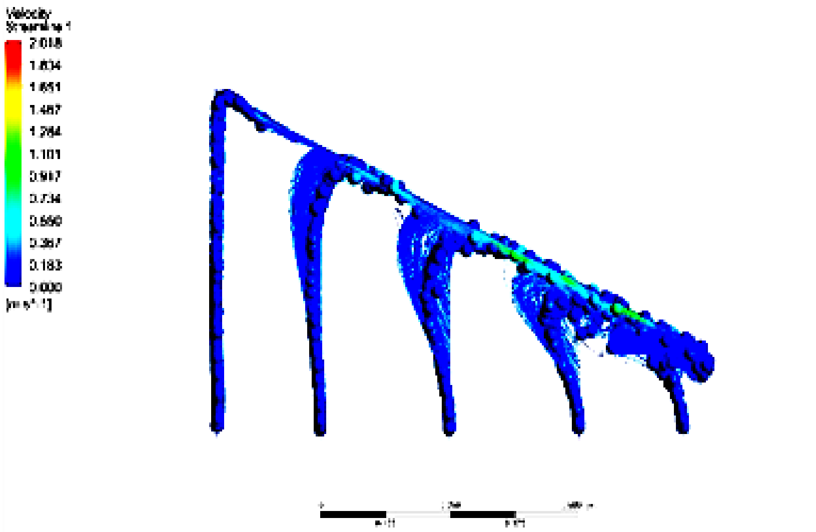

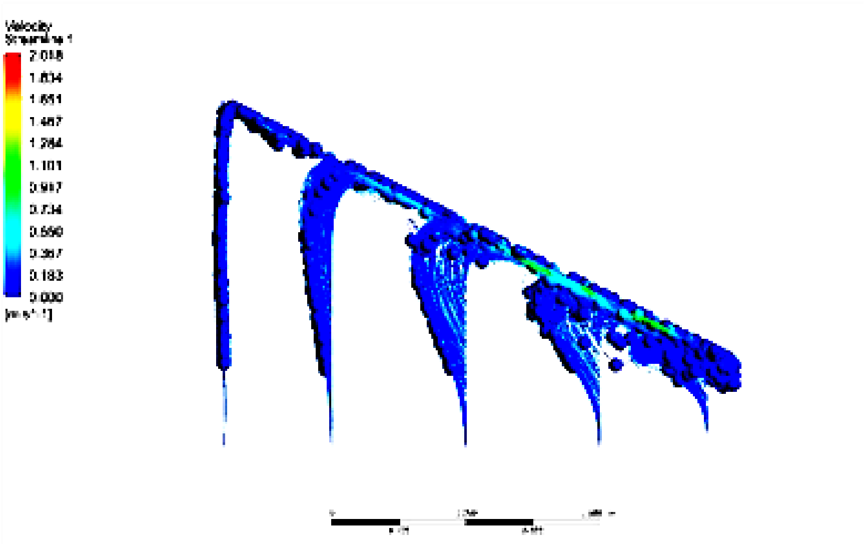

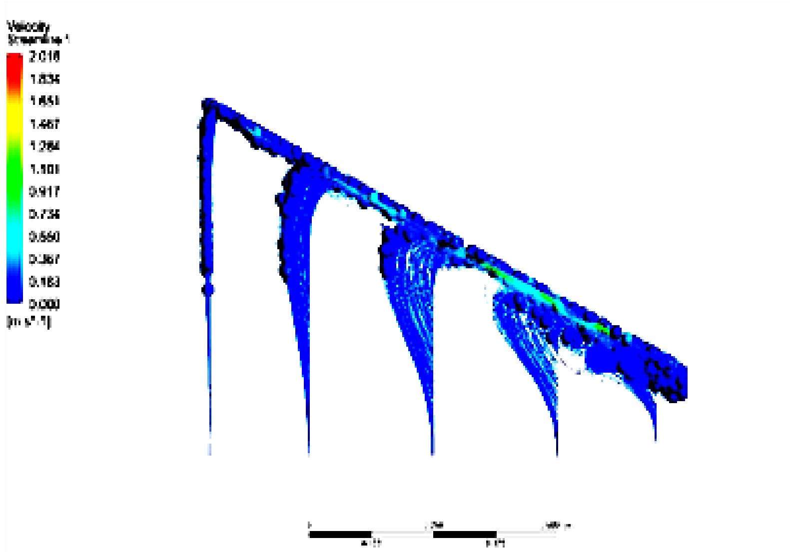

Figure 5. 6 The vapour movement starting from the base toward the glass cover during the evaporation-condensation process

5.4. Experimental work

Figures 5.7 (A and B) show the measured solar intensity and ambient temperature over time for March 21st and April 21st. The figures demonstrate the impact of the time of day on solar radiation. The solar radiation begins at 7:00 am, increases, and reaches a value of 1000 W/m^2 between 12:00 pm and 1:00 pm, then decreases. The earth stores heat; therefore, when solar radiation drops, it emits heat. This is why the ambient temperature rises and keeps rising even after the radiation drops. As a result, even when the sun's radiation decreases, the surrounding temperature stays high. After 3:00 pm, the outside temperature starts to drop slowly.

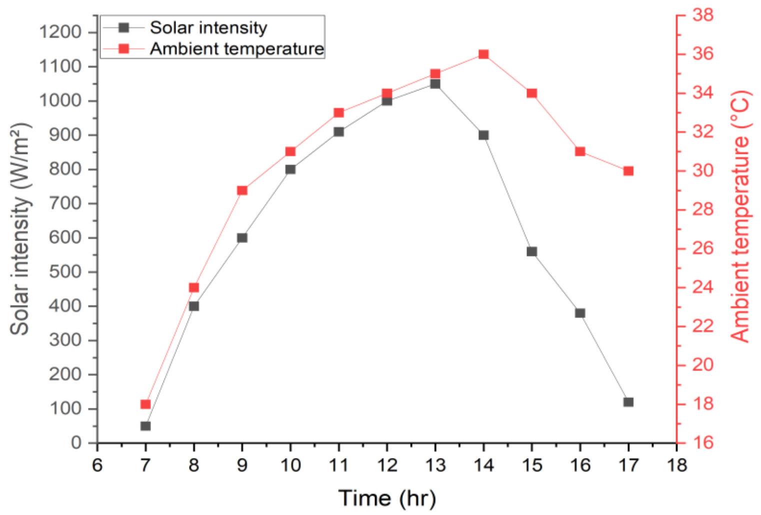

A

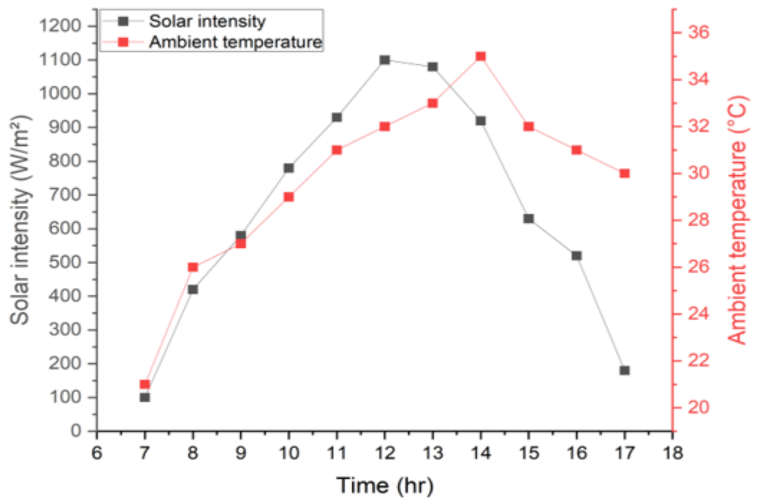

B

Figure 5. 7 The measured solar intensity and ambient temperature vs time (A) 21st March and (B) 21st April

Figure 5.8 (A) shows a temperature increase concerning solar radiation; the highest temperatures were from 12 p.m. to 2 p.m. The water's temperature and the glass's bottom surface increased by about 5°C on April 21st compared to

March 21st. This can be attributed to the increase in solar intensity in April compared to March, even though the ambient temperature dropped by 1°C, as illustrated in Figure 5.7 (A).

As shown in Figure 5.8 (B and C) April's productivity and cumulative productivity increased by 3.75% and 4.48% compared to March's due to an increase in solar intensity.

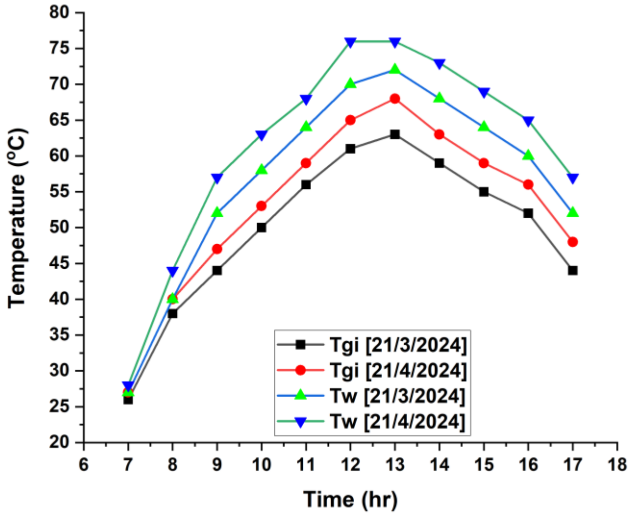

A

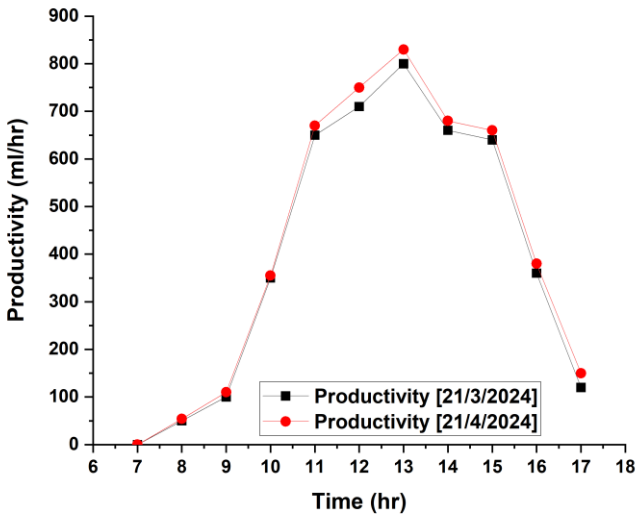

B

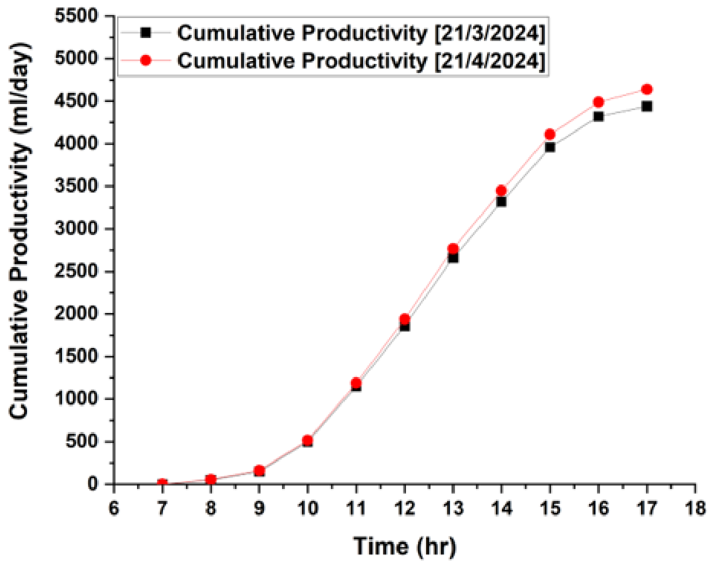

C

Figure 5. 8 Experimental results of tests carried out on 21st March and 21st April, (A) Temperatures of glass cover bottom and water, (B) Productivity and (C) Cumulative productivity

Figure 5.9 (A) shows the water temperature inside the SSSS and SSSS with absorbent materials. The water temperature rises as solar intensity increases, peaking at noon and gradually decreasing after 2 p.m. Using 4 cm of crushed black marble has resulted in the highest temperature of the water basin, rising by 13°C compared to the water temperature in SSSS. The black natural leather has also proved to work as a sound absorber material by raising the temperature by 8°C compared to SSSS. This increase in solar temperature has still increased productivity, as shown in Figure 5.9 (B).

Compared to SSSS, the yield of SSSS when using 4 cm crushed black marble increased by 53.92% of fresh water, as shown in Figure 5.9 (C).

Figure 5.9 (D) shows the efficiency of solar still with different types and sizes of absorbing materials. Even after 5 p.m., the temperature of the water inside the SSSS remains high enough to evaporate, indicating that the solar system will continue to produce energy.

Despite using the same amount of black marble, it was found that the 4 cm and 2 cm crushed marble produced the highest yield. This could be attributed to the fact that the basin water did not cover a portion of the marble stone, as the water level was kept at 1 cm, causing this part to heat up more quickly than the water-covered part. The crushed marble stone will absorb the sun's rays and work as a heater. Heat transfer through conduction and convection will be more significant in a larger-sized marble than in a smaller-sized marble.

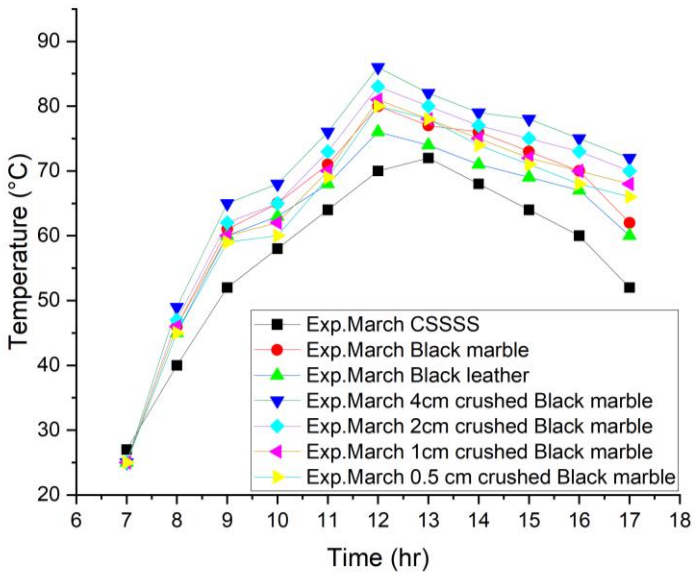

A

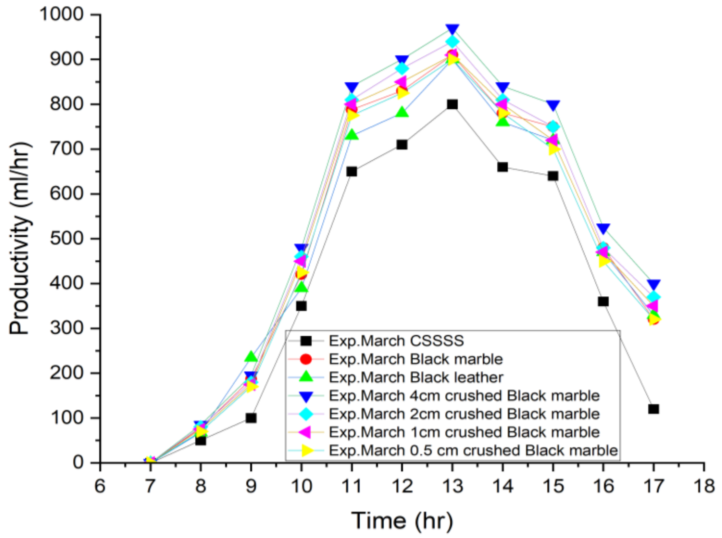
1000
900
800
700
600
500
400
300
200
100
0
Productivity (ml/hr)
6 7 8 9 10 11 12 13 14 15 16 17 18
Time (hr)
Exp.March CSSSS
Exp.March Black marble
Exp.March Black leather
Exp.March 4cm crushed Black marble
Exp.March 2cm crushed Black marble
Exp.March 1cm crushed Black marble
Exp.March 0.5 cm crushed Black marble

B

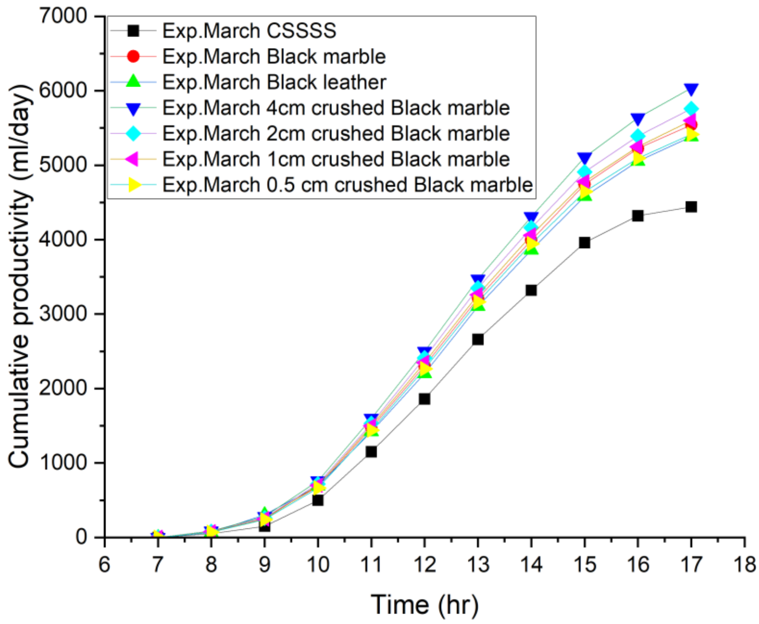
7000
6000
5000
4000
3000
2000
1000
0
Cumulative productivity (ml/day)
6 7 8 9 10 11 12 13 14 15 16 17 18
Time (hr)
Exp.March CSSSS
Exp.March Black marble
Exp.March Black leather
Exp.March 4cm crushed Black marble
Exp.March 2cm crushed Black marble
Exp.March 1cm crushed Black marble
Exp.March 0.5 cm crushed Black marble

C

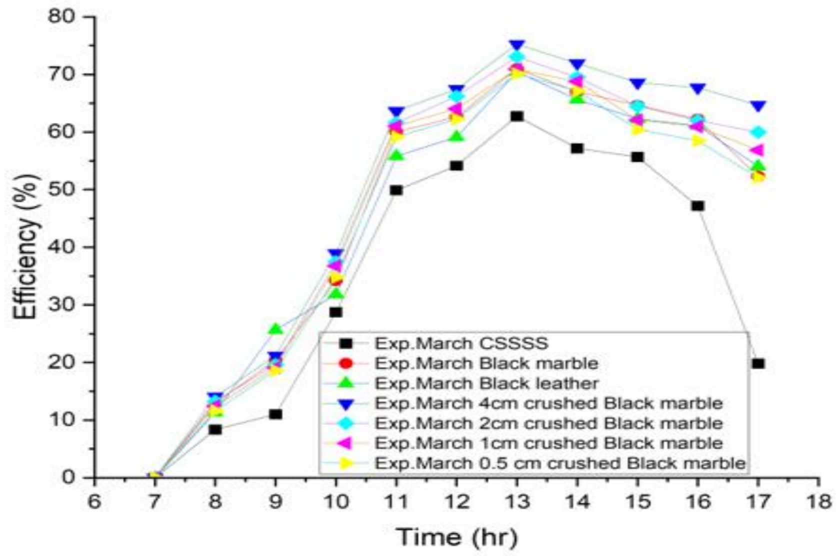

D

Figure 5. 9 Experimental result of tests carried out on 21st -27th March for different absorbing materials, (A) Temperatures of basin water, (B) Productivity and (C) Cumulative productivity, (D) Efficiency

Table 5.1 summarises the results obtained for all cases under study carried out in March.

Table 5. 1 Summary of the experimental work results in March for the six cases

Case under study	Maximum productivity mL/hr	Maximum cumulative productivity mL/day	Maximum Efficiency % Using eq. (3-25)	Percentage increase of cumulative productivity compared to SSSS
SSSS	800	4440	62.73%	
SSSS with 1 m^2 black marble basin	910	5543	70.97%	24.84%
SSSS with 1 m^2 1 m^2 black leather	900	5383	70.42%	21.23 %
SSSS with Crushed black marble 0.5 cm size	900	5415	70.11%	21.95%
SSSS with Crushed black marble 1 cm size	910	5600	70.89%	26.12%
SSSS with Crushed black marble 2 cm size	940	5760	73.07%	29.72%
SSSS with Crushed black marble 4 cm size	970	6035	75.24%	35.92%

5.5. Pre-heating and absorbing materials effect

Figure 5.10 (A) shows the measured solar intensity and air temperature over May 22nd. The figure demonstrates the impact of the time of day on solar radiation. The solar radiation begins at 7:00 am, increases, and reaches a value of 1100 W/m² between 11:00 pm and 12:00 pm, then decreases. The earth stores heat; therefore, when solar radiation drops, it emits heat. This is why the air temperature rises and keeps rising even after the radiation drops. As a result, even when the sun's radiation decreases, the surrounding temperature stays high. After 1:00 pm, the outside temperature starts to drop slowly.

Figure 5.10 (B) Comparison of the water temperature of the tested solar still on 22nd May, 7 am to 5 pm for conventional solar still with and without preheating and on 23rd May with the crushed black marble 4 cm preheating. The highest temperature was 77^{o}C at 1 p.m. for the first case without preheating. In the second case with preheating, the highest temperature was 90^{o}C at 1 p.m. with an increase of about 17% compared to the first case without preheating, whereas for the third case, 23rd May SSSS preheating and adding absorbing crushed black marble 4 cm, the highest temperature was 95^{o}C at 1 p.m. at with an increase of about 23% comparing to the first case without preheating. This indicates the effectiveness of preheating and absorbing materials, as increased water basin temperature means more water evaporates, leading to better thermal performance.

Figure 5.10 (C) The glass temperature of the tested solar still, 22nd May, 7 am to 5 pm, was also monitored for conventional solar still with and without preheating and for 23rd May with the crushed black marble 4 cm preheating. For the first case without preheating, the highest temperature was 74^{o}C at 1 p.m. 75^{o}C was recorded at 1 p.m. for the second case with preheating, while for the third case, 23rd May, with the crushed black marble 4 cm and preheating, the highest temperature was 75ºC at 1 p.m. This shows that despite using preheating and absorbing materials, there is no significant change in glass temperatures as the glass cover is affected mainly by the outside weather.

Similarly, the productivity of the tested solar still Figure 5.10 (D) has also been compared for conventional solar still with and without preheating and with the preheating crushed black marble 4 cm. The highest productivity for the first case without preheating was 1100 mL/m^2/hr at 1 p.m. In the second case with preheating, the highest productivity was 1200 mL/m^2/hr at 1 p.m., with an increase of about 9% compared to the first case without preheating. In contrast, for the third case with the crushed black marble 4 cm preheating, the highest productivity was 1450 mL/m^2/hr. At 1 p.m., with an increase of about 31% compared to the first case without preheating. This comparison indicates that incorporating preheating, especially with crushed black marble, significantly improves the productivity of the solar still, leading to enhanced water production efficiency.

The cumulative productivity of the above tested solar stills, which is the result of productivity curves as shown in figure 5.10 (E) showed 5690 mL/m^2/day for SSSS, while in the case of preheating was 6860 mL/m^2/day, an increase of 20.5%. The SSSS with the crushed black marble 4 cm and preheating yielded 8140 mL/m^2/day with a rise of 43% compared to the SSSS. Preheating and adding cheap absorbing materials, such as crushed black marble, significantly affects productivity in solar still systems, which in turn leads to more effective solar stills.

Figure 5.10 (F) Comparing the efficiency of the tested solar still for SSSS with and without preheating and with the crushed black marble 4 cm preheating. For the case without preheating, the highest efficiency was 67.40%, while in the second case with preheating, the highest efficiency was 72.65%. The third case with the crushed black marble 4 cm and preheating showed a maximum efficiency of 83.13%. These results highlight that preheating, particularly with crushed black marble, significantly enhances the efficiency of the solar still, resulting in higher water production per unit area. The results gained are aligned with those of previous research [102], [103], [104]. Indicating that preheating techniques substantially improve productivity and thermal efficiency. Preheating expedites the evaporation process, resulting in enhanced system performance. The heightened production rates shown in our findings may be ascribed to the expedited evaporation enabled by preheating, consistent with the improved efficiency documented in the literature.

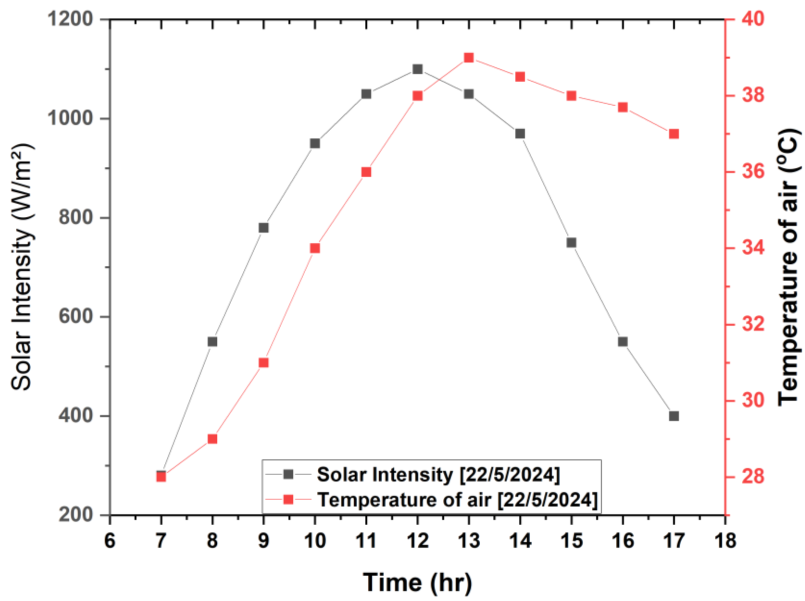

A

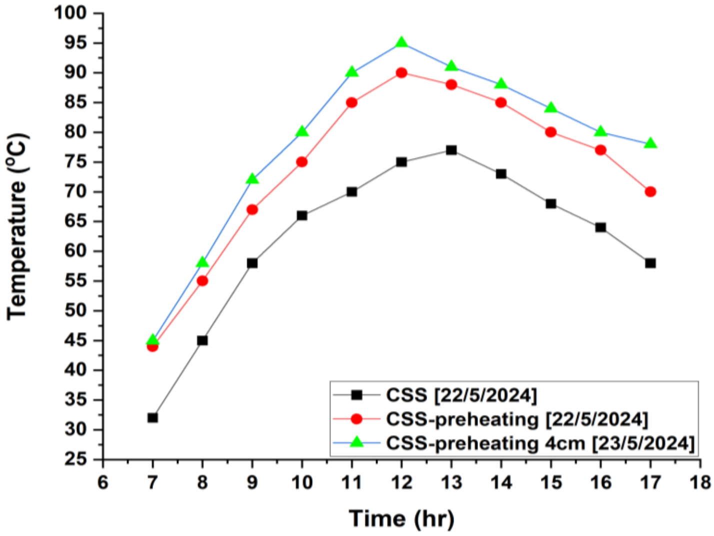
Temperature (°C)
Time (hr)
CSS [22/5/2024]
CSS-preheating [22/5/2024]
CSS-preheating 4cm [23/5/2024]

B

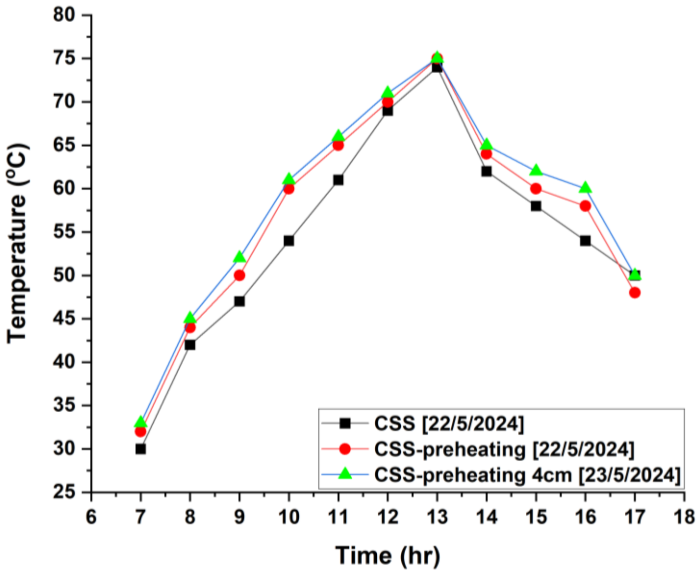
Temperature (°C)
Time (hr)
CSS [22/5/2024]
CSS-preheating [22/5/2024]
CSS-preheating 4cm [23/5/2024]

C

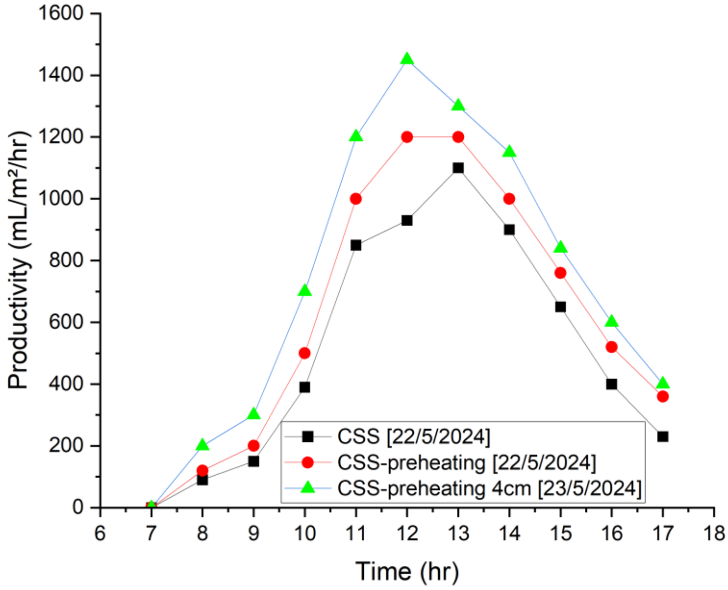
Productivity (mL/m²/hr)
Time (hr)
CSS [22/5/2024]
CSS-preheating [22/5/2024]
CSS-preheating 4cm [23/5/2024]

D

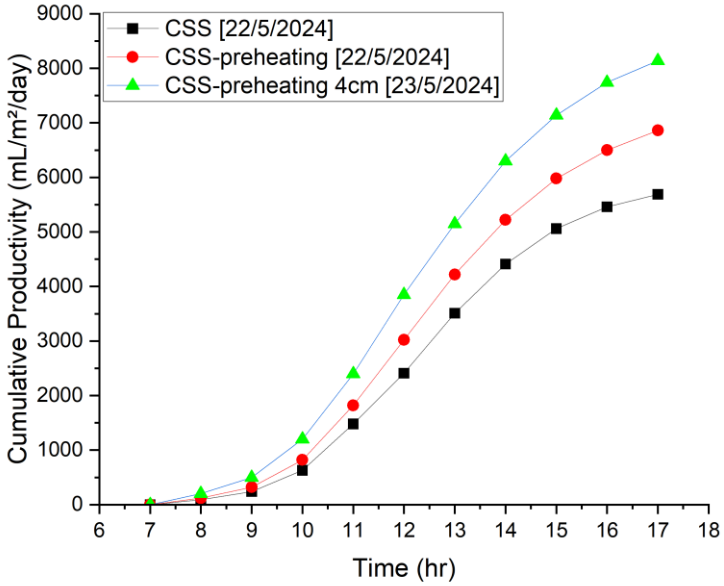
Cumulative Productivity (mL/m²/day)
Time (hr)
CSS [22/5/2024]
CSS-preheating [22/5/2024]
CSS-preheating 4cm [23/5/2024]

E

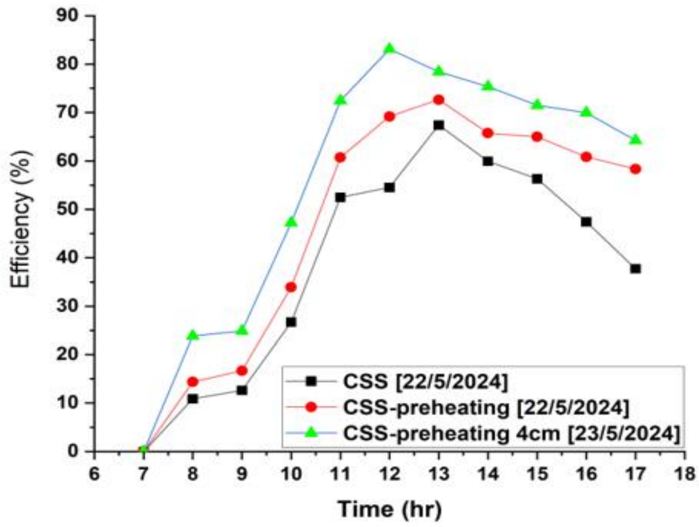

F

Figure 5. 10 Experimental result of tests carried out on SSSS on May (A) solar intensity vs temperature of air, (B) water temperature, (C) glass temperature, (D) Productivity, (E) Cumulative productivity, (F) Efficiency.

Figure 5.11 Shows a comparison of the experimental results of tests carried out on 21st March, 21st April and 22nd May for SSSS from 7 am to 5 pm. It was assumed that the variation in weather conditions due to the differences in testing dates (March 21st, April 21st, and May 22nd) was minimal.

In Figure 5.11 (A) the highest hourly productivity was set on 22nd May at 1100 mL/hr at 1 pm; in Figure 5.11 (B) the highest daily cumulative productivity was found on 22nd May, which was 5690 mL/day. The solar intensity in May, as shown in Figure 5.11 (C) played a significant parameter in the productivity increase, as the solar is still a closed system, and more solar radiation means more heat gained. Thus, the water temperature increases, causing more water to evaporate. As shown in Figure 5.11 (D), the higher efficiency was on 22nd May at 67.4% at 1 pm compared to efficiencies for SSSS on 21st March and 21st April, which were 62.73% and 64.80%, respectively. According to equation (3-25), this resulted from the highest productivity and water temperature in May, caused by higher solar intensity during the day. which depends on the parameters mentioned above.

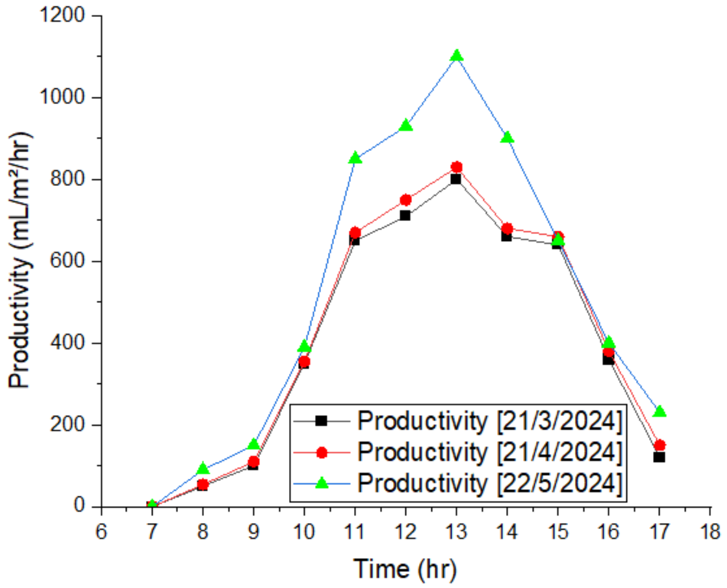

A

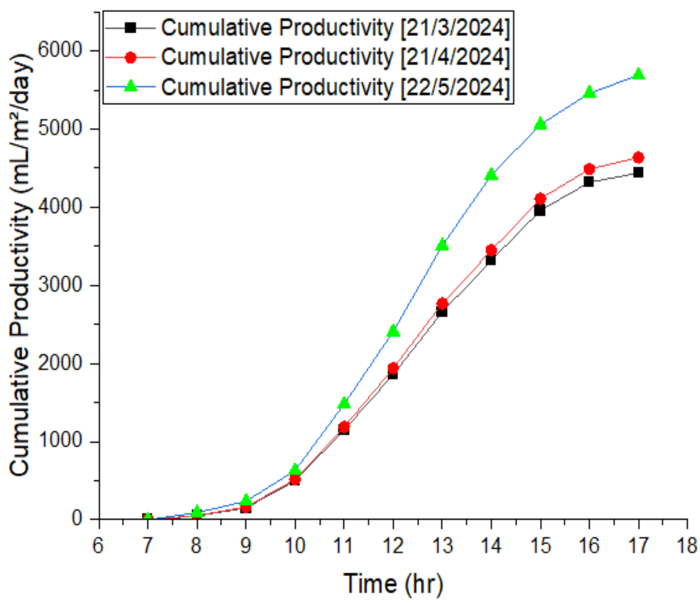

B

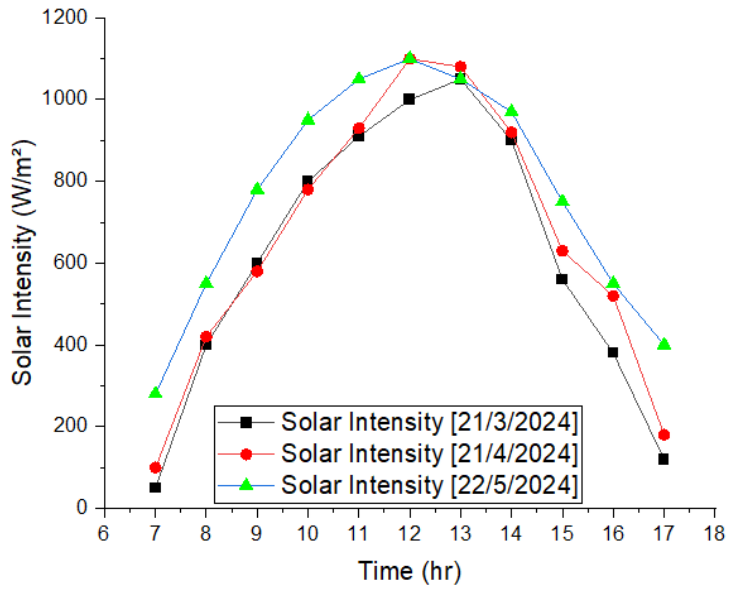

C

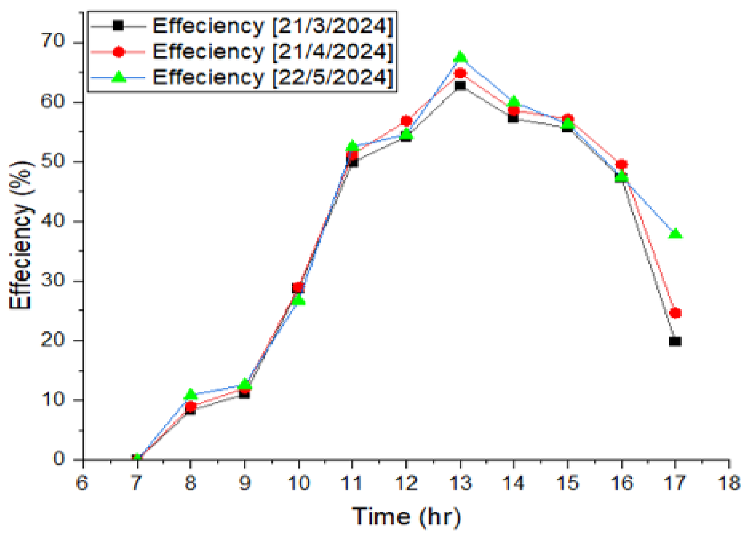

D

Figure 5. 11 Experimental result of tests carried out on SSSS on 21st March, 21st April and 22nd May (A) Productivity (B) Cumulative productivity (C) Solar intensity (D) Efficiency

5.6. Stepped solar still

Figure 5.12 (A) shows the measured solar intensity and air temperature over time on May 22nd for a stepped SS. The figure demonstrates the impact of the time of day on solar radiation. It illustrates a consistent increase in solar intensity and air temperature from early morning (7:00 am) to midday, culminating around 1:00 pm. Solar intensity attains a maximum of slightly over 1050 W/m² before experiencing a sharp decline in the afternoon, whereas air temperature peaks at approximately 39°C and gradually decreases. Both variables exhibit a diurnal pattern, with solar intensity diminishing more swiftly than air temperature post-1:00 pm.

Figure 5.12 (B & C) show the water and glass temperatures in stepped SS concerning solar radiation from 7 am to 5 pm. Tests have been done for three cases from the 22nd to the 24th of May. It should be noted that no significant solar intensity or wind speed was found on the days mentioned above of tests.

Figure 5.12 (B) Compares the glass temperature of the stepped SS for a stepped SS with preheating and a stepped SS combined with preheating and 4cm crushed black marble. For the first-stepped SS alone, the highest temperature was 76ºC at 1 p.m., whereas, for the second-stepped SS with preheating, the highest temperature was 78ºC at 1 p.m. The third case stepped SS with the crushed black marble 4 cm preheating recorded a temperature of 77ºC at 1 p.m. This shows that despite preheating and absorbing materials, there is no significant change in glass temperature as the glass cover is affected mainly by the outside weather.

Figure 5.12 (C) Compares the stepped SS's water temperature for the abovementioned cases. For the first case stepped SS alone, the highest temperature was 83ºC at 1 p.m., while the second case stepped SS with preheating; the highest temperature was 95ºC at 1 p.m. with an increase of about

14.45% compared to the first case, whereas for the third case stepped SS preheating and adding absorbing crushed 4 cm black marble the highest temperature was 97ºC at 1 p.m. with an increase of about 17% in comparison with the first case. This comparison highlights that incorporating preheating methods to stepped SS, particularly with crushed black marble, both incorporated with stepped SS, has significantly enhanced the solar still's water basin temperature, which means more water to evaporate, leading to better thermal performance.

Similarly, the productivity of the tested solar still shown in Figure 5.12 (D) has also been compared to stepped SS with and without preheating and with the preheating crushed black marble 4 cm. For the first case stepped SS alone, the highest productivity was 1350 mL/m^2/hr at noon, whereas for the second case stepped SS with preheating, the highest productivity was 1550 mL/m^2/hr at 1 p.m. with an increase of about 14.81% comparing to the first. In the third case stepped, SS with the crushed black marble 4 cm preheating; the highest productivity was 1620 mL/m^2/hr at 1 p.m. with an increase of about 20% compared to the first case. This comparison indicates that incorporating preheating, especially with crushed black marble incorporated with stepped SS, significantly improves the productivity of the solar still, leading to enhanced water production efficiency.

The cumulative productivity of the stepped SS, which is the result of productivity curves, is shown in Figure 5.12 (E); for the first case stepped SS alone, the highest cumulative productivity was 7100 mL/m^2/day; for the second case stepped SS with preheating; the highest cumulative productivity was 9000 mL/m^2/day with an increase of about 26.76% in comparison with the first case. In the third case, stepped SS with the crushed black marble 4 cm preheating, the highest cumulative productivity was 9990 mL/m^2/day, with an increase of about 40.70% in comparison with the first case. This comparison demonstrates that preheating methods, especially with cheap absorbing materials such as crushed black marble incorporated with stepped SS, significantly enhance the cumulative productivity of the solar still, leading to more efficient water collection.

Figure 5.12 (F) Comparing the efficiency of the tested solar still for stepped SS with and without preheating and with the preheating crushed black marble 4 cm. For the first case, stepped SS alone, the highest efficiency was 79.14%, while in the second case, stepped SS with preheating, the highest efficiency was 93.09%, and for the third case, stepped SS with the crushed black marble 4 cm preheating, the highest efficiency was 97.07%. The preheating, particularly with crushed black marble, has significantly enhanced the efficiency of the solar still, resulting in higher water production per unit area.

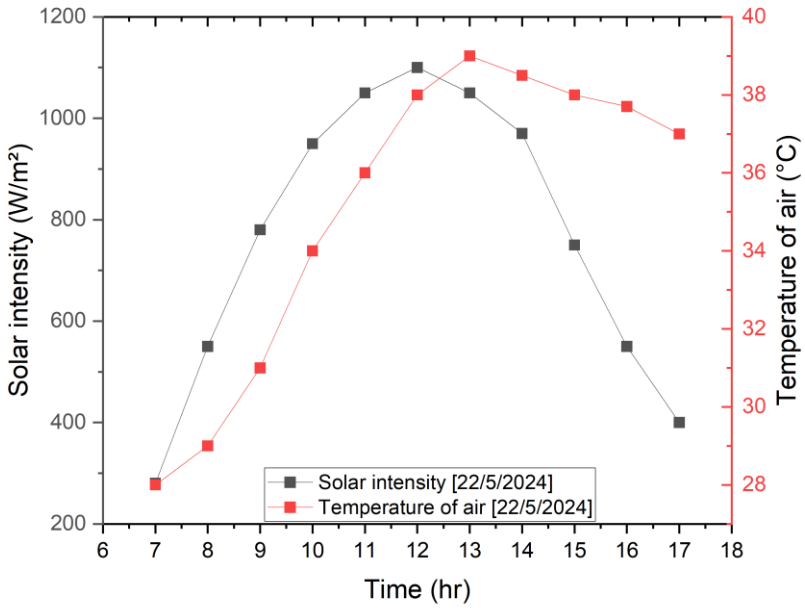

A

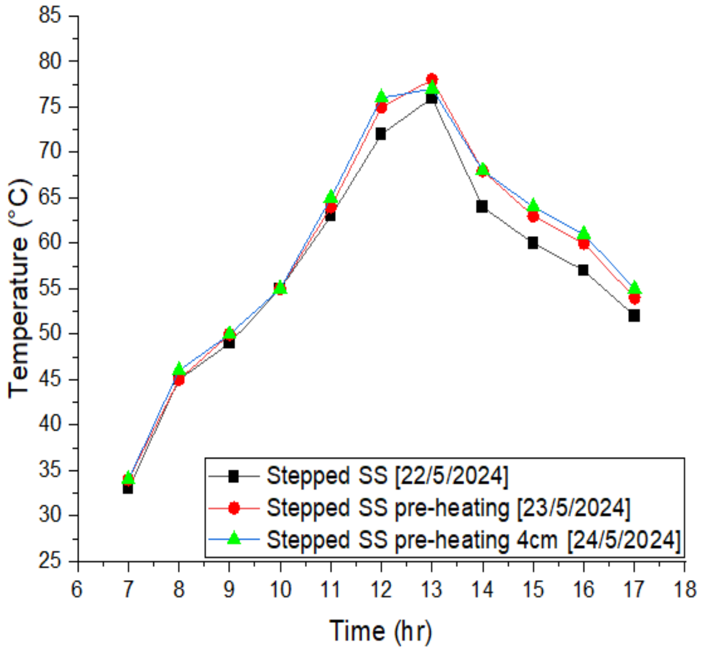

Temperature (°C)
Time (hr)
Stepped SS [22/5/2024]
Stepped SS pre-heating [23/5/2024]
Stepped SS pre-heating 4cm [24/5/2024]

B

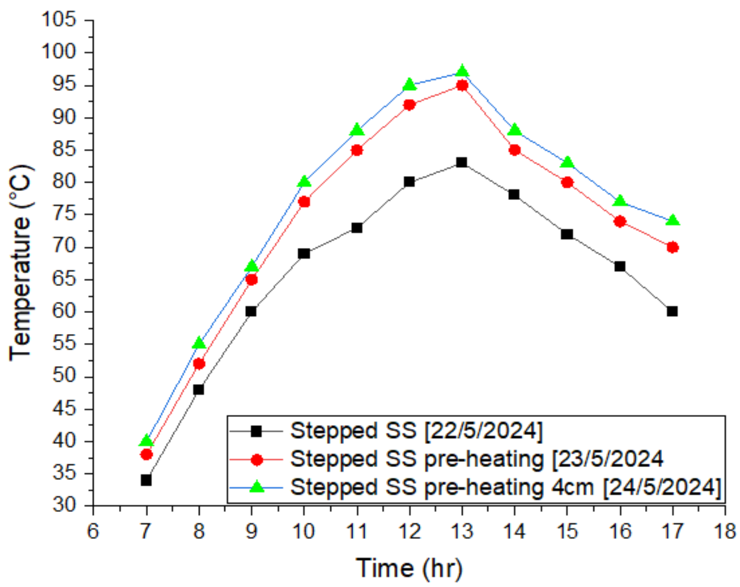

Temperature (°C)
Time (hr)
Stepped SS [22/5/2024]
Stepped SS pre-heating [23/5/2024
Stepped SS pre-heating 4cm [24/5/2024]

C

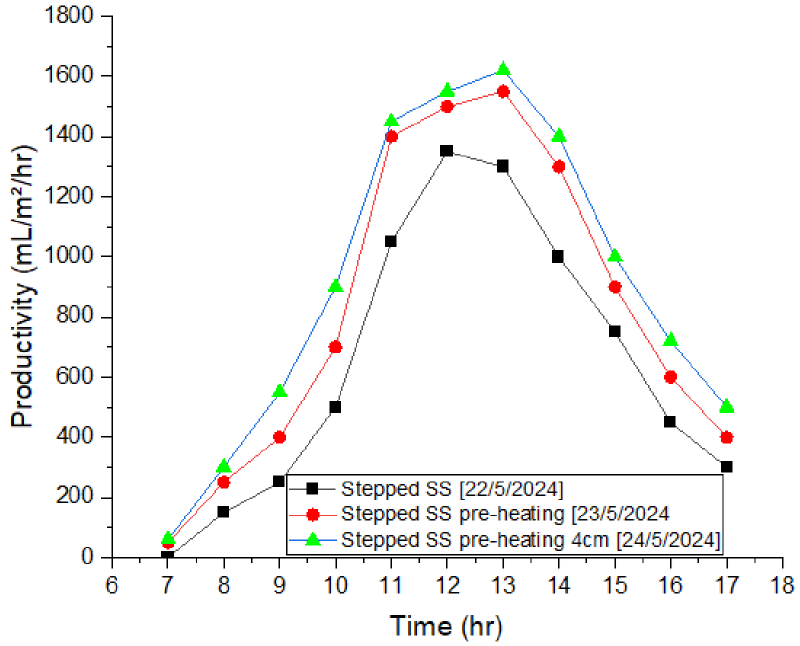
1800
1600
1400
1200
1000
800
600
400
200
0
Productivity (mL/m²/hr)
6
7
8
9
10
11
12
13
14
15
16
17
18
Time (hr)
Stepped SS [22/5/2024]
Stepped SS pre-heating [23/5/2024
Stepped SS pre-heating 4cm [24/5/2024]

D

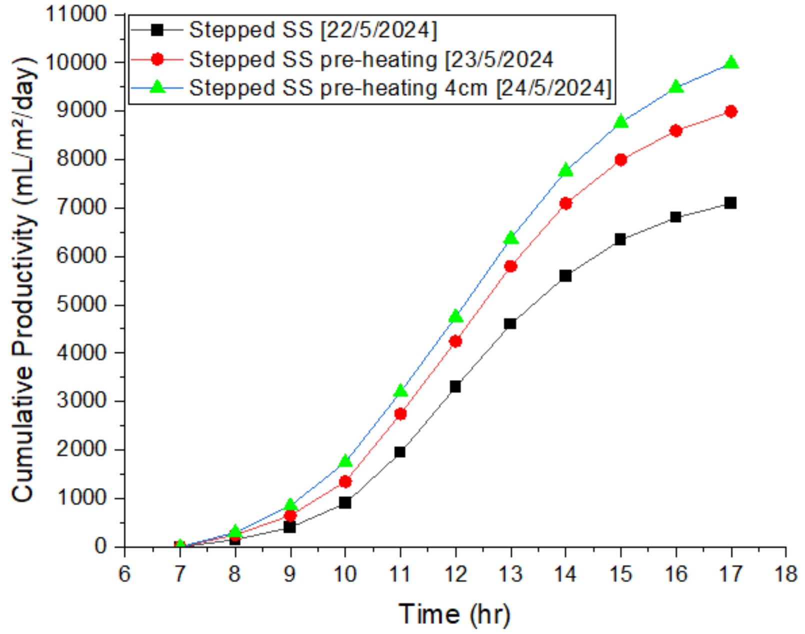
11000
10000
9000
8000
7000
6000
5000
4000
3000
2000
1000
0
Cumulative Productivity (mL/m²/day)
6
7
8
9
10
11
12
13
14
15
16
17
18
Time (hr)
Stepped SS [22/5/2024]
Stepped SS pre-heating [23/5/2024
Stepped SS pre-heating 4cm [24/5/2024]

E

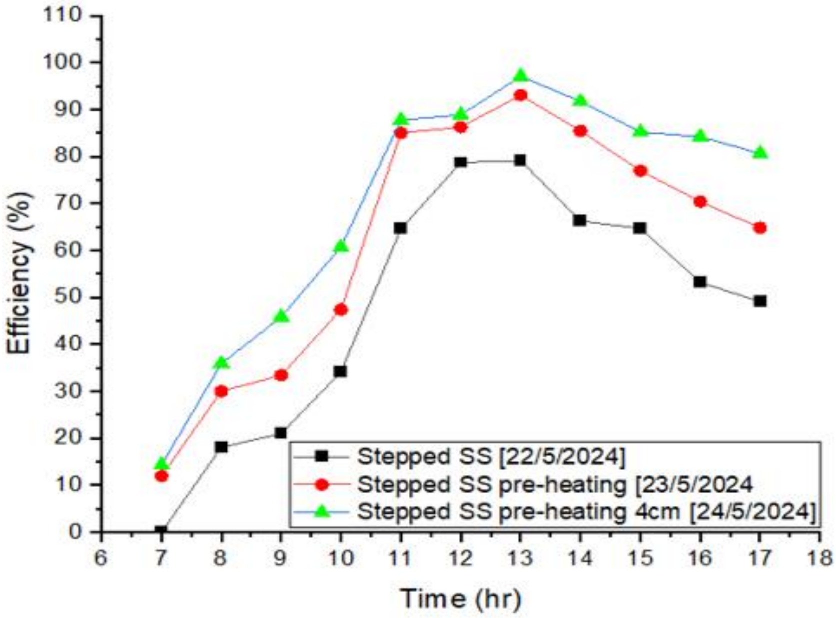

F

Figure 5. 12 Experimental results of tests carried out on stepped solar on May (A) solar still vs temperature of air (B) glass temperature (C) water temperature (D) Productivity (E) Cumulative productivity (F) Efficiency

5.7. Comparison of all studied cases

A comparison for all cases under study in May has been carried out to get the best design optimisation of the solar stills. Figure 5.13 (A) shows that the highest hourly productivity of stepped SS with preheating and 4cm black marble was 1620 mL/hr at 1 pm, with an increase of 47.27% compared to SSSS. In Figure 5.13 (B) the highest daily productivity of stepped SS with preheating and 4cm black marble was 9990 mL/day at 5 pm, with an increase of 75.57% compared to SSSS. The highest efficiency of stepped SS with preheating and 4cm black marble, as shown in Figure 5.13 (C) was 97.07 %, with an increase of 30% compared to SSSS, which has an efficiency of 67.40%.

Table 5.2 summarises the results obtained for all cases under study.

Table 5. 2 summary of the results obtained for all cases under study in May

Case under study	Maximum productivity mL/hr	Maximum cumulative productivity mL/day	Maximum Efficiency (%) Using eq. (3-25)	Percentage increase of cumulative productivity compared to SSSS
SSSS	1100	5690	67.40%	
SSSS with pre-heating	1200	6860	72.65%	20.56%
SSSS with pre-heating and 4cm black marble	1450	8140	64.27%	43.05%
Stepped SS	1350	7100	79.14%	24.78%
Stepped SS with pre-heating	1550	9000	93.09%	58.17%
Stepped SS with pre-heating and 4cm black marble	1620	9990	97.07%	75.57%

The primary factor contributing to the peak production, cumulative productivity, and efficiency recorded in the stepped SS with pre-heating and 4cm black marble is the integration of three methodologies. Due to its shape, the stepped solar still offers an expanded surface area for evaporation compared to the SSSS. The stepped solar still has a surface area of 1.6 m^2, representing a 60% increase compared to the SSSS. The expanded area facilitates more effective water evaporation, and the stepped structure enhances the effective surface area exposed to solar radiation. Each stage creates an enormous expanse for water dispersion, augmenting the evaporation surface area. Research on solar distillation indicates that optimising the water surface area exposed to heat is critical for enhancing the evaporation rate. Also, the water vapour will condense faster on the glass cover, as the distance between the solar basin and the glass is smaller than in SSSS.

Furthermore, the preheating device allows the water to enter the system at an elevated temperature, requiring less thermal energy to attain the evaporation threshold. Preheating significantly decreases the time needed to evaporate water, mainly when used with the stepped design. The temperature disparity between the warmed water and the surrounding environment enhances thermodynamic evaporation conditions, increasing total system efficiency.

Furthermore, using heat-absorbing materials such as 4 cm of crushed marble amplifies heat absorption, augmenting the volume of evaporated water relative to the SSSS alone. Crushed marble has a substantial thermal mass, absorbing and retaining considerable heat. The extensive surface area promotes accelerated heat transfer to the water. When water contacts heated marble, it undergoes localised heating, facilitating quick evaporation despite less direct sunlight. This creates a more uniform and prolonged evaporation after 2 pm., where the solar radiation decreases until the sun sets, improving total water production.

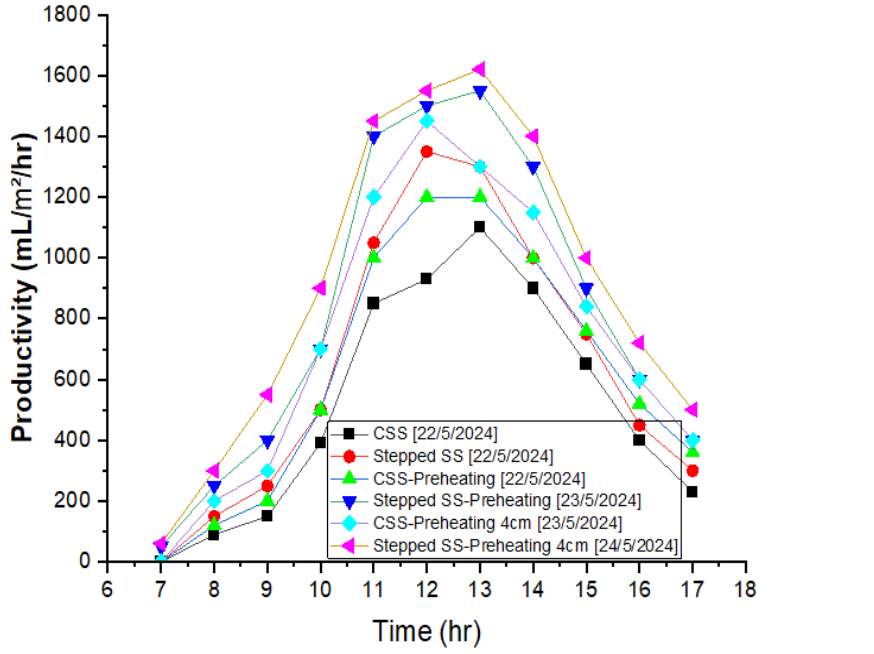

A

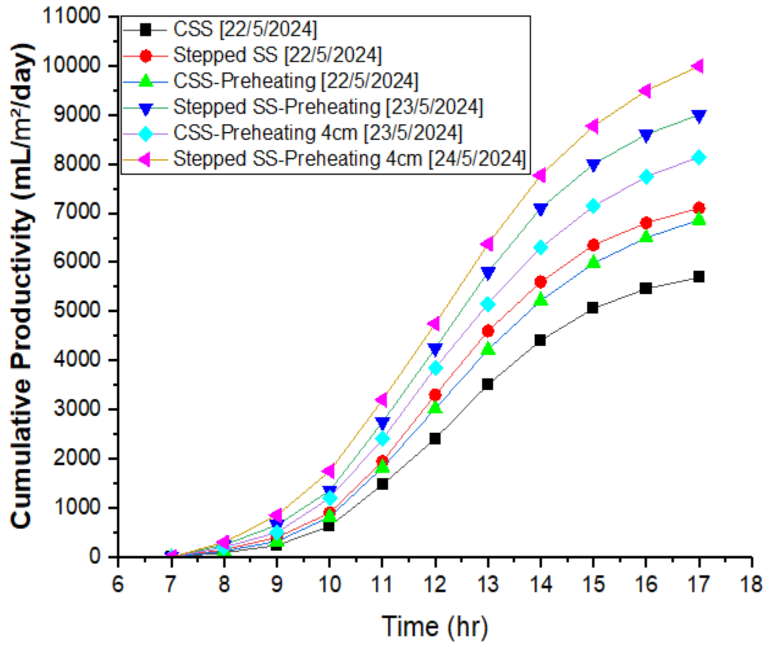

B

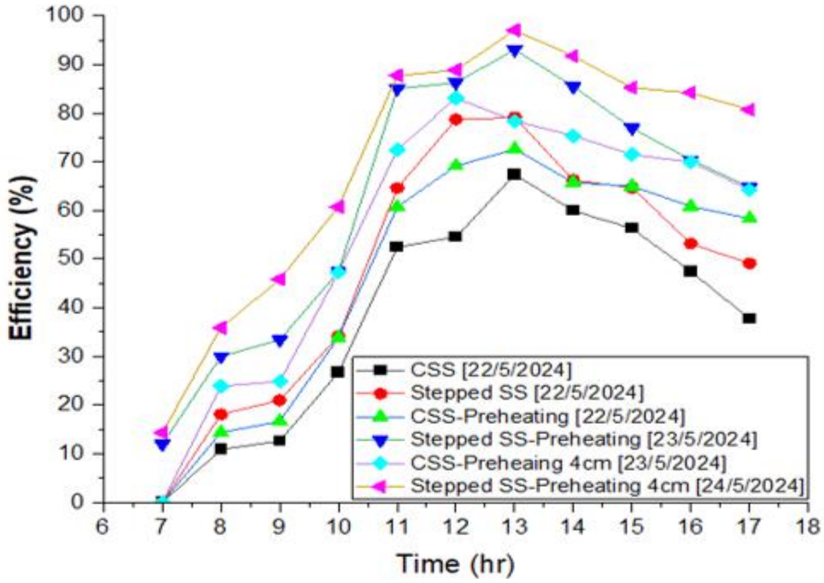

C

Figure 5. 13 Experimental results of tests carried out on SSSS and stepped SS alone were incorporated with different techniques in March, April, and May: (A) Productivity, (B) Cumulative productivity, and (C) Efficiency

Table 5.3 shows the economical side of the conducted work

Table 5. 3 Economical side of the conducted work

Item		**Cost**
SSSS		50000 IQD
Stepped solar still		75000 IQD
Absorbing materials (marble)		5000 IQD for each 20 kg

Chapter Six

Conclusions and Recommendations

6.1. Conclusion

The numerical and experimental findings of this study provide the following conclusions:

1) Applying CFD simulation is a powerful technique to predict and develop the SSSS for better efficiency. The CFD model can reduce the cost of experiments by suggesting suitable absorbing materials and practical design. The results from the current CFD model closely matched the experimental findings.

2) The percentage difference between measured and simulated temperatures, productivity, and cumulative productivity is lower than 5%, which indicates that the CFD model is accurate and suitable for enhancing the SSSS's efficiency.

3) The intensity of solar radiation has favourably influenced the production and efficiency of the solar system. An increase in radiation intensity correlates with heightened production and efficiency. The quality of the system diminishes around sunset. It was found that the peak output of distilled water occurs during five hours, from 10 a.m. to 3 p.m.

4) Using absorbing materials has increased the solar still efficiency by 19.94 % when using 4 cm of crushed black marble. This could be because the basin only submerged a small portion of the marble stone (maintaining the water level at 1 cm), causing the exposed portion to heat up more quickly than the submerged portion. When the size of the crushed marble was reduced (2 cm), productivity decreased; however, it was still higher than the productivity of SSSS by 29.72%.

5) The black natural leather has also increased the SS productivity by about 21.23% due to its high specific heat, which allows it to absorb heat despite its low thickness (2 mm).
6) The water temperature inside the SSSS when using the absorbing materials is high enough even after 5 p.m., indicating that the solar will still yield.
7) Using preheated water units has increased the SSSS and stepped solar still cumulative productivity by 20.56% and 58.17%, respectively, compared to SSSS. Preheating significantly enhances the productivity and efficiency of a solar still by elevating the water temperature before it enters the system, hence decreasing the energy required for evaporation. This expedites evaporation and enhances energy efficiency since less solar energy is used to heat the water.
8) Using stepped solar still has increased cumulative productivity by 24.78% compared to SSSS. The reason for this could be that the stepped solar still has enhanced the productivity and efficiency by increasing the evaporation surface area since the stepped solar still has a surface area of 1.6 m^2, representing a 60% increase compared to the SSSS, so exposing a greater volume of water to solar radiation. Also, the water vapour was condensed faster on the glass cover because the distance between the solar basin and the glass was smaller than in SSSS.
9) Using the combination (preheated water unit and absorbing materials) has increased the SSSS and stepped solar still cumulative productivity by 43.05% and 75.57%, respectively, compared to SSSS.
10) Comparing all the cases under study, the combination of three techniques (absorbing materials, preheated water unit, and stepped solar still) has the highest enhancement rate, about 75.57%, compared to SSSS.

6.2. Recommendations and future works

Various methods may be used to enhance the productivity and efficiency of the solar system, as outlined in the following points:

1) Increasing the evaporation using Fresnel lenses.
2) Increase the condensation by cooling the glass cover

References

[1] Akeel Salman Ahmoed, "AN EXPERIMENTAL STUDY THE PERFORMANCE OF SINGLE - SLOPE SOLAR STILL UTILIZING PARABOLIC TROUGH COLLECTOR WITH FRESNEL LENSES," Al-Furat Al-Awsat Technical University, Al-Najaf, 2023.

[2] S. A. Kalogirou, "Solar thermal collectors and applications," *Prog Energy Combust Sci*, vol. 30, no. 3, pp. 231–295, 2004, doi: 10.1016/j.pecs.2004.02.001.

[3] M. A. S. Malik, G. N. Tiwari, A. Kumar, and M. S. Sodha, "Solar distillation (a practical study of a wide range of stills and their optimum design, construction, and performance)," 1982.

[4] H. A. Kazem and M. T. Chaichan, "Status and future prospects of renewable energy in Iraq," *Renewable and Sustainable Energy Reviews*, vol. 16, no. 8, pp. 6007–6012, Oct. 2012, doi: 10.1016/j.rser.2012.03.058.

[5] M. S. Sachit, H. Z. M. Shafri, A. F. Abdullah, and A. S. M. Rafie, "Combining Re-Analyzed Climate Data and Landcover Products to Assess the Temporal Complementarity of Wind and Solar Resources in Iraq," *Sustainability*, vol. 14, no. 1, p. 388, 2021.

[6] Zahraa Abdulkareem Jaafar, "INVESTIGATION THE EFFECT OF ENHANCING EVAPORATION – CONDENSATION PROCESS ON A CONVENTIONAL SOLAR STILL PERFORMANCE," Al-Furat Al-Awsat Technical University, Al-Najaf., 2020.

[7] Doaa Chfat Hasan, "Thermal Design Of A Single Slope Solar Still With Preheater Unit By Fresnel Lens Applications," Al-Furat Al-Awsat Technical University, Al-Najaf, 2023.

[8] S. KALOGIROU, “Seawater desalination using renewable energy sources,” *Prog Energy Combust Sci*, vol. 31, no. 3, pp. 242–281, 2005, doi: 10.1016/j.pecs.2005.03.001.

[9] M. A. Sharaf, A. S. Nafey, and L. García-Rodríguez, “Exergy and thermo-economic analyses of a combined solar organic cycle with multi effect distillation (MED) desalination process,” *Desalination*, vol. 272, no. 1–3, pp. 135–147, May 2011, doi: 10.1016/j.desal.2011.01.006.

[10] E. Kabir, P. Kumar, S. Kumar, A. A. Adelodun, and K.-H. Kim, “Solar energy: Potential and future prospects,” *Renewable and Sustainable Energy Reviews*, vol. 82, pp. 894–900, Feb. 2018, doi: 10.1016/j.rser.2017.09.094.

[11] V. K. Chauhan, S. K. Shukla, J. V. Tirkey, and P. K. Singh Rathore, “A comprehensive review of direct solar desalination techniques and its advancements,” *J Clean Prod*, vol. 284, p. 124719, Feb. 2021, doi: 10.1016/j.jclepro.2020.124719.

[12] K. Kalidasa Murugavel, P. Anburaj, R. Samuel Hanson, and T. Elango, “Progresses in inclined type solar stills,” *Renewable and Sustainable Energy Reviews*, vol. 20, pp. 364–377, Apr. 2013, doi: 10.1016/j.rser.2012.10.047.

[13] Hussein Oleiwi Abdulridha, “Experimental Investigation for Performance of a Single Slope Solar Still Integrated with A Solar Collector and External Condenser System,” Al-Furat Al-Awsat Technical University, Al-Najaf., 2023.

[14] A. Muthu Manokar, K. Kalidasa Murugavel, and G. Esakkimuthu, “Different parameters affecting the rate of evaporation and condensation on passive solar still – A review,” *Renewable and Sustainable Energy Reviews*, vol. 38, pp. 309–322, Oct. 2014, doi: 10.1016/j.rser.2014.05.092.

[15] L. García-Rodríguez, “Assessment of most promising developments in solar desalination,” in *Solar desalination for the 21st century*, Springer, 2007, pp. 355–369.

[16] A. Kaushal and Varun, “Solar stills: A review,” *Renewable and Sustainable Energy Reviews*, vol. 14, no. 1, pp. 446–453, Jan. 2010, doi: 10.1016/j.rser.2009.05.011.

[17] P. Prakash and V. Velmurugan, “Parameters influencing the productivity of solar stills – A review,” *Renewable and Sustainable Energy Reviews*, vol. 49, pp. 585–609, Sep. 2015, doi: 10.1016/j.rser.2015.04.136.

[18] A. Muthu Manokar, K. Kalidasa Murugavel, and G. Esakkimuthu, “Different parameters affecting the rate of evaporation and condensation on passive solar still – A review,” *Renewable and Sustainable Energy Reviews*, vol. 38, pp. 309–322, Oct. 2014, doi: 10.1016/j.rser.2014.05.092.

[19] V. Sivakumar and E. Ganapathy Sundaram, “Improvement techniques of solar still efficiency: A review,” *Renewable and Sustainable Energy Reviews*, vol. 28, pp. 246–264, Dec. 2013, doi: 10.1016/j.rser.2013.07.037.

[20] V. Velmurugan and K. Srithar, “Performance analysis of solar stills based on various factors affecting the productivity—A review,” *Renewable and Sustainable Energy Reviews*, vol. 15, no. 2, pp. 1294–1304, Feb. 2011, doi: 10.1016/j.rser.2010.10.012.

[21] S. Yadav and K. Sudhakar, “Different domestic designs of solar stills: A review,” *Renewable and Sustainable Energy Reviews*, vol. 47, pp. 718–731, Jul. 2015, doi: 10.1016/j.rser.2015.03.064.

[22] T. Rajaseenivasan, K. K. Murugavel, T. Elango, and R. S. Hansen, “A review of different methods to enhance the productivity of the multi-effect

solar still," *Renewable and Sustainable Energy Reviews*, vol. 17, pp. 248–259, Jan. 2013, doi: 10.1016/j.rser.2012.09.035.

[23] K. Sampathkumar, T. V. Arjunan, P. Pitchandi, and P. Senthilkumar, "Active solar distillation—A detailed review," *Renewable and Sustainable Energy Reviews*, vol. 14, no. 6, pp. 1503–1526, Aug. 2010, doi: 10.1016/j.rser.2010.01.023.

[24] G. Xiao *et al.*, "A review on solar stills for brine desalination," *Appl Energy*, vol. 103, pp. 642–652, Mar. 2013, doi: 10.1016/j.apenergy.2012.10.029.

[25] K. Kalidasa Murugavel, P. Anburaj, R. Samuel Hanson, and T. Elango, "Progresses in inclined type solar stills," *Renewable and Sustainable Energy Reviews*, vol. 20, pp. 364–377, Apr. 2013, doi: 10.1016/j.rser.2012.10.047.

[26] V. Manikandan, K. Shanmugasundaram, S. Shanmugan, B. Janarthanan, and J. Chandrasekaran, "Wick type solar stills: A review," *Renewable and Sustainable Energy Reviews*, vol. 20, pp. 322–335, Apr. 2013, doi: 10.1016/j.rser.2012.11.046.

[27] C. Elango, N. Gunasekaran, and K. Sampathkumar, "Thermal models of solar still—A comprehensive review," *Renewable and Sustainable Energy Reviews*, vol. 47, pp. 856–911, Jul. 2015, doi: 10.1016/j.rser.2015.03.054.

[28] R. Sathyamurthy, H. J. Kennady, P. K. Nagarajan, and A. Ahsan, "Factors affecting the performance of triangular pyramid solar still," *Desalination*, vol. 344, pp. 383–390, Jul. 2014, doi: 10.1016/j.desal.2014.04.005.

[29] G. N. Tiwari, V. Dimri, and A. Chel, "Parametric study of an active and passive solar distillation system: Energy and exergy analysis," *Desalination*, vol. 242, no. 1–3, pp. 1–18, Jun. 2009, doi: 10.1016/j.desal.2008.03.027.

[30] G. N. Tiwari, S. K. Shukla, and I. P. Singh, "Computer modeling of passive/active solar stills by using inner glass temperature," *Desalination*, vol. 154, no. 2, pp. 171–185, Apr. 2003, doi: 10.1016/S0011-9164(03)80018-8.

[31] S. K. Nougriaya, M. K. Chopra, B. Gupta, P. Baredar, and H. Parmar, "Influence of basin water depth and energy storage materials on productivity of solar still: A review," *Mater Today Proc*, vol. 44, pp. 1589–1603, 2021, doi: 10.1016/j.matpr.2020.11.796.

[32] D. Dsilva Winfred Rufuss, S. Iniyan, L. Suganthi, and P. A. Davies, "Solar stills: A comprehensive review of designs, performance and material advances," *Renewable and Sustainable Energy Reviews*, vol. 63, pp. 464–496, Sep. 2016, doi: 10.1016/j.rser.2016.05.068.

[33] D. Das, U. Bordoloi, P. Kalita, R. F. Boehm, and A. D. Kamble, "Solar still distillate enhancement techniques and recent developments," *Groundw Sustain Dev*, vol. 10, p. 100360, Apr. 2020, doi: 10.1016/j.gsd.2020.100360.

[34] H. N. Panchal and P. K. Shah, "Charperformance analysis of different energy absorbing plates on solar stills," *Iranica Journal of Energy & Environment*, vol. 2, no. 4, 2011.

[35] D. W. Medugu and L. G. Ndatuwong, "Theoretical analysis of water distillation using solar still," *International Journal of Physical Sciences*, vol. 4, no. 11, pp. 705–712, 2009.

[36] Y. H. Zurigat and MousaK. Abu-Arabi, "Modeling and performance analysis of a solar desalination unit with double-glass cover cooling," *Desalination*, vol. 138, no. 1–3, p. 145, Sep. 2001, doi: 10.1016/S0011-9164(01)00256-9.

[37] N. Rahbar and J. A. Esfahani, "Productivity estimation of a single-slope solar still: Theoretical and numerical analysis," *Energy*, vol. 49, pp. 289–297, Jan. 2013, doi: 10.1016/j.energy.2012.10.023.

[38] N. Setoodeh, R. Rahimi, and A. Ameri, "Modeling and determination of heat transfer coefficient in a basin solar still using CFD," *Desalination*, vol. 268, no. 1–3, pp. 103–110, Mar. 2011, doi: 10.1016/j.desal.2010.10.004.

[39] V. Sivakumar, E. G. Sundaram, and M. Sakthivel, "Investigation on the effects of heat capacity on the theoretical analysis of single slope passive solar still," *Desalination Water Treat*, vol. 57, no. 20, pp. 9190–9202, Apr. 2016, doi: 10.1080/19443994.2015.1026284.

[40] H. Tanaka, "Monthly optimum inclination of glass cover and external reflector of a basin type solar still with internal and external reflector," *Solar Energy*, vol. 84, no. 11, pp. 1959–1966, Nov. 2010, doi: 10.1016/j.solener.2010.07.013.

[41] H. Tanaka, "A theoretical analysis of basin type solar still with flat plate external bottom reflector," *Desalination*, vol. 279, no. 1–3, pp. 243–251, Sep. 2011, doi: 10.1016/j.desal.2011.06.016.

[42] M. Boubekri and A. Chaker, "Yield of an improved solar still: numerical approach," *Energy Procedia*, vol. 6, pp. 610–617, 2011, doi: 10.1016/j.egypro.2011.05.070.

[43] P. K. Srivastava and S. K. Agrawal, "Experimental and theoretical analysis of single sloped basin type solar still consisting of multiple low thermal inertia floating porous absorbers," *Desalination*, vol. 311, pp. 198–205, Feb. 2013, doi: 10.1016/j.desal.2012.11.035.

[44] R. Manivel, S. Sivakumar, and D. D. Rufuss, “Experimental investigation of solar desalination system with roof heating,” *Int J Earth Sci Eng*, vol. 7, pp. 1459–1464, 2014.

[45] D. Dsilva, W. Rufuss, and S. Sivakumar, “Enhancing the performance by increasing the productivity of water in solar desalination system with roof heating,” *Int J Adv Technol Eng Res*, vol. 4, pp. 41–45, 2014.

[46] K. Kalidasa Murugavel, S. Sivakumar, J. Riaz Ahamed, Kn. K. S. K. Chockalingam, and K. Srithar, “Single basin double slope solar still with minimum basin depth and energy storing materials,” *Appl Energy*, vol. 87, no. 2, pp. 514–523, Feb. 2010, doi: 10.1016/j.apenergy.2009.07.023.

[47] K. Kalidasa Murugavel and K. Srithar, “Performance study on basin type double slope solar still with different wick materials and minimum mass of water,” *Renew Energy*, vol. 36, no. 2, pp. 612–620, Feb. 2011, doi: 10.1016/j.renene.2010.08.009.

[48] M. Abdelgaied, M. F. Seleem, and M. M. Bassuoni, “Recent technological advancements in membrane distillation and solar stills: preheating techniques, heat storage materials, and nanomaterials—a detailed review,” *Environmental Science and Pollution Research*, vol. 29, no. 26, pp. 38879–38898, 2022.

[49] S. Shoeibi, H. Kargarsharifabad, and N. Rahbar, “Effects of nano-enhanced phase change material and nano-coated on the performance of solar stills,” *J Energy Storage*, vol. 42, p. 103061, Oct. 2021, doi: 10.1016/j.est.2021.103061.

[50] T. Arunkumar *et al.*, “Energy efficient materials for solar water distillation - A review,” *Renewable and Sustainable Energy Reviews*, vol. 115, p. 109409, Nov. 2019, doi: 10.1016/j.rser.2019.109409.

[51] N. H. A. Rahim, “New method to store heat energy in horizontal solar desalination still,” *Renew Energy*, vol. 28, no. 3, pp. 419–433, Mar. 2003, doi: 10.1016/S0960-1481(02)00030-7.

[52] V. Velmurugan, K. J. Naveen Kumar, T. Noorul Haq, and K. Srithar, “Performance analysis in stepped solar still for effluent desalination,” *Energy*, vol. 34, no. 9, pp. 1179–1186, Sep. 2009, doi: 10.1016/j.energy.2009.04.029.

[53] M. Dashtban and F. F. Tabrizi, “Thermal analysis of a weir-type cascade solar still integrated with PCM storage,” *Desalination*, vol. 279, no. 1–3, pp. 415–422, Sep. 2011, doi: 10.1016/j.desal.2011.06.044.

[54] K. Swetha and J. Venugopal, “Experimental investigation of a single slope solar still using PCM,” *International Journal of Research in Environmental Science and Technology*, vol. 1, no. 4, pp. 30–33, 2011.

[55] O. Badran, “Theoretical analysis of solar distillation using active solar still,” *Int. J. of Thermal & Environmental Engineering*, vol. 3, no. 2, pp. 113–120, 2011.

[56] W. Su, J. Darkwa, and G. Kokogiannakis, “Review of solid–liquid phase change materials and their encapsulation technologies,” *Renewable and Sustainable Energy Reviews*, vol. 48, pp. 373–391, Aug. 2015, doi: 10.1016/j.rser.2015.04.044.

[57] E. Rubio-Cerda, M. A. Porta-Gándara, and J. L. Fernández-Zayas, “Thermal performance of the condensing covers in a triangular solar still,” *Renew Energy*, vol. 27, no. 2, pp. 301–308, Oct. 2002, doi: 10.1016/S0960-1481(01)00196-3.

[58] A. Kianifar, S. Zeinali Heris, and O. Mahian, “Exergy and economic analysis of a pyramid-shaped solar water purification system: Active and

passive cases," *Energy*, vol. 38, no. 1, pp. 31–36, Feb. 2012, doi: 10.1016/j.energy.2011.12.046.

[59] A. Ahsan, M. Imteaz, U. A. Thomas, M. Azmi, A. Rahman, and N. N. Nik Daud, "Parameters affecting the performance of a low cost solar still," *Appl Energy*, vol. 114, pp. 924–930, Feb. 2014, doi: 10.1016/j.apenergy.2013.08.066.

[60] W. Jamal and M. A. Siddiqui, "Effect of water depth and still orientation on productivity for passive solar distillation," *Int J Eng Res Appl*, vol. 2, no. 2, pp. 1659–1665, 2012.

[61] T. Arunkumar, R. Jayaprakash, A. Prakash, P. U. Suneesh, M. Karthik, and S. Kumar, "Study of thermo physical properties and an improvement in production of distillate yield in pyramid solar still with boosting mirror," *Indian J Sci Technol*, vol. 3, no. 8, pp. 879–884, 2010.

[62] Z. Chen *et al.*, "Analysis of the characteristics of heat and mass transfer of a three-effect tubular solar still and experimental research," *Desalination*, vol. 330, pp. 42–48, Dec. 2013, doi: 10.1016/j.desal.2013.09.017.

[63] N. Rahbar, J. A. Esfahani, and E. Fotouhi-Bafghi, "Estimation of convective heat transfer coefficient and water-productivity in a tubular solar still – CFD simulation and theoretical analysis," *Solar Energy*, vol. 113, pp. 313–323, Mar. 2015, doi: 10.1016/j.solener.2014.12.032.

[64] A. Ahsan, M. Imteaz, A. Rahman, B. Yusuf, and T. Fukuhara, "Design, fabrication and performance analysis of an improved solar still," *Desalination*, vol. 292, pp. 105–112, Apr. 2012, doi: 10.1016/j.desal.2012.02.013.

[65] T. Arunkumar *et al.*, “An experimental study on a hemispherical solar still,” *Desalination*, vol. 286, pp. 342–348, Feb. 2012, doi: 10.1016/j.desal.2011.11.047.

[66] R. Dev, H. N. Singh, and G. N. Tiwari, “Characteristic equation of double slope passive solar still,” *Desalination*, vol. 267, no. 2–3, pp. 261–266, Feb. 2011, doi: 10.1016/j.desal.2010.09.037.

[67] H. Aburideh, A. Deliou, B. Abbad, F. Alaoui, D. Tassalit, and Z. Tigrine, “An Experimental Study of a Solar Still: Application on the sea water desalination of Fouka,” *Procedia Eng*, vol. 33, pp. 475–484, 2012, doi: 10.1016/j.proeng.2012.01.1227.

[68] M. R. Rajamanickam and A. Ragupathy, “Influence of Water Depth on Internal Heat and Mass Transfer in a Double Slope Solar Still,” *Energy Procedia*, vol. 14, pp. 1701–1708, 2012, doi: 10.1016/j.egypro.2011.12.1155.

[69] T. Abderachid and K. Abdenacer, “Effect of orientation on the performance of a symmetric solar still with a double effect solar still (comparison study),” *Desalination*, vol. 329, pp. 68–77, Nov. 2013, doi: 10.1016/j.desal.2013.09.011.

[70] M. Boukar and A. Harmim, “Parametric study of a vertical solar still under desert climatic conditions,” *Desalination*, vol. 168, pp. 21–28, Aug. 2004, doi: 10.1016/j.desal.2004.06.165.

[71] H. Tanaka, “Experimental study of vertical multiple-effect diffusion solar still coupled with a flat plate reflector,” *Desalination*, vol. 249, no. 1, pp. 34–40, Nov. 2009, doi: 10.1016/j.desal.2008.10.022.

[72] H. Tanaka and Y. Nakatake, “A simple and highly productive solar still: a vertical multiple-effect diffusion-type solar still coupled with a flat-plate

mirror," *Desalination*, vol. 173, no. 3, pp. 287–300, Mar. 2005, doi: 10.1016/j.desal.2004.08.035.

[73] A. A. El-Sebaii, "Parametric study of a vertical solar still," *Energy Convers Manag*, vol. 39, no. 13, pp. 1303–1315, Sep. 1998, doi: 10.1016/S0196-8904(98)00011-9.

[74] S. Aboul-Enein, A. A. El-Sebaii, and E. El-Bialy, "Investigation of a single-basin solar still with deep basins," *Renew Energy*, vol. 14, no. 1–4, pp. 299–305, May 1998, doi: 10.1016/S0960-1481(98)00081-0.

[75] M. S. Sodha, A. Kumar, G. N. Tiwari, and R. C. Tyagi, "Simple multiple wick solar still: Analysis and performance," *Solar Energy*, vol. 26, no. 2, pp. 127–131, 1981, doi: 10.1016/0038-092X(81)90075-X.

[76] S. Suneja and G. N. Tiwari, "Optimization of number of effects for higher yield from an inverted absorber solar still using the Runge-Kutta method," *Desalination*, vol. 120, no. 3, pp. 197–209, Dec. 1998, doi: 10.1016/S0011-9164(98)00218-5.

[77] H. Tanaka, T. Nosoko, and T. Nagata, "Experimental study of basin-type, multiple-effect, diffusion-coupled solar still," *Desalination*, vol. 150, no. 2, pp. 131–144, Nov. 2002, doi: 10.1016/S0011-9164(02)00938-4.

[78] H. Tanaka, "Tilted wick solar still with flat plate bottom reflector," *Desalination*, vol. 273, no. 2–3, pp. 405–413, Jun. 2011, doi: 10.1016/j.desal.2011.01.073.

[79] H. Al-Hinai, M. S. Al-Nassri, and B. A. Jubran, "Parametric investigation of a double-effect solar still in comparison with a single-effect solar still," *Desalination*, vol. 150, no. 1, pp. 75–83, Oct. 2002, doi: 10.1016/S0011-9164(02)00931-1.

[80] A. A. El-Sebaii, “Thermal performance of a triple-basin solar still,” *Desalination*, vol. 174, pp. 23–37, Apr. 2005, doi: 10.1016/j.desal.2004.08.038.

[81] G. M. Cappelletti, “An experiment with a plastic solar still,” *Desalination*, vol. 142, no. 3, pp. 221–227, Mar. 2002, doi: 10.1016/S0011-9164(02)00203-5.

[82] M. K. Phadatare and S. K. Verma, “Influence of water depth on internal heat and mass transfer in a plastic solar still,” *Desalination*, vol. 217, no. 1–3, pp. 267–275, Nov. 2007, doi: 10.1016/j.desal.2007.03.006.

[83] A. Madhlopa and C. Johnstone, “Numerical study of a passive solar still with separate condenser,” *Renew Energy*, vol. 34, no. 7, pp. 1668–1677, Jul. 2009, doi: 10.1016/j.renene.2008.12.032.

[84] F. Nematollahi, A. Rahimi, and T. T. Gheinani, “Experimental and theoretical energy and exergy analysis for a solar desalination system,” *Desalination*, vol. 317, pp. 23–31, May 2013, doi: 10.1016/j.desal.2013.02.021.

[85] M. Arslan, “Experimental investigation of still performance for different active solar still designs under closed cycle mode,” *Desalination*, vol. 307, pp. 9–19, Dec. 2012, doi: 10.1016/j.desal.2012.09.003.

[86] T. Rajaseenivasan, P. Nelson Raja, and K. Srithar, “An experimental investigation on a solar still with an integrated flat plate collector,” *Desalination*, vol. 347, pp. 131–137, Aug. 2014, doi: 10.1016/j.desal.2014.05.029.

[87] A. E. Kabeel, A. Khalil, Z. M. Omara, and M. M. Younes, “Theoretical and experimental parametric study of modified stepped solar still,”

Desalination, vol. 289, pp. 12–20, Mar. 2012, doi: 10.1016/j.desal.2011.12.023.

[88] O. O. Badran, "Experimental study of the enhancement parameters on a single slope solar still productivity," *Desalination*, vol. 209, no. 1–3, pp. 136–143, Apr. 2007, doi: 10.1016/j.desal.2007.04.022.

[89] H. Taghvaei *et al.*, "A thorough investigation of the effects of water depth on the performance of active solar stills," *Desalination*, vol. 347, pp. 77–85, Aug. 2014, doi: 10.1016/j.desal.2014.05.038.

[90] M. A. Eltawil and Z. M. Omara, "Enhancing the solar still performance using solar photovoltaic, flat plate collector and hot air," *Desalination*, vol. 349, pp. 1–9, Sep. 2014, doi: 10.1016/j.desal.2014.06.021.

[91] S. Kumar, A. Dubey, and G. N. Tiwari, "A solar still augmented with an evacuated tube collector in forced mode," *Desalination*, vol. 347, pp. 15–24, Aug. 2014, doi: 10.1016/j.desal.2014.05.019.

[92] E. G. Marı, R. P. G. Colomer, and C. A. Blaise-Ombrecht, "Performance analysis of a solar still integrated in a greenhouse," *Desalination*, vol. 203, no. 1–3, pp. 435–443, Feb. 2007, doi: 10.1016/j.desal.2006.04.020.

[93] A. A. El-Sebaii, S. Aboul-Enein, M. R. I. Ramadan, and A. M. Khallaf, "Thermal performance of an active single basin solar still (ASBS) coupled to shallow solar pond (SSP)," *Desalination*, vol. 280, no. 1–3, pp. 183–190, Oct. 2011, doi: 10.1016/j.desal.2011.07.004.

[94] J. A. Esfahani, N. Rahbar, and M. Lavvaf, "Utilization of thermoelectric cooling in a portable active solar still — An experimental study on winter days," *Desalination*, vol. 269, no. 1–3, pp. 198–205, Mar. 2011, doi: 10.1016/j.desal.2010.10.062.

[95] Z. S. Abdel-Rehim and A. Lasheen, “Experimental and theoretical study of a solar desalination system located in Cairo, Egypt,” *Desalination*, vol. 217, no. 1–3, pp. 52–64, Nov. 2007, doi: 10.1016/j.desal.2007.01.012.

[96] T. Arunkumar, D. Denkenberger, A. Ahsan, and R. Jayaprakash, “The augmentation of distillate yield by using concentrator coupled solar still with phase change material,” *Desalination*, vol. 314, pp. 189–192, Apr. 2013, doi: 10.1016/j.desal.2013.01.018.

[97] F. F. Tabrizi and A. Z. Sharak, “Experimental study of an integrated basin solar still with a sandy heat reservoir,” *Desalination*, vol. 253, no. 1–3, pp. 195–199, Apr. 2010, doi: 10.1016/j.desal.2009.10.003.

[98] K. Sampathkumar and P. Senthilkumar, “Utilization of solar water heater in a single basin solar still—An experimental study,” *Desalination*, vol. 297, pp. 8–19, Jul. 2012, doi: 10.1016/j.desal.2012.04.012.

[99] A. S. Abdullah, “Improving the performance of stepped solar still,” *Desalination*, vol. 319, pp. 60–65, Jun. 2013, doi: 10.1016/j.desal.2013.04.003.

[100] A. M. El-Zahaby, A. E. Kabeel, A. I. Bakry, S. A. El-Agouz, and O. M. Hawam, “Enhancement of solar still performance using a reciprocating spray feeding system—An experimental approach,” *Desalination*, vol. 267, no. 2–3, pp. 209–216, Feb. 2011, doi: 10.1016/j.desal.2010.09.028.

[101] M. Younes, W. H. Alawee, A. S. Abdullah, Z. Omara, and F. A. Essa, “Techniques used to reduce back wall losses of solar stills - A review,” *Journal of Contemporary Technology and Applied Engineering*, vol. 1, no. 1, pp. 62–74, Oct. 2022, doi: 10.21608/jctae.2022.158802.1008.

[102] A. S. Zedan and S. A. M. Nasr Eldin, “An Experimental Investigation of the Factors Which Affect on the Performance of a Single Basin Typical

Double Slope Solar Still for Water Desalination," *Energy Power Eng*, vol. 07, no. 06, pp. 270–277, 2015, doi: 10.4236/epe.2015.76026.

[103] V. S. Winstor Jebakumar and S. Dharmalingam, "http://www.deswater.com/DWT_abstracts/vol_212/212_2021_v.pdf," *Desalination Water Treat*, vol. 212, pp. 1–7, 2021, doi: 10.5004/dwt.2021.26634.

[104] A. S. Abdullah, L. Hadj-Taieb, M. M. Hikal, Z. M. Omara, and M. M. Younes, "Enhancing a solar still's performance by preheating the feed water and employing phase-change material," *Alexandria Engineering Journal*, vol. 77, pp. 395–405, Aug. 2023, doi: 10.1016/j.aej.2023.07.002.

[105] V. R. Khare, A. P. Singh, H. Kumar, and R. Khatri, "Modelling and Performance Enhancement of Single Slope Solar Still Using CFD," *Energy Procedia*, vol. 109, pp. 447–455, Mar. 2017, doi: 10.1016/j.egypro.2017.03.064.

[106] M. S. El-Sebaey, A. Ellman, A. Hegazy, and T. Ghonim, "Experimental analysis and CFD modeling for conventional basin-type solar still," *Energies (Basel)*, vol. 13, no. 21, p. 5734, 2020.

[107] H. G. Hameed, H. A. N. Diabil, and M. A. Al-Moussawi, "A numerical investigation of the enhancement of single-slope single-basin solar still productivity," *Energy Reports*, vol. 9, pp. 484–500, Dec. 2023, doi: 10.1016/j.egyr.2022.11.199.

[108] S. Gorjian, B. Ghobadian, T. Tavakkoli Hashjin, and A. Banakar, "Experimental performance evaluation of a stand-alone point-focus parabolic solar still," *Desalination*, vol. 352, pp. 1–17, Nov. 2014, doi: 10.1016/j.desal.2014.08.005.

[109] C. Multiphysics, “Fluid governing equations. What are the Navier–Stokes equations,” 2021.

[110] S. A. Kalogirou, *Solar energy engineering: processes and systems*. Elsevier, 2023.

[111] J. C. Torchia-Núñez, J. Cervantes-de-Gortari, and M. A. Porta-Gándara, “Thermodynamics of a Shallow Solar Still,” *Energy Power Eng*, vol. 06, no. 09, pp. 246–265, 2014, doi: 10.4236/epe.2014.69022.

[112] G. Mittal, “An unsteady CFD modelling of a single slope solar still,” *Mater Today Proc*, vol. 46, pp. 10991–10995, 2021, doi: 10.1016/j.matpr.2021.02.090.

[113] H. Fadhel, Q. A. Abed, and D. M. Hachim, “Numerical simulation of heat exchanger inside the single solar still with PTC,” 2023, p. 050009. doi: 10.1063/5.0136232.

[114] S. K. Singh, S. C. Kaushik, V. V. Tyagi, and S. K. Tyagi, “Comparative Performance and parametric study of solar still: A review,” *Sustainable Energy Technologies and Assessments*, vol. 47, p. 101541, Oct. 2021, doi: 10.1016/j.seta.2021.101541.

[115] S. Kumar Nougriaya, M. K. Chopra, B. Gupta, and P. Baredar, “Stepped solar still: A review on designs analysis,” *Mater Today Proc*, vol. 46, pp. 5647–5660, 2021, doi: 10.1016/j.matpr.2020.09.598.

[116] April weather, “Spring 2024 ,” *Najaf, Iraq (weather-atlas.com)*.

[117] E. Papanicolaou, K. Voropoulos, and V. Belessiotis, “NATURAL CONVECTIVE HEAT TRANSFER IN AN ASYMMETRIC GREENHOUSE-TYPE SOLAR STILL--EFFECT OF ANGLE OF INCLINATION,” *Numeri Heat Transf A Appl*, vol. 42, no. 8, pp. 855–880, Dec. 2002, doi: 10.1080/104077802900598

Appendix A: Density, specific heat, and viscosity of water-liquids as functions of temperature

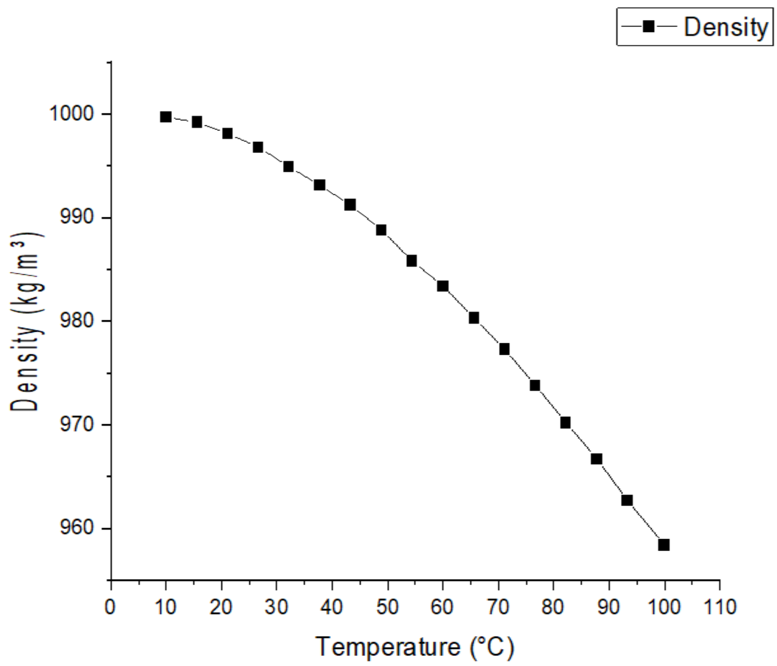

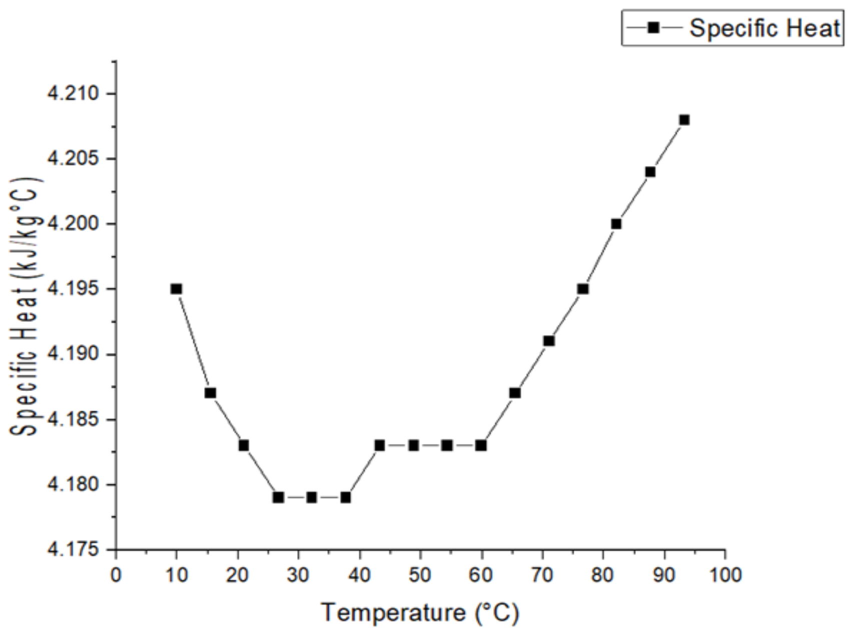

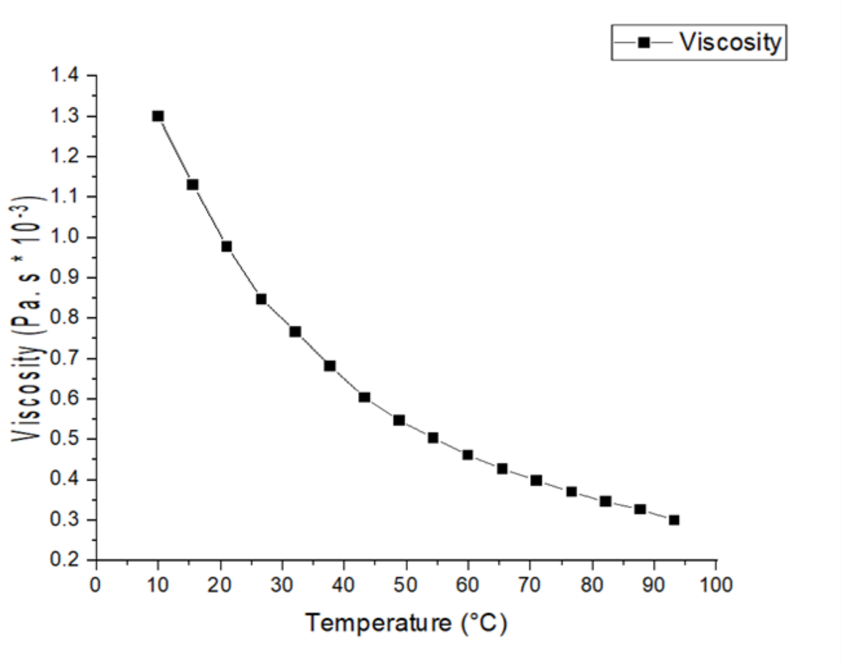

Figure (A) Density, specific heat, and viscosity of water-liquids as functions of temperature

Appendix B: Solar Power Meter Calibration

This investigation used a solar power meter to quantify global radiation. It was employed because it was simple to use and had adequate accuracy. The device may be simply calibrated using compatible equipment with an accurate measurement standard. The meteorological station at Al-Najaf Airport / Iraq has been chosen as a benchmark for calibrating the pyrometer. With the capacity to measure solar radiation ranging from 0 - 1368 W/m^2 and with an accuracy of ±0.3%. Values between 0 and 1365 W/m^2 were acquired for calibration as in Figure below:

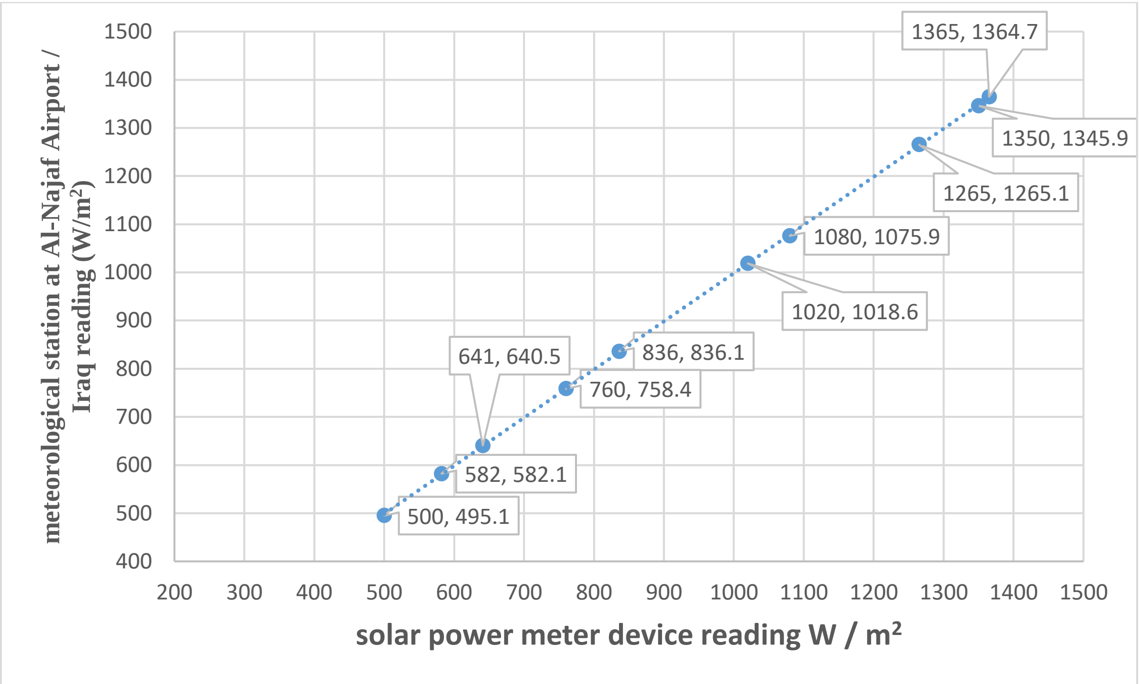

Figure (B) Solar Power Meter Calibration

Appendix C: Wind Velocity Calibration

The Anemometer was used in all the trials to quantify the velocity of the wind. It was chosen for its user-friendly design and easy handling in all experimental circumstances. The anemometer was calibrated using wind speed data from the meteorological station at Al-Najaf Airport in Iraq. It has a wind speed range of 0.1 to 89 m/s with an accuracy of ± 5%. As seen in the Figure below:

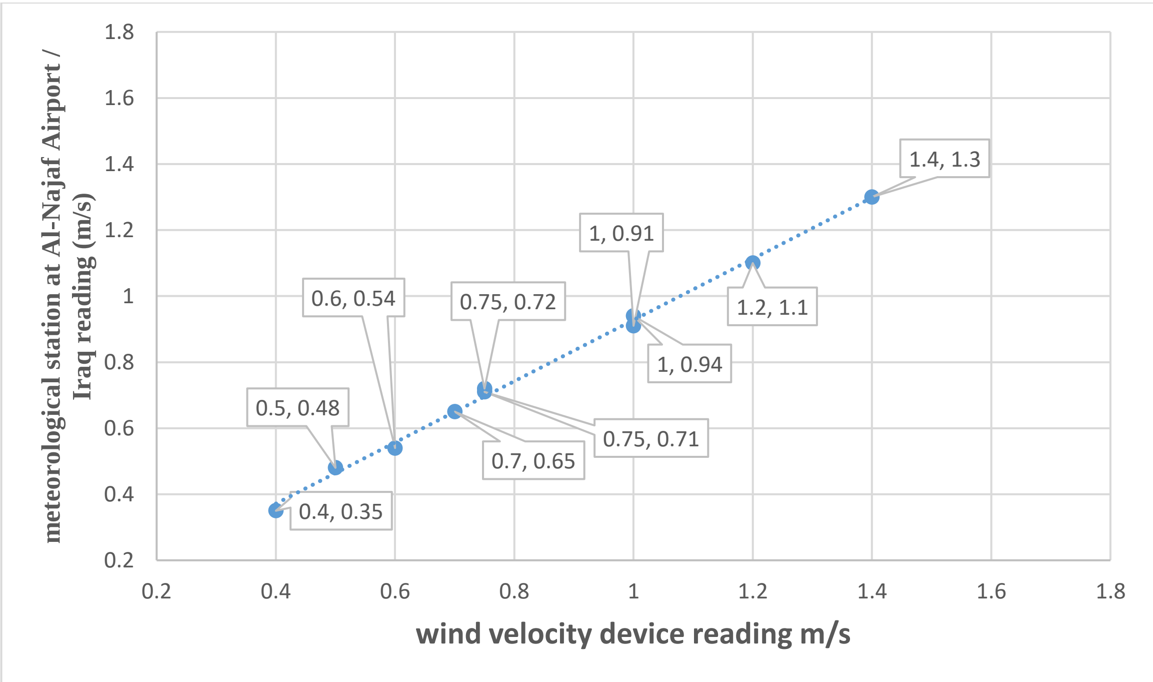

Figure (C) Wind Velocity Calibration

Appendix D: Acceptance Paper

NUMERICAL HEAT TRANSFER, PART A: APPLICATIONS
2024, VOL. , NO. ,
https://

Taylor & Francis
Taylor & Francis Group

OPEN ACCESS Check for updates

Increasing the productivity of single slope solar still using absorbing materials: a numerical and experimental study

Mays Alaa. Noori[1], Almoussawi Montadhar. Aboodi.[2],*, Basil Noori. Merzah[3] , Masoumah Faraji[4]

1,2,3 Engineering Technical College of Najaf, Al-Furat Al-Awsat Technical University, Najaf, Iraq 3001

4 Coventry University, centre of manufacturing and materials, Coventry, UK.

ABSTRACT

The demand for freshwater is increasing due to diverse human activities and a rapidly growing worldwide population. The extensive use of conventional fuel sources for freshwater production contributes to environmental contamination, prompting the exploration of alternative solutions like solar energy. There needs to be more access to clean water in rural locations around the world. People have created various desalination technologies to address this problem. This study applied an effective numerical CFD model to simulate the evaporation-condensation process and productivity of a single-slope solar still (SSSS). The model is based on the evaporation-condensation mechanism, which involves three phases of fluids: air, water liquid, and water vapor. In the model, solar radiation was the only source of heating, and the density, specific heat, and viscosity of water liquids were considered to be temperature-dependent. We calculated and validated the temperature, productivity, and efficiency by comparing them with previous published work. The model aims to analyze the experiments and select the most appropriate absorbing material for the solar still's basin. The SSSS basin utilized a variety of absorbent materials, such as crushed black marble in varying sizes (0.5–4 cm) and natural black leather. We determined the best material based on the highest productivity of SSSS. It was found that crushed black marble with a size of 4 cm and 2 cm yielded the highest productivity of 7 kg/day and 6.5 kg/day, respectively, while natural black leather produced 6 kg of productivity. The experiments yielded results in agreement with the CFD model. The main objective of this study is to use the CFD model to represent an effective and promising technique for developing the efficiency of solar stills. Furthermore, the study investigated how to improve the efficiency and productivity of the CSSSS by incorporating new absorbent materials such as marble and black leather.

ARTICLE HISTORY
Received
Accepted

KEYWORDS
Solar still, CFD, productivity, absorbing materials

1. Introduction

The most prominent indication of the water crisis is the shortage of safe and inexpensive water for home use among 1.2 billion individuals [1]. Generally speaking, there is a need for more documentation regarding the significant proportion of the 900 million individuals residing in rural regions whose income falls below the poverty threshold of one dollar per day and who face a lack of access to water essential for their sustenance. Insufficient water accessibility significantly affects individuals' welfare [1].

CONTACT M. A. Almoussawi mun.inj@atu.edu.iq Engineering Technical College of Najaf, Al-Furat Al-Awsat Technical University, Najaf, Iraq 3001

Appendix E: Acceptance Paper

Mays A. Noori <mays.ms.etcn2@student.atu.edu.iq>

ESM'2024 RESULT

2 messages

Philippe Geril <philippe.geril@eurosis.org> Sun, Aug 25, 2024 at 6:05 PM
To: mays.ms.etcn2@student.atu.edu.iq, inj.mun@atu.edu.iq, coj.bas@atu.edu.iq

Dear Mays,

I have the pleasure to announce that the paper
you submitted for ESM'2024, which will be held at the
University of the Basque Country, San Sebastian, Spain
from October 23-25, 2024, has been accepted as a

REGULAR 5 PAGE PAPER

for the aforementioned conference.

The paper code for this paper is:

SIM_METH_01
A Numerical Model for Single Slope Solar Still

(USE YOUR CODE NUMBER IN ALL FURTHER COMMUNICATION)

Enclosed in this email are your paper files and reviews

The authorkit consists of:
- acceptxx.doc: acceptance letter
- authagre.doc: author agreement form (*)
- authfinxxx.doc: author registration form (*)
- authin3xxx.doc: author instructions
- authinnew2023.doc: paper formatting instructions WHICH HAVE TO BE FOLLOWED TO THE LETTER
- authkeyw.doc: keywords (*)
- biograph.doc: biography info (*)
- copyrigh.doc: the copyright form (*)

Appendix F: Published Paper

Journal of Contemporary Technology and Applied Engineering (JCTAE), 3(1), 2024, 32-53

DOI: 10.21608/JCTAE.2024.289814.1027 Published by: *Faculty of Engineering, Kafrelsheikh University*

THE LATEST DEVELOPMENT IN WATER DISTILLATION: A REVIEW

Received: 15-05-2024
Accepted: 28-05-2024

A.N. Mays [a], M.A. Al-Moussawi [a,*], N.M. Basil [a]

[a] *Engineering Technical College of Najaf, Al-Furat Al-Awsat Technical University, Najaf, Iraq*

[*] corresponding author: M.A. Al-Moussawi (inj.mun@atu.edu.iq)

ABSTRACT. The global freshwater demand production is steadily growing due to demographic expansion and industrial expansion. The utilization of desalination technology is experiencing a rise in order to fulfill this growing demand. SSs, a type of desalination technology, possess the advantages of low maintenance and affordability. Nevertheless, their productivity is constrained. This paper aims to offer an extensive examination of different classifications of SS. This includes an analysis of designs that are both passive and active, as well as both single- and multiple-effect variations. Additionally, the paper will explore various enhancements aimed at increasing productivity, such as the implementation of reflectors, mechanisms for storing heat, fins, collectors, and techniques for improving thermal and fluid transport. The inclusion of greenhouse and photovoltaic-thermal SS is additionally encompassed within the scope of this study. The capabilities of PCM in improving performance are highly encouraging, suggesting the need for future research in these and related domains to promote wider adoption of SS technology.

KEYWORDS: Solar stills; Development; Productivity; Distillation.

1. INTRODUCTION

Insufficiency of water poses a significant worldwide dilemma. According to projections, by 2025, approximately 25% of the global population is expected to encounter water scarcity, while approximately 66% will face water-stressed conditions. According to a study, it is estimated that by 2030, approximately 50% of the worldwide populace will encounter significant hydrological scarcity [1]. Currently, regions in Africa are facing significant hydrological scarcity, impacting approximately 31% of the populace. Asia, America, and Europe follow this, where Severe water scarcity affects 25%, 7%, and 2% of the population, respectively [2-5]. The utilization of desalination is increasingly significant in addressing the need for potable water.

Numerous techniques exist for the desalination of seawater and brackish water. The category includes a range of techniques such as flash distillation, multi-effect distillation, membrane distillation, reverse osmosis, forward osmosis, ion exchange, capacitive deionization, electrodialysis, and seawater greenhouse technology [6,7]. The energy needed for desalination can be obtained from either traditional fossil fuels or alternative sources of energy such as biomass, wind, solar, geothermal energy, or industrial waste heat. SSs possess several advantages within the realm of solar desalination, namely their simplicity, affordability, ease of maintenance, and minimal ecological footprint. Nevertheless, it is important to acknowledge that these technologies also possess certain drawbacks, notably their subpar performance, which acts as a deterrent to their widespread adoption in commercial settings.

SSs function on the basis of the principles of evaporation and condensation. Solar energy is utilized to evaporate the brine contained within the SS, resulting in the collection of condensed water as the output of purified water. Within a dual-or multi-effect SS, the procedure above is iterated in a manner that utilizes the heat generated during condensation to facilitate a subsequent evaporation phase. The utilization of multiple effects has been observed to enhance performance; however, it is accompanied by a concomitant cost penalty. The utilization of dynamic elements, such as pumps and fans, presents an alternative approach to enhance performance; however, it also entails certain drawbacks in terms of increased expenses and heightened intricacy.

The quantification of a SS's performance can be assessed through the metrics of efficiency and productivity. The efficiency of a singular-effect still can be described as the proportion of stored thermal

الخلاصة

تم إجراء الدراسة العددية باستخدام برنامج ANSYS Fluent الإصدار 18.2. تم استخدام نموذج عددي لديناميكا الموائع الحاسوبية (CFD) لاختيار أفضل المواد الماصة. المواد الماصة المستخدمة في هذا العمل كانت الرخام الأسود المهشم بأحجام متوسطة مختلفة (0.5–4 سم) والجلد الأسود الطبيعي، وهما من المواد المتوفرة بسهولة وذات تكلفة منخفضة.

وُجد أن الرخام الأسود المهشم بحجم 4 سم و2 سم أعطى أعلى إنتاجية بلغت 6035 مل/اليوم و5760 مل/اليوم على التوالي، بينما أنتج الجلد الأسود الطبيعي 5600 مل/اليوم. أظهرت النتائج توافقًا كبيرًا بين النتائج التجريبية لهذه الدراسة والبيانات العددية. تم التحقق من صحة نتائج CFD من خلال المقارنة مع أعمال منشورة سابقة وكذلك مع النتائج التجريبية، حيث أظهرت نسبة خطأ أقل من 0.5%

تم إجراء الاختبارات التجريبية في أيام محددة من شهري مارس وأبريل ومايو وفي أوقات معينة، بدءًا من الساعة 7 صباحًا وحتى الساعة 5 مساءً .تشير النتائج من الدراسات التجريبية والعددية إلى أن التقنيات المستخدمة في هذا العمل يمكن أن تعزز أداء المقطر الشمسي. وقد يتحقق ذلك عن طريق تحسين إنتاجية المقطر من خلال رفع درجة حرارة الماء وتسهيل عملية التبخر السريع.

كان استخدام مقطر شمسي مدرج مزود بمواد ماصة ووحدة تسخين مسبق هو الطريقة الأكثر فعالية لتحقيق هذا الهدف. وكانت وظيفة المواد الماصة أقل تأثيرًا نسبيًا مقارنة بوظيفة المقطر المدرج ووحدة التسخين المسبق. وبالتالي، فإن الاستخدام المدمج لهذه الاستراتيجيات (المقطر الشمسي المدرج مع وحدة تسخين مسبق ومادة الرخام المهشم بحجم 4 سم) أدى إلى تحسين كفاءة وإنتاجية المياه العذبة للمقطر الشمسي بنسبة 44.02% و75.57% على التوالي مقارنة بالمقطرات الشمسية التقليدية.

جمهورية العراق

وزارة التعليم العالي والبحث العلمي

جامعة الفرات الاوسط التقنية

الكلية التقنية الهندسية – نجف

انتاج المياه العذبة باستخدام الطاقة الشمسية الفعالة باستخدام مواد ماصة مختلفة

رسالة مقدمة الى

قسم هندسة تقنيات ميكانيك القوى

كجزء من متطلبات نيل درجة الماجستير في هندسة تقنيات ميكانيك القوى (حراريات)

تقدمت بها الطالبة

ميس علاء نوري

(بكالوريوس هندسة تقنيات ميكانيك القوى 2021)

اشراف

المدرس الدكتور باسل نوري عبد

الأستاذ الدكتور منتظر عبودي محمد الموسوي

1446 ه　　　　**2024 م**